



HAL
open science

The role of mechanosensitive ion channels during zebrafish heart regeneration

Nathalie Nasr

► **To cite this version:**

Nathalie Nasr. The role of mechanosensitive ion channels during zebrafish heart regeneration. Human health and pathology. Université Montpellier, 2018. English. NNT : 2018MONTT001 . tel-01748056

HAL Id: tel-01748056

<https://theses.hal.science/tel-01748056>

Submitted on 29 Mar 2018

HAL is a multi-disciplinary open access archive for the deposit and dissemination of scientific research documents, whether they are published or not. The documents may come from teaching and research institutions in France or abroad, or from public or private research centers.

L'archive ouverte pluridisciplinaire **HAL**, est destinée au dépôt et à la diffusion de documents scientifiques de niveau recherche, publiés ou non, émanant des établissements d'enseignement et de recherche français ou étrangers, des laboratoires publics ou privés.

THÈSE POUR OBTENIR LE GRADE DE DOCTEUR DE L'UNIVERSITÉ DE MONTPELLIER

En Electrophysiologie et médecine régénératrice

École doctorale Sciences Chimiques et biologiques pour la santé (CBS2)

Unité de recherche CNRS UMR5203-INSERM U1191, Montpellier

The role of mechanosensitive ion channels during zebrafish heart regeneration

Présentée par Nathalie NASR

Le 23 février 2018

Sous la direction de Dr. Chris JOPLING
et Dr. Hamid MOHA OU MAATI

Devant le jury composé de

Dr. Chris JOPLING, CR (HDR) INSERM, CNRS UMR5203-INSERM U1191, Montpellier

Dr. Hamid MOHA OU MAATI, Maître de conférences, CNRS UMR5203-INSERM U1191, Montpellier

Dr. Marc BORSOTTO, DR (HDR), CNRS UMR7275, Nice

Dr. Flavien CHARPENTIER, DR (HDR), CNRS UMR6291-INSERM UMR1087, Nantes

Dr. Delphine BICHET, CR (HDR), CNRS UMR7275, Nice

Pr. Jean-Yves LE GUENNEC, Professeur, CHU Arnaud de Villeneuve INSERM U1061, Montpellier

Directeur de thèse

Codirecteur de thèse

Rapporteur

Rapporteur

Examineur

Examineur



UNIVERSITÉ
DE MONTPELLIER



The role of mechanosensitive ion channels during zebrafish heart regeneration and
development

Funding: Labex Ion Channel Science and Therapeutics (ICST) 2014-2017

Laboratoire : Chris Jopling, physiology department, CNRS UMR 5203 - INSERM U1191,
141 Rue de la Cardonille, 34094 Montpellier Cedex 5, France.

Table of Contents

Abbreviation list.....	1
Abstract.....	3
Aims of my thesis	5
1_ Overview on cardiovascular diseases	7
2_ Heart regeneration	8
2.1_ Zebrafish (zf) heart regeneration	8
2.1a_ Methods of adult zebrafish cardiac injury.....	9
2.1b_ Methods of embryonic zebrafish cardiac injury.....	9
2.1c_ The mechanism of zebrafish heart regeneration.....	10
2.1d_ Hypoxia positively regulates zebrafish heart regeneration	12
2.1e_ p38 MAPK negatively regulates zebrafish heart regeneration	13
2.2_ Mouse heart regeneration.....	16
2.2a_ Methods of mouse cardiac injury	16
2.2b_ The mechanism of neonatal heart regeneration	17
2.2c_ Hypoxia positively regulates mouse heart regeneration	18
2.2d_ p38 induces mouse cardiac hypertrophy	19
2.2e_ Adult mouse heart regeneration	20
2.3_ Summary I.....	21
2.4_ Human heart regeneration	22
2.4a_ Stem cell therapy	23
2.4a.1_ Embryonic stem cells	23
2.4a.2_ Induced pluripotent cells	24
2.4a.3_ Adult stem cells	24
2.4b_ Ventricular unloading promotes heart regeneration.....	25
2.5_ Summary II.....	26
3_ Mechanotransduction	26
3.1_ The types of mechanotransducers.....	27
3.2_ Mechanosensation between physiological and pathological mechanisms	30
3.3_ Mechanosensation in the heart	32
3.3a_ Mechanosensitive ion channels in the heart	32
3.3a.1_ Mechanically modulated ion channels (MMC)	33
3.3a.2_ Mechano gated ion channels (MGC)	35
3.3a.2.1_ Cation non selective ion Channel (SAC _{NS})	36
3.3a.2.2_ Transient receptor potential channel (TRP)	37
3.3a.2.3_ PIEZO channels.....	41
3.3a.3_ Stretch-Activated Channels, K ⁺ -Selective (SAC _K).....	43
3.4_ Summary III.....	44

4_ Potassium channel	45
5_ TREK-1 channel	48
5.1_ TREK-1 structure	48
5.2_ TREK-1 homodimers	50
5.3_ TREK-1 heterodimers	58
5.4_ TREK-1 between physiology and pathology	60
5.5_ Summary IV	64
6_ Hypothesis	66
7_ Objectives	68
7.1_ The characterization of zTREK-1a and zTREK-1b	68
7.2_ The role of zTREK-1a and zTREK-1b during zebrafish heart regeneration	69
7.3_ The role of zTREK-1a and zTREK-1b in physiological zebrafish heart function	69
Chapter 1: Electrophysiology	71
1_ Introduction	72
2_ Materials and methods	75
2.1_ Cloning	75
2.2_ Cell culture and transfection	75
2.3_ Adult zf cardiomyocyte primary culture	76
2.3.1_ Cardiomyocyte isolation	76
2.3.2_ Coating	76
2.4_ Electrophysiological recordings	77
2.4.1_ Stretch experiment	77
2.4.1.1_ Inside out configuration	77
2.4.1.2_ Cell attached configuration	78
2.4.2_ Polyunsaturated fatty acids experiment	78
2.4.3_ pH experiment	79
2.4.4_ Statistical analysis	80
2.5_ Immunofluorescence and immunohistochemistry	80
3_ Results	81
3.1_ Characterization of zTREK-1a and zTREK-1b (zTREK-1a/b)	81
3.1.1_ Effect of the membrane stretch on zTREK-1a/b	81
3.1.2_ Effect of the PUFs on zTREK-1a/b	84

3.1.3_ Effect of the intracellular pH on zTREK-1a/b	87
3.1.4_ Effect of the spadin on zTREK-1a/b.....	89
3.2_ zTREK-1a/b expression in zf cardiomyocytes	91
3.3_ Effect of the DN forms of zTREK-1 on zTREK-1a/b.....	93
3.3.1_ Effect of the DN TREK-1 del ex4 on zTREK-1a/b.....	93
3.3.2_ Effect of the DN TREK-1 del ex3 on zTREK-1a/b.....	95
3.4_ Validation of the mouse TREK-1 antibody	97
4_ Discussion.....	99
5_ Perspectives.....	102
Chapter 2: Implication of zTREK-1a/b during zf heart regeneration	103
1_ Introduction.....	104
2_ Materials and methods.....	107
2.1_ Making an antisense RNA probes for in situ hybridization.....	107
2.2_ In situ hybridization	107
2.3_ Zebrafish heart cDNA	108
2.3.1_ Embryonic zf heart cDNA	108
2.3.2_ Adult zf heart cDNA	108
2.4_ Zf heart amputation.....	109
2.5_ Zf pharmacological treatment	109
2.6_ Preparing heart for sectioning	109
2.7_ Immunohistochemistry	110
2.8_ AFOG staining	110
2.9_ Immunofluorescence	111
2.10_ Imaging	111
2.11_ Generating a transgenic conditional dominant negative TREK-1 del ex4 fish line.....	112
2.11.1_ Construct	112
2.11.2_ Generating the conditional DN TREK-1 del ex4 line	115
2.12_ Cre/Tamoxifen induction.....	116
2.12.1_ Embryos Cre/Tamoxifen induction.....	116
2.12.2_ Adult Cre/Tamoxifen induction.....	116
3_ Results.....	117
3.1_ Localization/expression of zTREK-1a and zTREK-1b	117
3.2_ Validation of the DN TREK-1 del ex4 transgenic line	121
3.3_ Implication of zTREK-1a/b during zf heart regeneration	122
3.3.1_ Effect of zTREK-1a/b Pharmacological inhibition on zf heart regeneration	122
3.3.2_ Effect of the conditional transgenic zf line expressing a dominant form of zTREK-1a/b on zf heart regeneration	123
4_ Discussion.....	125

5_Perspectives	129
Chapter 3: Implication of zTREK-1a and zTREK-1b in zebrafish normal cardiac function	131
1_ Introduction	132
2_ Materials and methods	134
2.1_ Embryonic heart rate recording	134
2.2_ Optical mapping	134
2.3_ Statistical analysis	135
2.4_ Zf pharmacological treatment	135
3_ Results	136
3.1_ Effect of zTREK-1a/b on embryonic heart rate.....	136
3.2_ Effect of zTREK-1a/b on adult heart activity	137
3.2.1_ Effect of zTREK-1a/b on adult heart rate	137
3.2.2_ Effect of zTREK-1a/b on speed of conduction	138
4_ Discussion	139
5_Perspectives	141
General discussion	143
French summary	150
References	157
Acknowledgement.....	169

Abbreviation list:

AA: arachidonic acid
AKAP 150: A-kinase anchor protein 150
 α MHC: α myosin heavy chain promoter
BDNF: Brain derived neurotrophic factor
CA: Cell attached
 Ca^{2+} : Calcium
ca MKK6: constitutively active Mitogen activated Kinase Kinase
cmlc2a: Cardiac myosin light chain 2a
cAMP: Cyclic AMP
CPC: Cardiac progenitor cells
CreER: Cre recombinase
CVDs : Cardiovascular disease
DAG: Diacylglycerol
Dag1: α -dystroglycan
DGC: Dysophin-glycoprotein complex
DHA: docosahexaenoic acid
DN: Dominant negative
DN zTREK-1a deletion exon 4: zTREK-1a del ex4
DN zTREK-1a deletion exon 3: zTREK-1a del ex3
dpa: Days post amputation
dpr: Days post-resection
DTA: Diphtheria toxin A chain
E: Glutamic acid
E3: Fish medium
ECM : Extracellular matrix
ETOH: Ethanol
ESC : Embryonic stem cells
FAK: Focal adhesion kinase
 Gd^{3+} : Gadolinium ions
GFP: Green fluorescent protein
HEK cells: Human Embryonic Kidney
hESC : human ESC
HIF1 α : Hypoxia inducible factor 1 α
hpf: Hours post fertilization
HSC : Hematopoietic stem cells
IP3: Inositol trisphosphate
IF: Immunofluorescence
iPSC : Induced pluripotent stem cells
IO: inside out
 K^+ : Potassium
 K_{ir} : Inward rectifier potassium channel
Kv: Voltage gated potassium channels family
LP: Lysophospholipids
LPC: Lysophosphatidylcholine
MAPK: Mitogen-Activated Protein Kinase
MF-20: Myosin heavy chain
MGC: Mechano gated ion channels
Mtap2: Microtubule associated protein 2

mTREK-1: Mouse TREK-1
MSC: Mesenchymal stem cell
MI: Myocardial infarction
Mtz: Metronidazole
MMC: Mechanically modulated ion channels
Na⁺: Sodium
NFAT: Nuclear factor of activated T cells
NO: nitric oxide
NTR: Nitroreductase
PC1: Polycystin-1
PCR: Polymerase Chain Reaction
PIP2: Phosphatidylinositol 4,5-bisphosphate
PKA: Protein kinase A
PKC: Protein kinase C
PKG: Protein kinase G
PLC: Phospholipase C
PLD 1: Phospholipase D 1
PLD 2: Phospholipase D 2
POPDC: Popeye domain-containing
PUFAs: polyunsaturated fatty acids
RFP: Red fluorescent protein
RI: Retroinverso
ROS: Reactive oxygen species
RR: Ruthenium red
RUNX1: Runt-related transcription factor 1
S: Serine
SAC: Stretch activated ion channels
SAC_K: Potassium SAC
SAC_{NS}: Cation non selective SAC
TGY: Thr-Gly-Tyr
TRAAK: TWIK related arachidonic acid stimulated potassium channel
TREK-1: TWIK-Related K⁺ Channel 1
TREK-2: TWIK-Related K⁺ Channel 2
TRP: Transient receptor potential channel
TRPA1: Ankyrin transmembrane protein 1
TRPC: Canonical TRP
TRPM: Melastatin TRP
TRPML: Mucolipins TRP
TRPP: Polycystins TRPs
TRPV: Vanilloid receptor TRPs
U2Os cell: Human Bone Osteosarcoma Epithelial Cells
VAD: Ventricular assist device
WC: Whole cell
WT: Wilde type
Zf: Zebrafish
Zebrafish TREK-1a: zTREK-1a
Zebrafish TREK-1b: zTREK-1b
zTREK-1a and zTREK-1b: zTREK-1a/b
(4-HT): 4-hydroxytamoxifen

Abstract:

In humans, most cardiovascular disorders lead to the destruction of cardiac tissue which will be replaced by fibrosis, leading to arrhythmia and reduced contractile function, resulting in an increase in ventricular load. In order to maintain an overall cardiac output, cardiomyocytes undergo a hypertrophic response, leading to pathological hypertrophy and heart failure. This increase in ventricular load, has to be sensed by mechanosensors such as mechanosensitive ion channels like TREK-1. Unlike mammals, adult zebrafish (zf) can fully regenerate their heart after an extensive insult through cardiomyocyte dedifferentiation followed by proliferation. We believe that in adult mammals, cardiomyocyte proliferation has been blocked/inhibited. Therefore it's likely that genes which respond to increased ventricular load in mammals and trigger pathological hypertrophy will trigger cardiomyocyte proliferation during heart regeneration in zf. We found that the mechanosensitive ion channels zTREK-1a and zTREK-1/b are expressed in zebrafish cardiomyocytes, they have similar biophysical and pharmacological properties to mammalian TREK-1, regarding their activation by membrane stretch, polyunsaturated fatty acids and intracellular acidification and their inhibition by a pharmacological agent (

) and the cytoskeleton. We have demonstrated that zTREK-1a/b don't affect normal zf heart function under normal conditions but they are important for successful heart regeneration. Their inhibition after heart amputation leads to impaired regeneration.

Key words: Regeneration, mechanosensitive ion channels, cardiomyocyte proliferation, electrophysiology, zebrafish.

Résumé:

Chez l'Homme, la plupart des maladies cardio-vasculaires provoquent une destruction du tissu cardiaque. Ce dernier est remplacé par de la fibrose conduisant à une diminution de la fonction contractile et une augmentation de la charge ventriculaire avec des risques d'arythmie. Pour maintenir un débit cardiaque constant, les cardiomyocytes vont alors s'hypertrophier, induisant sur le long terme le développement d'une insuffisance cardiaque. L'augmentation de la charge ventriculaire pourrait être perçue par des mécanosenseurs tels que les canaux ioniques mécanosensibles TREK-1. Contrairement aux mammifères adultes, le cœur du poisson zèbre se régénère suite à une destruction massive du ventricule. Cette régénération se fait par un mécanisme de dédifférenciation, suivie d'une étape de prolifération des cardiomyocytes. Chez les mammifères adultes, la prolifération des cardiomyocytes pourrait être bloquée / inhibée empêchant ainsi la régénération. L'hypothèse que les gènes responsables de l'hypertrophie pathologique chez les mammifères adultes suite à l'augmentation de la charge ventriculaire, soient également responsables de la prolifération des cardiomyocytes au cours de la régénération cardiaque chez le poisson zèbre est ainsi consistante. Cette étude, a montré que les canaux TREK-1a et TREK-1b du poisson zèbre possèdent des propriétés biophysiques et pharmacologiques, similaires à ceux du canal TREK-1 de mammifères, et qu'ils jouent un rôle fondamental dans la régénération cardiaque.

Mots clés : Régénération, canaux ioniques mécanosensibles, prolifération des cardiomyocytes, électrophysiologie, poisson zèbre.

The aims of my thesis:

The aims of my thesis are to directly address the role of zTREK-1a and zTREK-1b (zTREK-1a/b) during zebrafish heart regeneration and physiology. For that reason, it is important to characterize the channels (zTREK-1a/b), to localize their tissue expression which allow us to investigate their role during zebrafish heart regeneration and function. Achieving my objectives, will allow us to further investigate TREK-1 downstream effectors and the signaling pathways in which they are implicated during zebrafish heart physiology and pathophysiology.

In order to characterize zTREK-1a/b I have performed electrophysiological recordings using a patch clamp technique on HEK cells transfected with either zTREK-1a or zTREK-1b. This technique will allow us to obtain zTREK-1a/b biophysical and pharmacological properties. I have tested the efficiency of a DN form of zTREK-1a/b (DN TREK-1 del ex4 and DN TREK-1 del ex3) in order to use them for further experiments. Establishing zTREK-1a/b biophysical and pharmacological properties served us to evaluate the expression of functional channels in our cells of interest: cardiomyocytes. I have tested the efficiency of a mouse TREK-1 (mTREK-1) antibody by performing immunofluorescence on U2OS cells transfected with either zTREK-1a or zTREK-1b. I have used this mTREK-1 antibody to investigate the presence of zTREK-1a protein in zf hearts and cardiomyocytes.

Subsequently, we wanted to investigate the role of TREK-1a/b during heart regeneration. In order to induce heart regeneration in zf, I have used the amputation as a method for cardiac injury. Heart amputation consists of cutting up to 20% of the ventricular apex with iridectomy scissors. To test the effect of zTREK-1a/b on heart regeneration, I have adopted 2 strategies.

The first strategy consists of zTREK-1a/b pharmacological inhibition during heart regeneration for 30days post amputation through spadin injections (functional pharmacological inhibitor of zTREK-1a/b tested by patch clamp technique). The second strategy consists of using a conditional DN zf transgenic line based on the conditional Cre/lox system. This line expresses under the control of the cardiomyocyte specific promoter (cardiac myosin light chain 2a (cmlc2a)), a 4-hydroxytamoxifen (4-HT) inducible Cre recombinase (CreER) and a floxed stop cassette that targets the expression of a dominant negative form of the channels (DN TREK-1 del ex4) in the cardiomyocytes upon 4-HT treatment. 4-HT treatment leads to an irreversible expression of the DN TREK-1 del ex4 in zf cardiomyocytes. For this reason I have treated this line 2 times before heart amputation with 4-HT to have a better effect on the DN TREK-1 del ex4 expression, to investigate its effect on heart regeneration. This experiment allows us to establish if zTREK-1a/b are required for successful heart regeneration.

We next sought to determine whether zTREK-1a/b inhibition affected cardiac physiology. For that reason, I have used 2 models: embryonic and adult zebrafish model. I have expressed the DN TREK-1 del ex4 in zebrafish cardiomyocytes in vivo and I have determined whether this affected the heart rate of zf embryos. For the adult zf model, I have performed optical mapping experiments with the help of Dr. Angelo TORRENTE on the hearts extracted from pharmacologically treated zebrafish. I have treated adult zebrafish with spadin injections in order to inhibit zTREK-1a and zTREK-1b. This experiment allowed us to evaluate the effect of zTREK-1a/b inhibition on zf embryo heart rate, adult heart automatism and on conduction velocity.

1_ Overview on cardiovascular diseases:

According to the World Health Organization, the death rate from cardiovascular diseases (CVDs) between 2012 and 2015 has fallen about 14% (15 million deaths in 2015 while it was 17.5 million in 2012). Despite this decrease, CVDs remain the first cause of death worldwide, and the death risk factor remains alarmingly high. Ischemic heart disease is the major cause of CVDs due to myocardial infarction (MI). MI results in fibrotic scar formation, caused by the massive loss of cardiomyocytes, which leads to a disruption of the normal heart function. When the balance between cardiomyocyte death and cardiomyocyte formation is over taken by cell death, this leads to pathological hypertrophy and heart failure (Nadal-Ginard, Kajstura et al. 2003, Mercola, Ruiz-Lozano et al. 2011).

Until now, the best solution for patients suffering from heart failure is heart transplantation. The limitations of heart transplantation, are the restricted availability of donated organs, the risk of graft rejection and the chronic immunosuppression treatment. However, recent studies based on tissue engineering are quite promising for the future treatment for patients with heart diseases. This new approach consists of replacing/regenerating the damaged part of the myocardium using tissue or cell based strategies. This approach is quite promising but the parameters should be optimized to have successful therapeutic outcomes (Chiu, Iyer et al. 2012).

Recent studies have focused on the natural capacities of some species to regenerate their hearts after extensive insult, such as amphibians, lower vertebrates and

neonatal mammals. Trying to understand molecular and cellular mechanisms that allow these species to regenerate their heart, will lead us to understand why this mechanism has been blocked/inhibited in adult mammals.

2. Heart regeneration:

Regeneration is the mechanism of renewal or restoration of damaged tissues and organs. Unlike adult mammals, some species like amphibians have a high regenerative activity. Amphibians can regenerate removed or injured body parts like lens, retina, spinal cord, jaws, portions of intestine, brain tissue, and major appendages (Kikuchi and Poss 2012). Interestingly, amphibians are able to regenerate their heart after resection of their ventricular apex (Rumyantsev 1977). It has been shown that cardiomyocyte proliferation does occur during amphibian heart regeneration. Oberpriller J et al and Rumyantsev, have shown by electron microscopy, the presence of dividing cardiomyocytes in newt hearts after cardiac injury (Oberpriller and Oberpriller 1971, Rumyantsev 1977). Adding to that, Flink et al, showed the presence of DNA synthesis in cardiomyocytes in injured axolotl's heart after BrdU injections (Flink 2002). Heart regeneration was then investigated in neonatal mammals like mice as well as in lower vertebrates, like zebrafish (zf).

2.1_ Zebrafish heart regeneration:

Different methods have been developed to induce cardiac injury in order to stimulate heart regeneration. Adding to that there are 2 models of zebrafish heart regeneration: the adult model and the embryonic one.

2.1a_ Methods of adult zebrafish cardiac injury:

Amputation is the most common method of zebrafish heart injury. This method consists of cutting up to 20% of the ventricular apex with iridectomy scissors (Jopling, Sleep et al. 2010). Since the coronary artery in zebrafish is small, thus hard to manipulate, another method has been developed: cryoinjury, a technique able to induce myocardial infarction. This method consists of damaging the ventricular wall using a probe cooled in liquid nitrogen applied on the ventricle, causing necrotic death of the surrounding area (Chablais, Veit et al. 2011).

Another method of zebrafish heart injury has been developed, based on genetic cardiomyocyte depletion. This method consists of using a double transgenic line expressing 4-hydroxytamoxifen (4-HT) inducible Cre recombinase (CreER) under the control of the cardiomyocyte specific promoter (cardiac myosin light chain 2a (cmlc2a)), and a floxed stop cassette that targets cytotoxic DTA (diphtheria toxin A chain) expression to CreER-expressing cells upon 4-HT injection under the control of β -actin2 promoter. Translocation of Cre into the nucleus upon tamoxifen treatment, leads an irreversible expression of DTA in the cardiomyocytes, resulting in cardiomyocyte death through apoptosis. Cardiomyocyte depletion can be controlled by the dose of injected tamoxifen (Wang, Panakova et al. 2011).

2.1b_ Methods of zebrafish embryonic cardiac injury:

This method consists of using a transgenic line expressing a bacterial Nitroreductase (NTR) enzyme in the cardiomyocytes under the control of the cardiomyocyte specific promoter *cmlc2a*. This enzyme converts its substrate: metronidazole (Mtz) into a cytotoxic DNA cross-linking agent, causing cardiomyocyte death through caspase activation. Cardiomyocyte depletion can be controlled by the dose and the exposure time of the Mtz applied on zf embryos. To have the maximum regeneration after Mtz treatment, the dose and the exposure time of Mtz are 4mM for 5hours, applied on zf embryos at 48 hours post fertilization (hpf). Once the Mtz is removed from the medium (72 to 96 hours in Mtz free medium), 60% to 70% of zf embryos were able to regenerate their hearts (Curado, Anderson et al. 2007).

2.1c_ The mechanism of zebrafish heart regeneration:

After 20% of heart amputation, zebrafish can replace the missing part of their heart after around 30 days post amputation (dpa). After heart injury, there is a blood/fibrin clot formation in the amputation area, which disappears progressively to be replaced by cardiomyocytes. To determine the cellular source of the regenerated myocardium, Jopling et al, have used a genetic lineage tracing approach, based on the conditional Cre/loxp system. Jopling et al, generated a double transgenic line that expresses in their cardiomyocytes under the of the cardiomyocyte specific promoter (*cmlc2a*), a 4-hydroxytamoxifen (4-HT) inducible Cre recombinase (CreER) and a loxp reporter transgene consisting of a floxed STOP cassette followed by a GFP reporter. Upon treatment with tamoxifen, Cre recombinase induces the excision, of the loxp flanked stop sequence and permanently labels the cardiomyocytes with GFP. After amputation, the

newly formed cardiomyocytes express GFP, indicating that they are derived from pre-existing cardiomyocytes which express GFP (Fig1). Following heart injury, cardiomyocytes return to a primitive state, this process is called dedifferentiation, characterized by the disassembly of their sarcomeres. Dedifferentiation is a crucial step allowing pre-existing cardiomyocytes to proliferate and replace the damaged part of the heart (Fig2) (Jopling, Sleep et al. 2010).

At 30 dpa the missing/damaged part of the heart is replaced by newly formed tissue. It has been reported that the newly formed cardiomyocytes result from proliferation of pre-existing cardiomyocytes (Jopling, Sleep et al. 2010, Chablais, Veit et al. 2011, Wang, Panakova et al. 2011).

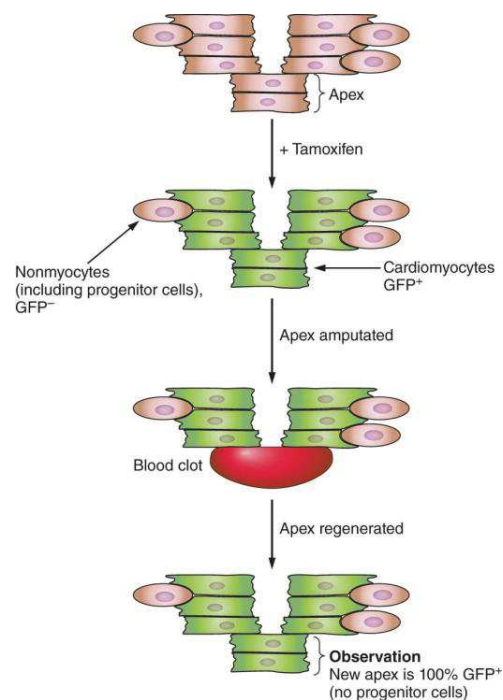
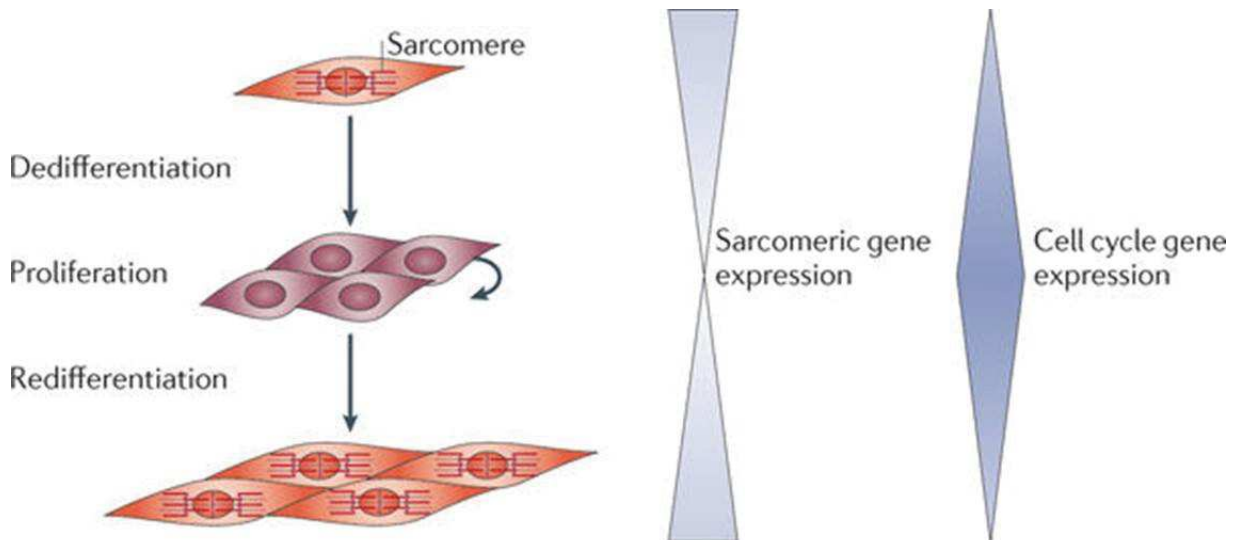


Figure1: Jopling C. and al., Nature, 2010. Schematic presentation of the lineage tracing done in zebrafish to determine the source of the newly form cardiomyocytes during zebrafish heart regeneration: Upon tamoxifen treatment the

GFP is expressed only in the cardiomyocytes. Following heart amputation the newly formed cardiomyocytes are all labeled with GFP reflecting that they come from preexisting cardiomyocytes.



*Figure2: Jopling C. and al., Nature, 2010. **Schematic presentation of the mechanism by which occurs zebrafish heart regeneration:** zebrafish heart regeneration occurs with the mechanism of cardiomyocyte dedifferentiation followed by proliferation where there is a downregulation of sarcomeric genes accompanied with an upregulation of the cell cycle genes. Once the redifferentiation takes place there is an upregulation of the sarcomeric genes accompanied with a downregulation of the cell cycle genes.*

2.1d Hypoxia positively regulates zebrafish heart regeneration:

Environmental factors regulate a number of biological processes. It has been shown that hypoxia affects zebrafish heart regeneration and cardiomyocyte proliferation (Jopling, Sune et al. 2012). Following heart amputation in zebrafish, there is an increase of hypoxia inducible factor 1 α (HIF1 α) in the cardiomyocytes, which positively regulates heart regeneration. A transgenic zebrafish line has been developed expressing a 4-HT

inducible CreER and a floxed red fluorescent protein (RFP) stop cassette that targets dominant negative (DN) HIF1 α expression in the cardiomyocytes, under the of the cardiomyocyte specific promoter *cmlc2a* promoter upon tamoxifen treatment. Upon treatment with tamoxifen, Cre recombinase induces the excision, of the loxp flanked stop sequence and permanently expresses the DN HIF1 α in the cardiomyocytes. After amputation, zebrafish that express the DN HIF1 α in their cardiomyocytes fail to regenerate their hearts. In addition, Jopling et al, have demonstrated that hypoxia positively regulates cardiomyocyte dedifferentiation/proliferation *in vitro*. They have performed immunohistochemistry on cultured zf cardiomyocytes under normoxic and hypoxic conditions, by using a marker for differentiated cardiomyocytes (alpha sarcomeric actin) and a cardiomyocyte marker (tropomyosin). Dedifferentiated cardiomyocytes display a reduced/disorganized alpha sacromeric actin expression but they conserve tropomyosin expression. They have quantified the percentage of dedifferentiated cardiomyocytes under normoxic and hypoxic conditions. They have demonstrated that the percentage of dedifferentiated cardiomyocytes increases by 2 fold in hypoxic conditions compared to normoxic conditions (Jopling, Sune et al. 2012).

2.1e_ Effect of p38 MAPK on zebrafish heart regeneration:

P38 Mitogen-Activated Protein Kinase (MAPK) is a proline-directed serine/threonine protein kinase. Four isoforms belong to the p38 MAPK subfamily: p38 α , p38 β , p38 γ and p38 δ . These isoforms have a conserved dual phosphorylation motif Thr-Gly-Tyr (TGY) that serves as an activation switch for kinases. p38 MAPK isoforms have different tissue-specific expression patterns. p38 α MAPK is ubiquitously expressed in

many cell types, in contrast p38 β MAPK is highly expressed in the brain and lungs, p38 γ MAPK is mostly detected in skeletal muscle and nervous system, and p38 δ MAPK is mostly expressed in the uterus and pancreas (Ono and Han 2000, Li, Liu et al. 2011). P38 MAPK are activated by an upstream kinase: MAPK kinase (MAPKK), which phosphorylates the TGY motif. P38 MAPK plays a role in several physiological and pathological mechanisms (Fig 3). It has been reported that p38 α is the main isoform expressed in the heart and it regulates different cell functions such as proliferation, differentiation, cell death, cell migration and cell adhesion (Liang and Molkentin 2003, Cuadrado and Nebreda 2010, Oeztuerk-Winder and Ventura 2012) (Fig 4). For this reason, several teams have been interested to investigate the role of p38 α during heart regeneration.

In order to directly address the role of p38 α in cardiomyocyte proliferation during heart regeneration, Jopling et al, have generated a double transgenic fish line that expresses a 4-hydroxytamoxifen (4-HT) inducible Cre recombinase (CreER) and a floxed stop cassette under the control of the cardiomyocyte specific promoter (cmlc2a) that targets the expression of a constitutively active Mitogen activated Kinase Kinase – (ca MKK6) in the cardiomyocytes upon tamoxifen treatment. The expression of the ca MKK6 in the cardiomyocytes leads to the activation of p38 α in these cells. Activated p38 α inhibits adult cardiomyocyte proliferation and cell cycle progression, resulting in blocked heart regeneration. Naturally, adult zebrafish cardiomyocytes have high levels of active p38 α MAPK. However, during heart regeneration zebrafish are able to downregulate p38 α activity allowing cardiomyocyte proliferation and successful heart regeneration (Jopling, Sune et al. 2012).

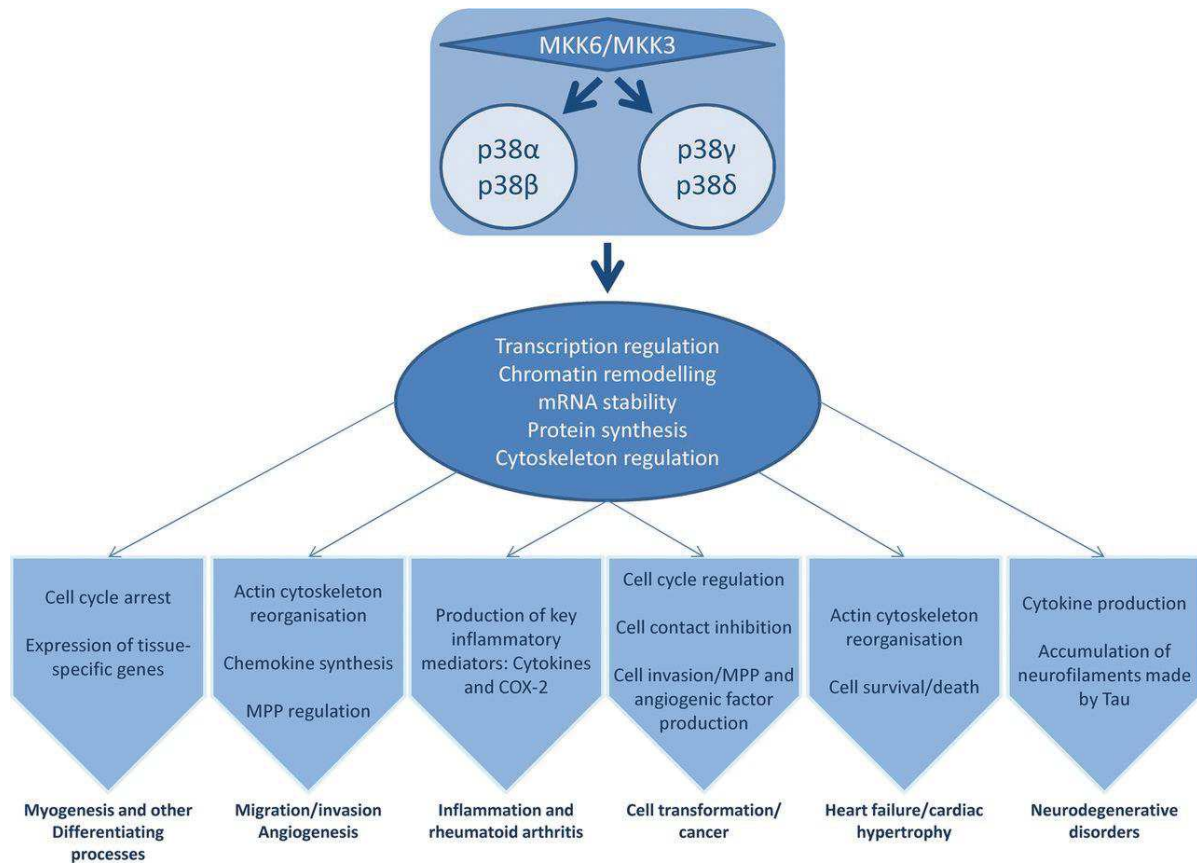


Figure3: Oeztuerk-Winder et al Biochem J. 2012: **Schematic presentation of p38 MAPK pathway and it's implication in biological processes: p38 signalization pathway affect several physiological and biological processes in contrast any disturbance in this signalization pathway lead to pathologies.**

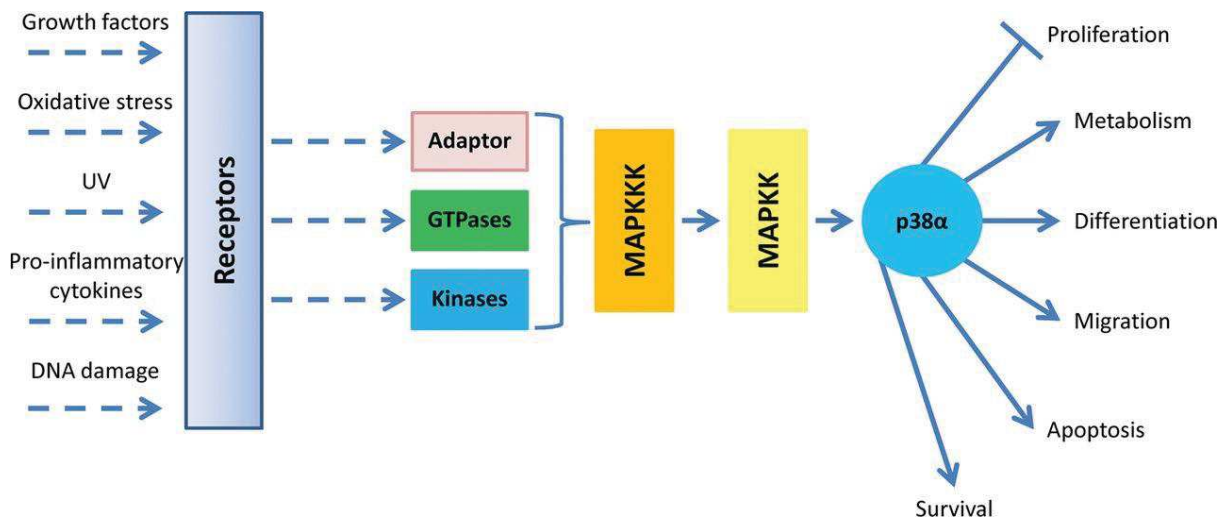


Figure 4: Cuadrado A et al Biochem. J 2010: **Schematic representation of p38 activation and its effect on several cellular processes.** p38 α activation influence several cellular processes including differentiation proliferation differentiation and migration.

2.2_ Mouse heart regeneration:

Neonatal mice represent mammalian models to study heart regeneration. The mechanism of heart regeneration is conserved between zfish and mice. Neonatal mice have the ability to regenerate their heart after up to 10% of ventricular apex resection. This ability of heart regeneration is blocked/inhibited one week after birth (Porrello, Mahmoud et al. 2011). Researchers have developed different methods of cardiac injury in mouse models.

2.2a_ Methods of mice cardiac injury:

The different methods of mice cardiac injury, are similar to the ones used in adult zfish. Ventricular apex resection (amputation) (Porrello, Mahmoud et al. 2011), and cryoinjury (Darehzereshki, Rubin et al. 2015). However microinjury in mice is different than the one developed in zfish and it consists of coronary artery occlusion resulting in myocardial infarction and cardiomyocyte death (Blom, Lu et al. 2016).

2.2b The mechanism of neonatal heart regeneration:

At 1 day post-resection (dpr), a large blood clot seals the entire apex. The blood clot will be resorbed gradually within 21 dpr to be replaced by normal myocardial tissue. In order to determine the source of the newly formed cardiomyocytes, Porrello et al, performed a lineage tracing. For that reason, they have generated a double transgenic line that expresses a floxed lacZ reporter under a ubiquitous promoter (Rosa26) and a 4-HTinducible CreER under the control of the cardiomyocyte specific promoter: α myosin heavy chain promoter (α MHC). Upon treatment with tamoxifen, Cre recombinase induces the excision, of the loxp flanked stop sequence and permanently expresses LacZ reporter in the cardiomyocytes. At 21 dpr most of the newly formed cardiomyocytes were lacZ positive visualized by a staining with X-gal to detect LacZ activity. This reflects that the newly formed cardiomyocytes come from pre-existing cardiomyocytes which express LacZ reporter. Like zf heart regeneration, neonatal mouse heart regeneration occurs by cardiomyocyte dedifferentiation, characterized by their sarcomere disassembly, allowing them to proliferate, and to give rise to the newly formed cardiomyocytes (Porrello, Mahmoud et al. 2011).

Neonatal mice show their ability to fully regenerate their heart within seven days following severe cardiac ischemia after MI. This regeneration is accompanied with a long term restoration of cardiac function. Genetic fate mapping shows that preexisting cardiomyocytes give rise to the newly formed cardiomyocytes by reentering cell cycle (Haubner, Adamowicz-Brice et al. 2012).

Naturally, adult mice fail to regenerate their heart, unless they undergo specific conditions such as hypoxia, or by stimulating particular signalization pathways (detailed later).

2.2c Hypoxia positively regulates mouse heart regeneration:

Soon after birth, the number of mitochondria increases in the cardiomyocytes, leading to an increase in oxidative stress. The increase in oxidative stress will lead to an increase of reactive oxygen species (ROS) production, causing oxidative DNA damage. The increase in ROS production, leads to an inhibition of cardiomyocyte proliferation caused by the activation of DNA damage response pathway that leads to cardiomyocyte cell cycle arrest, resulting in loss of mouse regenerative capacity. In addition, it has been shown that neonatal mice placed under hypoxic conditions show a high rate of proliferative cardiomyocytes compared to neonatal mice placed under normoxic or hyperoxic conditions (Puente, Kimura et al. 2014).

Following ischemia or acute coronary occlusion, HIF 1 α is a potential therapeutic target, because HIF-1 α has been shown to up-regulate expression of genes involved in protective effects, including angiogenesis, stress response, and extracellular matrix remodeling. The upregulation of HIF α enhances angiogenesis and vascularization, allowing by that to limit the infarct size, and to improve myocardial function (Kido, Du et al. 2005, Ziello, Jovin et al. 2007).

Recent studies show the presence of cardiomyocyte proliferation in non-injured adult mouse hearts placed under hypoxic conditions. After myocardial infarction, mice placed under hypoxic conditions, present a smaller fibrotic area and a significant increase in cardiomyocyte proliferation rate, compared to mice placed under normoxic conditions. Hypoxia leads to a decrease of ROS production in adult mouse hearts, resulting in a decrease of oxidative DNA damage decreasing the activation of DNA damage response pathway, thereby

inducing cardiomyocyte proliferation. In order to investigate the source of the newly formed cardiomyocytes, Nakada et al, have generated a double transgenic mouse line that expresses a 4-HT inducible CreER under the control of the cardiomyocyte specific promoter: α MHC and a floxed stop cassette that targets a bright red fluorescent protein: td tomato (under the control of a ubiquitous promoter). Upon tamoxifen treatment, Cre recombinase induces the excision, of the loxp flanked stop sequence and permanently expresses td tomato in the cardiomyocytes. Following MI, most of the newly formed cardiomyocytes were td tomato positive, this reflects that the newly formed cardiomyocytes come from pre-existing cardiomyocytes rather than from cardiac progenitors (Nakada, Canseco et al. 2017).

2.2d_ p38 MAPK induces mouse cardiac hypertrophy:

During fetal development, cardiomyocytes proliferate and increase in number. Soon after birth, cardiomyocytes switch to hypertrophic growth, and they increase in size rather than number (Li, Wang et al. 1996). Inducing p38 α activation in adult mouse hearts, results in lethal cardiomyopathy associated with cardiomyocyte hypertrophy and contractile dysfunction (Streicher, Ren et al. 2010). p38 α is inversely correlated with fetal cardiac growth and its activation leads to the inhibition of gene expression required for mitosis. p38 regulates mitosis in fetal cardiomyocytes, its inhibition is crucial for DNA synthesis. The inhibition of p38 leads to cell cycle progression by promoting G2/M transition. Regarding adult cardiomyocytes, P38 inhibition promotes growth-factor-induced DNA synthesis in adult cardiomyocytes, which allow cardiomyocyte proliferation (Engel, Schebesta et al. 2005).

2.2e_ Adult mouse heart regeneration:

Naturally, in response to stress or extensive heart insult, adult mice fail to regenerate their heart and they develop hypertrophy instead. However, studies showed that expressing a constitutively active tyrosine kinase receptor ERBB2 in adult mice after MI, leads to heart regeneration. In this case, heart regeneration was shown to occur due to cardiomyocyte dedifferentiation. Cardiomyocyte dedifferentiation was evaluated by their sarcomere disassembly and the evaluation of dedifferentiation markers such as Runt-related transcription factor 1 (RUNX1). Dedifferentiation allows cardiomyocyte proliferation, in order to replace the damaged part of the heart. Cardiomyocyte proliferation occurs due to the activation of ERK, AKT pathway triggered by the activation of ligand/receptor NRG/ERBB2 (D'Uva, Aharonov et al. 2015).

Another study showed the ability of adult mice to switch from hypertrophic response to regenerative response after MI. This switch occurs due to an extracellular matrix protein: Agrin. Agrin is a proteoglycan, it is expressed in several tissues including neurons and muscles. It has been shown that agrin is important in neuromuscular junction signaling (Kim, Stiegler et al. 2008). Neural and muscle agrins are shown to be involved in the cytoskeletal rearrangement (Denzer, Brandenberger et al. 1997, Uhm, Neuhuber et al. 2001, Lin, McCroskery et al. 2010). However, muscle agrin has more affinity to α -dystroglycan than neural agrin (Gesemann, Brancaccio et al. 1998). During mouse heart regeneration, agrin binds to α -dystroglycan (Dag1) receptor, which promotes ERK activation. ERK signalization pathways is already shown to be implicated during cardiomyocyte proliferation (D'Uva, Aharonov et al. 2015, Bassat, Mutlak et al. 2017). Adding to that, it has been demonstrated that Agrin/ Dag1 binding

leads to partial disassembly of the Dystrophin-glycoprotein complex (DGC) which plays the role of mechanical linkage between cardiac microenvironment and the inner contractile machinery. This step was suggested to play a key role in cardiomyocyte dedifferentiation, a crucial step allowing the cardiomyocytes to re-enter cell cycle (Bassat, Mutlak et al. 2017).

These studies suggest that adult mammalian heart regeneration has been blocked/inhibited and it is possible to reverse this inhibition by controlling environmental and molecular factors that promote cardiomyocyte dedifferentiation and proliferation to replace the damaged part of the heart.

2.3_ Summary I:

Adult zf heart regeneration shares similarities with neonatal and adult mammalian (mouse) heart regeneration. Heart regeneration occurs by cardiomyocyte dedifferentiation followed by proliferation that gives rise to the newly formed cardiomyocytes. The mechanism of heart regeneration in zf or mice is influenced by environmental factors such as hypoxia that positively regulates cardiomyocyte proliferation. Adult mice fail to naturally regenerate their heart. Recent studies show that controlling environmental and molecular factors that induce the activation of signalization pathway, which promote cardiomyocyte dedifferentiation and proliferation, allow adult mice to switch their heart response from hypertrophy to regeneration (D'Uva, Aharonov et al. 2015, Bassat, Mutlak et al. 2017) . Molecular mechanisms that regulate cardiomyocyte proliferation are also similar between species where p38 and its upstream activator (MAPKK), negatively regulate cardiac development and cardiomyocyte proliferation. Inhibition of p38 results in positive regulation of cardiomyocyte proliferation. It seems that adult

mammalian heart regeneration occurs with the same mechanism as neonatal mice, through cardiomyocyte dedifferentiation followed by proliferation.

For that reason zfish is an appropriate model to study heart regeneration, to better understand molecular and cellular mechanisms that influence cardiac regeneration. This allows us to determine different effectors and signalization pathways implicated during heart regeneration.

2.4 Human heart regeneration:

CVDs are the first cause of death in the world. Most of them lead to ventricular destruction, for that reason it is important to replace the damaged part of the heart to increase the chances of survival for the patients. In Humans, cardiomyocyte proliferation occurs during fetal development. Cardiomyocytes continue to proliferate during the first few months after birth and then their proliferative capacity significantly decreases (Li, Wang et al. 1996). However, a study based on the atomic bomb and the release of radioactive carbon 14 to the environment and its incorporation into cardiomyocyte DNA, brought evidences about cardiomyocyte renewal in Humans. Individuals born after the atomic the release of the atomic bomb have incorporated carbon-14 into their DNA. If they continue to produce cardiomyocytes after the levels of environmental carbon-14 have dropped, these new cardiomyocytes would not have incorporated carbon-14 into their DNA. This study showed that less than 45% of cardiomyocytes are replaced during life span. However, the source of the newly formed cardiomyocytes remains unknown. The amount of cardiomyocyte proliferation, is not sufficient to enhance recovery after heart injury (Bergmann, Bhardwaj et al. 2009).

2.4a_ Stem cell therapy:

According to the World Health Organization CVDs represent 31% of global death worldwide in 2012. The majority of cardiac arrest occurs in patients who have had myocardial infarction (Zaman and Kovoov 2014). For that reason, it is important to develop an efficient therapeutic approach for patients suffering from CVDs. Regenerative medicine is quite promising to treat CVDs and replace the damaged part of the heart.

2.4a.1_ Embryonic stem cells:

Embryonic stem cells (ESC) are pluripotent stem cells, they come from the isolation of the inner cell mass of blastocyst stage embryos. ESC remain pluripotent in an undifferentiated state *in vitro* for a long time. This allows them to reserve their capacity to differentiate into any cell types according to the stimuli and the signalization pathway provided (Thomson, Itskovitz-Eldor et al. 1998, Lev, Kehat et al. 2005). It has been reported that overexpression of transcription factors such as GATA4, Nkx2-5, or MEF2C induces differentiation of human ESC (hESC) into cardiomyocytes, while their inhibition prevents cardiomyocyte formation (Skerjanc, Petropoulos et al. 1998). When ESC-derived cardiomyocytes are transplanted in a pro-survival cocktail, they show an enhanced survival properties *in vivo* (Laflamme, Chen et al. 2007). Human ESC-derived cardiomyocytes can also electromechanically couple with host cells to allow synchronous contraction between the grafted cells and the host tissue (Shiba, Fernandes et al. 2012). However, hESC approach presents several limitations, regarding ethical problems, because it involves the destruction of human embryos (Evans and Kaufman 1981). hESC derive from embryos that don't have the same genome as the patients, increasing the risk of immune rejection (Murata, Tohyama et al. 2010). In addition, the number of differentiated

cardiomyocytes, generated from hESC remains small and not efficient to regenerate the damaged part of injured heart. One critical point is the safety of the patients, where in vivo implantation of hESC results in teratomas formation (Amit, Carpenter et al. 2000).

2.4a.2_ Induced pluripotent stem cells:

Induced pluripotent stem cells (iPSC) derive from reprogramming somatic cells to a pluripotent state (Takahashi, Tanabe et al. 2007). iPSC have the ability to differentiate into functional cardiomyocytes (Zhang, Wilson et al. 2009, Yoshida and Yamanaka 2011). iPSC bypass ethical problems, however, the major problem of these cells is the small amount of cell survival after transplantation (Yoshida and Yamanaka 2011) as well as their capacity to develop teratomas (Gutierrez-Aranda, Ramos-Mejia et al. 2010).

2.4a.3_ Adult stem cells:

Adult stem cells have an advantage over hESC and hiPSC where they bypass ethical problems, and immune rejection because they are isolated from adult patients (Leri, Kajstura et al. 2008). The presence of multipotent cells has been reported in the heart, which correspond to cardiac progenitor cells (CPC). They have the ability to differentiate into many cardiac cell types. However, the amount of cells isolated from *in vitro* culture used for therapies is not sufficient (Urbanek, Quaini et al. 2003, Leri, Kajstura et al. 2008).

Mesenchymal stem cells (MSC) have been used to treat patients suffering from pathological hypertrophy or myocardial infarction (Novotny et al 2008; Wang et al 2010). Implanted MSC can repair the damaged tissue due to their paracrine activity, their ability to fuse with the damaged cell as well as their ability to differentiate into cardiomyocytes. MSC are easy

to access. They can be isolated from peripheral blood or umbilical cord (Gnecchi, Zhang et al. 2008, Avitabile, Crespi et al. 2011). However, preconditioning MSC requires a hypoxic, highly acidic and nutrient deprived environment. Once implanted, MSC will be exposed to traumatic physical load and high levels of inflammatory mediators which affect their survival (Richardson, Hoyland et al. 2010).

Hematopoietic stem cells (HSC) are multipotent stem cells that can differentiate into many cell types *in vitro* and *in vivo*. However, they lack the ability of transdifferentiation into cardiomyocytes *in vivo* after myocardial infarction. The injection of HSC into the peri-infarcted area of mouse left ventricle, results in an improvement of heart function with an increased angiogenesis (Murry, Soonpaa et al. 2004).

2.4b_ Ventricular unloading promotes heart regeneration:

An important study realized by Birks et al, shows that using a ventricular assist device (VAD), which promotes ventricular unloading in patients suffering from severe heart failure with cardiac dysfunction, results in an improvement of their prognosis and reversal of their heart failure. The reversal of patient heart failure was accompanied by a reduction of myocyte hypertrophy. The patient follow up showed that they have a better life style with an improvement of their heart function (Zafeiridis, Jeevanandam et al. 1998, Birks, Tansley et al. 2006). The improvement of heart function and physiology is due to cardiomyocyte proliferation. Cardiomyocyte proliferation was accompanied with a decrease of mitochondrial DNA (Canseco, Kimura et al. 2015). It has been shown that the depletion of mitochondrial DNA reduces oxidative DNA damage, resulting in an increase of the chances for cardiomyocyte survival and proliferation as we have described before (Chen, Wang et al. 2016).

2.5_ Summary II:

Stem cell therapy for human heart regeneration, seems to be promising and leads to an improvement of patient heart function. However, there is a lot of limitations, regarding ethical problems, high risk of cancer formation or immune rejection problems. Stem cell therapy needs a lot of improvement before it can be used for patients. However, human ventricular unloading in patients suffering from severe heart failure, results in an improvement of their prognosis. This strongly supports the hypothesis made by Faucherre and Jopling, based on high blood pressure in human that prevents cardiac regeneration and cardiomyocyte proliferation. Adult zebrafish, have low blood pressure, allowing them to survive after heart amputation, by sealing the wound with a blood clot, and initiating heart regeneration. In contrast, adult mammals have high blood pressure, they risk cardiac rupture if they try to regenerate their heart in the same way as zebrafish. Removing pressure on adult mammal heart by using a ventricular assist device, enhances cardiac regeneration. (Faucherre and Jopling 2013). This suggests that mechanosensors play a key role during hypertrophy as well as during heart regeneration.

3_ Mechanotransduction:

Mechanotransduction is the mechanism by which cells convert mechanical stimuli into biochemical signals. This mechanism is conserved from bacteria to humans (Orr, Helmke et al. 2006). Mechanotransduction is important for cell and tissue morphology and functions. In addition mechanotransduction is important for many physiological processes such as blood pressure regulation, maintenance of muscle and perception of touch and hearing (Ernstrom and Chalfie 2002, Lehoux and Tedgui 2003, Garin and Berk 2006). Mechanotransduction also participates to pathological mechanisms such as hypertrophy and atherosclerosis (Thubrikar

and Robicsek 1995, Sadoshima and Izumo 1997). At the cellular level, mechanotransduction is involved in a large number of cellular mechanism such as cell cycle, cell migration, and cell shape (Kumar, Maxwell et al. 2006, Provenzano and Keely 2011, Fruleux and Hawkins 2016).

After a massive loss of cardiomyocytes, the heart attempts to maintain sufficient cardiac output. Maintaining constant cardiac output, leads to heart pressure overload. On one hand, this pressure overload leads to cardiac hypertrophy in adult mammals, on the other hand, we hypothesize that it induces cardiac regeneration in neonatal mammals and zf.

3.1_ The types of mechanotransducers:

It exists several types of mechanical stimuli: tension, compression and shear stress. The cells respond to these stimuli by adjusting their shape, function, migration, differentiation, and their cell death (Vogel and Sheetz 2006). The response of the cells can be different depending on the stimuli to which they are exposed (Nyman, Leng et al. 2009).

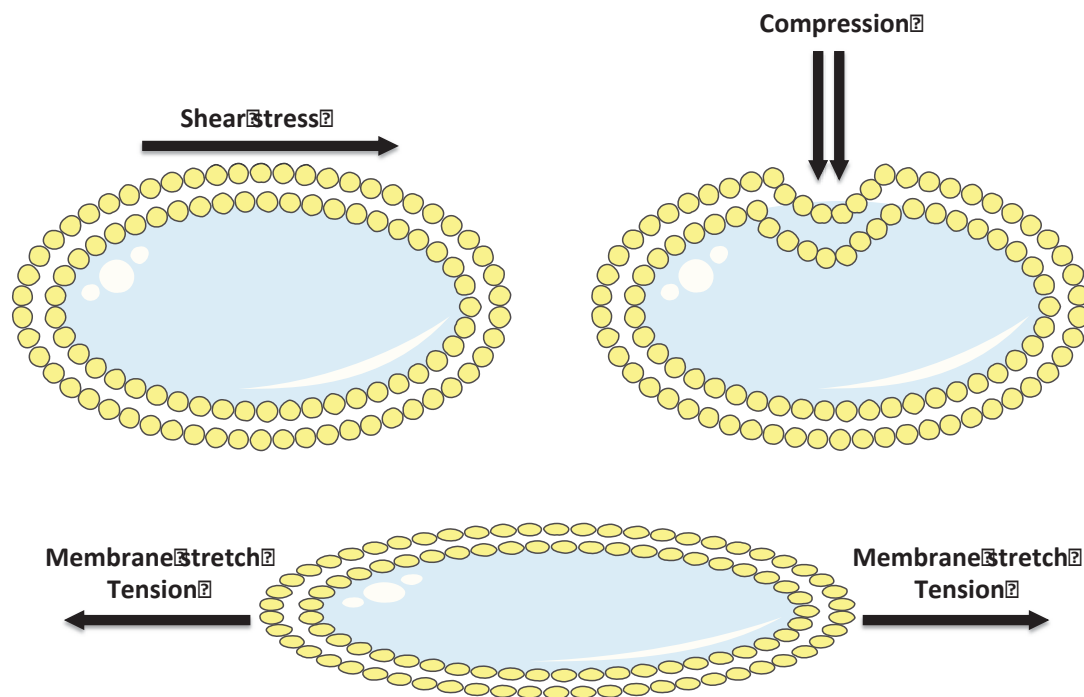


Figure 5: Different types of mechanical stress to which the cells are exposed: Different types of mechanotransducers are involved in the mechanotransduction mechanism. In order to sense the mechanical stimuli and transmit it into the cells to activate/inhibit different signalization pathways.

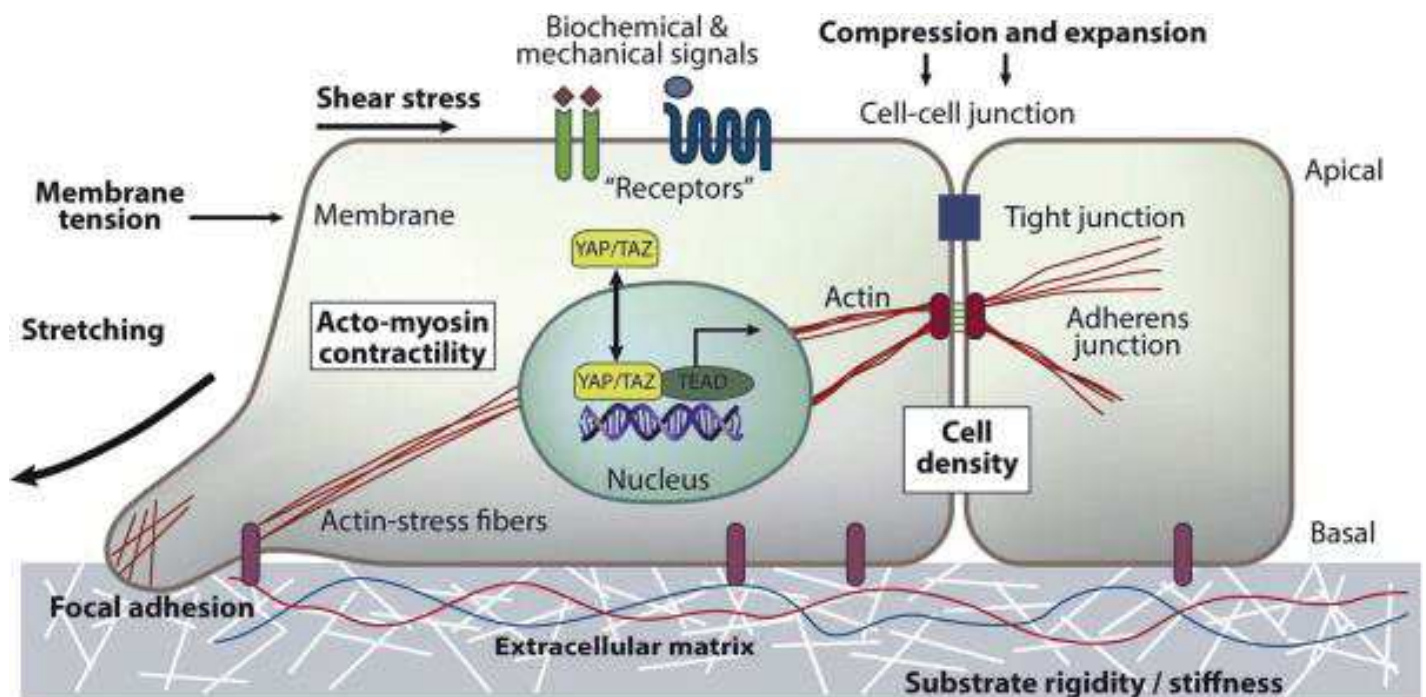


Figure 6: Low BC et al FEBS Lett 2014: **Schematic presentation of the different effectors of mechanotransduction:** Several biological components that acts as mechanotransducers and transmit the mechanical signal from the surrounding environment into the cell.

Cells are in close contact with their environment through cell adhesion molecules, tight junctions and cell surface receptors. Biochemical signals are transmitted into the cells through these protein complexes that sense mechanical stimuli generated in their environment, or through stretch activated/inhibited ion channels. This will lead to the activation/inhibition of signalization pathways in the cells (Schroeder and Halder 2012). Substrate rigidity, and extracellular matrix stiffness (through collagen secretion) provide mechanical signals to cells, resulting in adaptation of the cells to their environment. The deregulation of this process leads to pathologies, including cancer where it has been reported that tumor masses are more rigid than the surrounding tissue (Levental, Yu et al. 2009).

The crosslinking between myosin motor proteins or integrin and actin filaments, generate contractile forces and membrane tension which represent an important mechanotransduction complex that regulates cell shape (Liu, Calderwood et al. 2000, Luo, Mohan et al. 2012).

The nucleus has been proposed to be a mechanosensor since it interacts with actin cytoskeleton and its position changes during cellular processes such as cell division, migration and differentiation. Adding to that the nuclear deformation leads to chromatin changes (Guilluy, Osborne et al. 2014).

3.2_ Mechanosensation between physiological and pathological mechanisms:

Hair cells in the inner ear represent a good model to study a mechanotransduction process. These cells detect mechanical signals from their surrounding environment, they transduce it into the cells by chemical signals through the opening of non-selective ion channels, with high permeability for calcium (Ca^{2+}). Ca^{2+} binds to cadherin 23, controlling then the elasticity and the tip link integrity. Mutations in Ca^{2+} binding sites in cadherin 23 result in an unfolded protein leading to deafness (Vollrath, Kwan et al. 2007).

Mechanotransduction is crucial for normal embryogenesis. The stiffness of the embryo and other mechanical stresses such as membrane tension, change depending on the embryonic developmental stage. These mechanical forces, are necessary for the embryonic development to progress appropriately. Otherwise, changes in normal mechanical stimuli during embryogenesis, lead to embryonic malformation (Wozniak and Chen 2009).

Mechanotransduction is an important mechanism for organ development and maintenance such as muscles, bones, and the cardiovascular system. In skeletal muscle cells, forces are generated in the sarcomeres and they are transmitted to the extracellular matrix (ECM) through several protein complexes involving dystrophin and dystrophin associated proteins. When the forces between the cytoskeleton and ECM are disrupted, this will result in muscular dystrophy (Rahimov and Kunkel 2013).

The exposure to microgravity (zero gravity), or a long time rest in bed, leads to loss of the bone mass and muscle atrophy. Osteocytes detect mechanical loads by sensing fluid flow through the lacunar-canalicular network. In response to the mechanical loads, osteocytes change the expression of signaling molecules which regulate bone remodeling. These signalization pathways regulate osteoblast proliferation that affect bone mass formation. Gravity and compression generated by muscle contractions during locomotion, leads to deformations of the bones, resulting in pressure gradients that drive interstitial fluid through the lacunae-canalicular network. This process stimulates bone remodeling and optimizes physical performance of the bones through mechanotransduction signaling. (Burger and Klein-Nulend 1998, Klein-Nulend, Bacabac et al. 2005).

In cancer, increasing the extracellular pressure leads to an increase in intracellular Ca^{2+} , activating NF- κ B pathway, stimulating the proliferation of cancer cells. In large stiff tumors, there is an increase of intracellular pressure, and activation of NF- κ B pathway, which leads to stimulate further proliferation resulting in an increase in the tumor growth (Basson, Zeng et al. 2015).

3.3 Mechanosensation in the heart:

The heart is one of the organs that is submitted to mechanical forces since early stages of development. The heart is permanently exposed to mechanical stimuli. Cardiomyocytes can directly sense mechanical deformation of their environment including stretch, through several biological components that act as mechanosensors. Integrins, integrin-associated proteins, sarcomeric proteins (such as myosin) and cell surface receptors (such as G-protein-coupled receptors or angiotensin II type 1 receptors) can be activated by stretch, even in the absence of ligands. These mechanosensors, activate multiple signalization pathways including Ras/Rho, mitogen activated protein kinase (MAPK), phospholipase C activation, calcium/Calcineurin-mediated signaling, and micro RNAs. The activation of these signalization pathways induces hypertrophic gene expression, resulting in an increase in cardiomyocyte size (Barry, Davidson et al. 2008).

Mechanosensitive ion channels expressed on the cell surface, play an important role as mechanotransducers in the heart (Takahashi, Kakimoto et al. 2013).

3.3a Mechanosensitive ion channels in the heart:

Disturbing mechanical forces or mechanosensors in the heart, leads to severe consequences increasing the risk of mortality. A large number of mechanosensors which we have detailed before are present in the heart. We will focus on mechanosensitive ion channels which are divided into 2 major groups: mechanically modulated ion channels (MMC) and mechano gated ion channels (MGC).

3.3a.1_ Mechanically modulated ion channels (MMC):

MMC are channels that are normally activated by non-mechanical stimuli. They have a gain of function affected by mechanical stimulus, or they require coactivation by mechanical and non-mechanical stimuli. This group is divided into 2 subgroups, voltage gated channels and ligand gated channels (Peyronnet, Nerbonne et al. 2016).

MMC classed as voltage gated channels are potassium, calcium and sodium channels (Boycott, Barbier et al. 2013).

Among voltage gated channels, potassium channel Kv1.5, shows its ability to be modulated by stretch. Shear stretch stimulates integrin/focal adhesion kinase (FAK), a signaling pathway that increases Kv1.5 exocytosis, expression and density on the sarcolemma surface of atrial myocytes. Chronic hemodynamic overloaded atria, induces an up regulation of integrin/FAK signalization pathway, resulting in a decrease of Kv1.5 expression with a reduced response to shear stress. This process was observed in dilated atria and hypertrophied myocytes (Boycott, Barbier et al. 2013). The loss of Kv1.5 function leads to action potential prolongation in atrial myocytes. Kv1.5 is associated with atrial arrhythmias and fibrillation (Brendel and Peukert 2003, Olson, Alekseev et al. 2006).

Voltage dependent sodium channels are also reported to be modulated by their mechanical environment. Nav1.5 is the isoform expressed in the heart. Nav1.5 kinetics are accelerated by membrane stretch. Its voltage-dependent transition and the channel activation and inactivation are accelerated by membrane stretch. It has been shown that membrane stretch increases the number of Nav1.5 channels on the plasma membrane. However, the mechanism underling the

increase of channel number on the membrane upon stretch stimulation is poorly understood (Beyder, Rae et al. 2010). Nav1.5 promotes the propagation of action potentials in the heart and it contributes to the pacemaker activity in the sinoatrial node (Lei, Jones et al. 2004). The perturbation in voltage dependent motions or in mechanosensor domains of Nav1.5 will lead to diseases including heart arrhythmias. Nav1.7 and Nav1.8 are expressed in neurons. Nav1.8 is a major contributor to action potential in nociceptors while Nav1.7 plays a crucial role in subthreshold depolarization, facilitating the generation of action potentials (Momin and Wood 2008). Nav1.7 and Nav1.8 are mechanosensitive channels. The action potential generated after mechanical stimulation, doesn't propagate in mice deficient for Nav1.7 and Nav1.8 channels. (Raouf, Rugiero et al. 2012).

L type calcium channels are mechanical modulated ion channels. L type calcium channels are expressed in a wide range of tissues, such as smooth muscle surrounding blood vessels, and the bladder. Calcium MMC are also expressed in the cardiomyocytes. In smooth muscle, L type calcium channel plays a role in muscle cell differentiation and growth. Mechanical stretch of mouse portal veins, promotes contractile differentiation by activating the Rho-pathway. This mechanism depends on calcium via L-type calcium channels influx (Turczynska, Hellstrand et al. 2013).

L type calcium channels in the heart play an important role after load induced hypertrophic growth. In fact Polycystin-1 (PC1) is a G coupled protein receptor that plays the role of a mechanosensor. PC1 is implicated in activating mTOR calcineurin-NFAT pathways, which play a crucial role in cardiac hypertrophy (Puri et al 2004). During hypertrophy, there is an increase in intracellular calcium. This Ca^{2+} increase is due to the stabilization of L type calcium channel

by α C fragment of PC1 (Pedrozo, Criollo et al. 2015). L type calcium channels are responsible for excitation-contraction coupling in the heart, due to the mechanism of calcium induce calcium release. The activation of L type calcium channels, leads to an increase in intracellular Ca^{2+} which triggers Ca^{2+} release from the sarcoplasmic reticulum due to the activation of the ryanodine receptor 2 (RYR2). L type calcium channels also participate to the plateau phase during an action potential in the heart (Yamakage and Namiki 2002). The plateau phase is the phase of the action potential where the membrane potential remains almost constant. This is due to the balance of ion moving into and out of the cell. During this phase, delayed rectifier potassium channels and L-type calcium channels are activated. The activation of L type calcium channels are responsible of heart contraction as describe previously. The disruption in L type calcium channels lead to severe consequences on the heart, for that reason they represent potential therapeutic targeted to treat arrhythmias (Priest and McDermott 2015).

3.3a.2 Mechanically gated ion channels (MGC):

MGC are channels that are normally activated by a different number of stimuli. They are directly activated by mechanical stimuli. These channels are also called stretch activated ion channels (SAC).

SAC are reported to be present in different cell types including cardiomyocytes. They are subdivided into 2 major groups, depending on their ion selectivity: cation non selective SAC (SAC_{NS}) and potassium SAC (SAC_{K}) (Craelius, Chen et al. 1988, Kim 1992, Arnadottir and Chalfie 2010).

3.3a.2.1 _ Cation non selective ion channels (SAC_{NS}):

The current of SAC_{NS} has the typical linear current–voltage relationship of weakly selective ion channels with a reversal potential close to 0 mV. This reversal potential being positive compared to the resting potential of working cardiomyocytes, so activation of SAC_{NS} will depolarize resting cardiomyocytes (Kohl et al 2006). Candidates that belong to SAC_{NS} are the transient receptor potential channel (TRP) and piezo channels. Most of the currents have a pronounced sensitivity blocked by gadolinium ions (Gd³⁺) (Zeng, Bett et al. 2000). SAC_{NS} are inhibited by ruthenium red (RR) and a peptide isolated by from Chilean tarantula venom: GsMTx-4 (Bowman, Gottlieb et al. 2007). RR functions as a pore blocker for TRP channels while its mode of action on PIEZO channel is different. RR interacts with the C-terminal tail of PIEZO channel blocking by that the channel conduction (Nilius and Flockerzi 2014, Geng, Zhao et al. 2017). The mechanism of action proposed of GsMTx4 involves its insertion into the outer membrane leaflet in the proximity of the channels, relieving lipid stress sensed by the channels and favoring the closed state of SAC_{NS} (Peyronnet, Nerbonne et al. 2016).

3.3a.2.2_ Transient receptor potential channel (TRP):

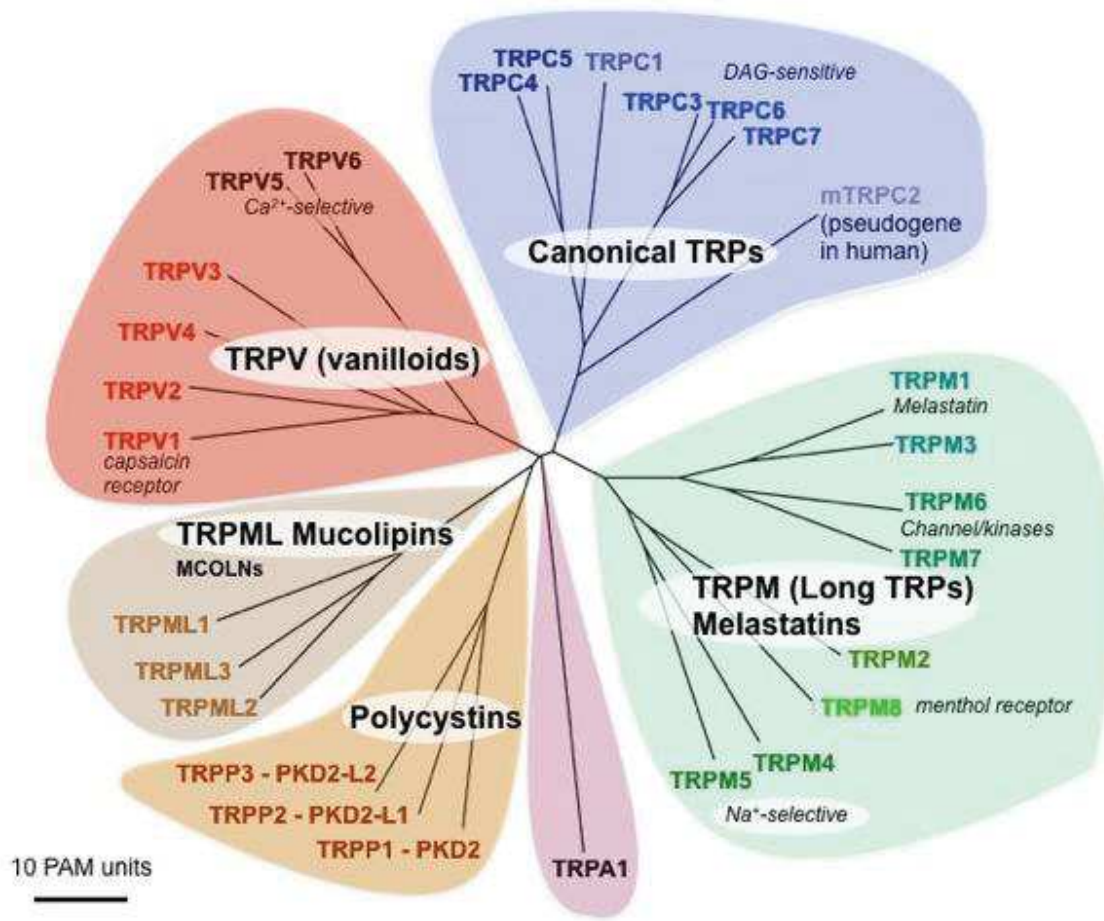


Figure 7: Clapham DE, Nature, 2003: **Mammalian TRP family tree:** The TRP channels are classified according to their sequence homology.

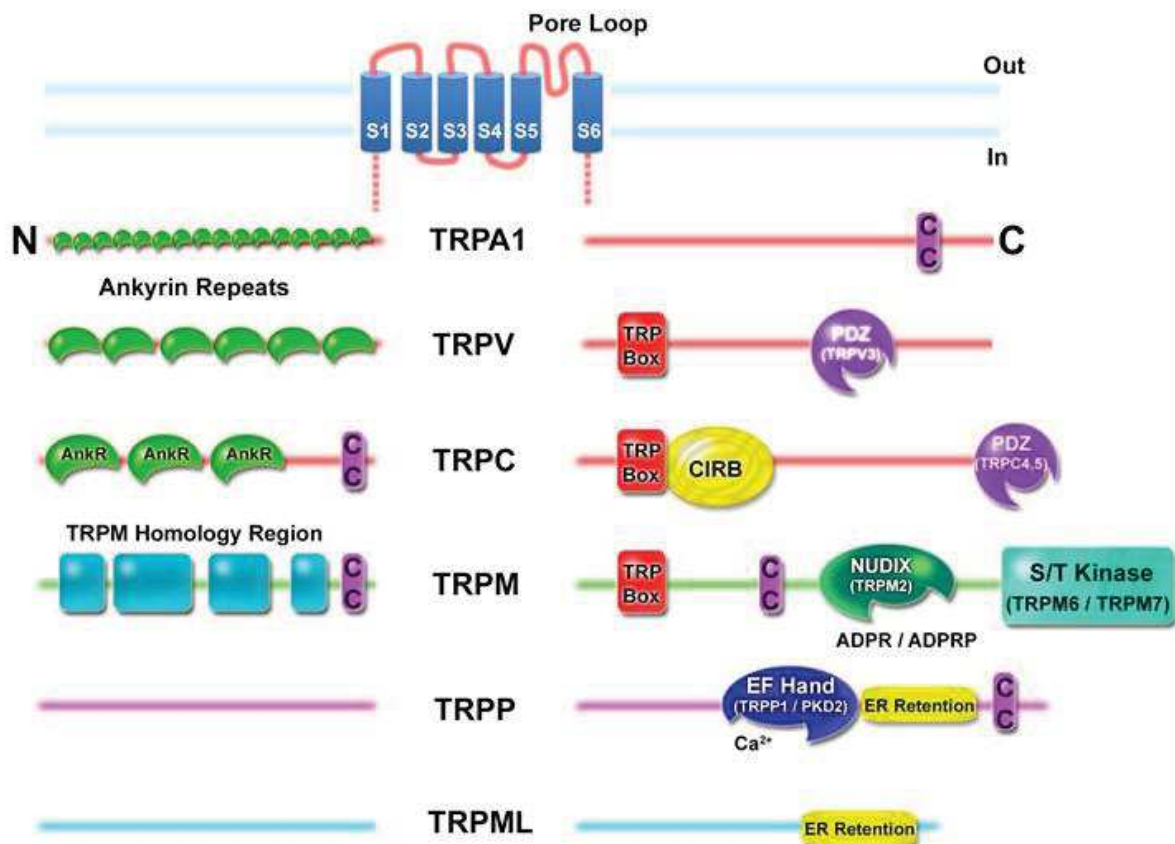


Figure 8: Clapham DE, Nature, 2003: **The TRP structures:** The TRP channel family is divided into 6 subfamilies depending on their sequence homology.

TRP channel classification is based on the sequence homology of TRP channels. They are divided into 6 subfamilies: canonical TRPs (TRPCs), vanilloid receptor TRPs (TRPVs), melastatin TRPs (TRPMs), mucolipins TRPs (TRPMLs), polycystins TRPs (TRPPs), and ankyrin transmembrane protein 1 (TRPA1) (Fig7).

TRP channel subunit structure is formed from 6 transmembrane domains and one pore loop. Most of TRP channels are cationic non selective ion channels. TRPM4 and TRPM5 are selective for sodium (Na⁺), TRPV5 and TRPV6 are selective to calcium (Ca²⁺). The TRP domain is located at the C terminus region. It is conserved in most of TRP channels except TRPA1,

TRPP and TRPML. The stretch sensitive region is localized in the TRP Box at the C terminus region and it is highly conserved among TRPC channels. Ankyrin repeats, which are localized at the N terminus region, play the role of scaffold proteins, and regulate the dimerization and the assembly of the TRP subunits. TRP channels can regulate different signalization pathways and they can be regulated by different proteins due to the protein interaction domains that they have, such as coiled/coil domains, calmodulin Ca^{2+} binding domain, C terminal PDZ binding domains as well as serine/threonine kinase domains (Clapham 2003) (Fig8).

TRP channels are expressed in a wide range of tissues, they are responsible for a variety of cellular functions. One of the characteristics of the TRP family is their polymodal regulation. TRP channels are activated by different stimuli including chemical stimuli, temperature, and mechanical interventions, ranging from local patch deformation to membrane stretch and shear strain (Inoue et al 2009). They are implicated in a wide range of physiological and pathological functions, especially in a wide range of cardiovascular diseases. TRPM7 is important in cardiac fibrosis by controlling $\text{TGF}\beta 1$ mediated fibrogenesis. TRPM4 participates in some features to cardiac arrhythmias. TRPM4 participates in the mechanism of membrane potential depolarization in the cardiomyocytes, which triggers spontaneous beating. TRPM4 could also be implicated in the prolongation of action potential duration reported to be present in the hypertrophied heart, triggering arrhythmias. TRPV1 regulates normal cardiac function, it also regulates the development of cardiac adaptation to ischemic stress. Activation of TRPV1 under ischemic conditions protects mouse hearts from injury after ischemia while its inhibition impairs preconditioning protection against myocardial injury after ischemia (Wang and Wang 2005).

The TRPC family play a key role in hypertrophy and heart failure (Yue, Zhang et al. 2013, Demion, Thireau et al. 2014).

There are 7 isoforms (TRPC1 to 7) in the TRPC family that have been divided into 2 general subfamilies based on structural and functional similarities: TRPC1/4/5 and TRPC3/6/7. However, TRPC2 is not expressed in humans. TRPC channels transduce mechanical stress, which is important in the cardiovascular system. This mechanical stress is due to the deformation of the vasculature and changes in cardiac contractility and hemodynamic stretch.

It has been shown, an upregulation of TRPC channel expression and activity in pathological hypertrophy and heart failure. An upregulation of TRPC3 has been reported due to pressure overload in the heart of mice and rats. In addition an upregulated of TRPC6 in cardiac hypertrophy and heart failure has also been reported. TRPC5 was shown also to be increased in failing human heart samples. TRPC1 is upregulated in pressure overload–induced cardiac hypertrophy in mice (Bush, Hood et al. 2006, Kuwahara, Wang et al. 2006, Seth, Zhang et al. 2009).

The overexpression of TRPC family members, leads to the activation of calcium/calmodulin-dependent serine/threonine protein phosphatase, which is important for pathological hypertrophy and cardiac remodeling. This leads to the activation of the nuclear factor of activated T cells (NFAT) transcription factors which are involved in hypertrophic cardiac remodeling (Kuwahara, Wang et al. 2006, Ohba, Watanabe et al. 2007).

There is an interaction between isoforms of the TRPC family. DN TRPC3 and DN TRPC6 block currents from TRPC3/6/7 subfamily in the heart. DN TRPC4 blocks the current from

TRPC1/4/5 subfamily in the heart. Transgenic mice expressing either DN TRPC3, TRPC6 or TRPC4 show an attenuated cardiac hypertrophic response following pressure overload stimulation compared to control mice. This suggests that TRPC subfamilies function in coordinated complexes in the heart. (Wu, Eder et al. 2010).

3.3a.2.3_ PIEZO channels:

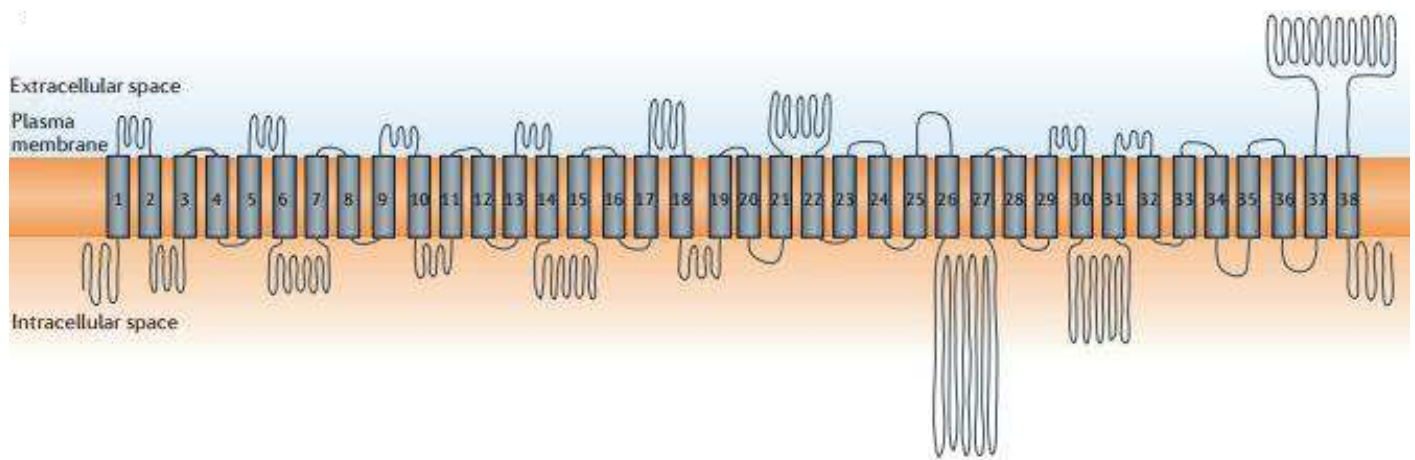


Figure 9: Murthy SE et al, Nat Rev Mol Cell Biol. 2017: the structure of PIEZO subunit

PIEZO proteins are large transmembrane proteins, they have between 16 and 40 transmembrane domains (Delmas and Coste 2013, Murthy, Dubin et al. 2017) (Fig 9).

PIEZO 1 is expressed in the lungs, the skin, the bladder and the heart. It is implicated in many physiological and pathophysiological processes. PIEZO 1 is expressed in embryonic endothelial cells where it can sense fluid shear stress, allowing a normal organization and alignment of these cells, promoting the formation of normal vasculature. The loss of PIEZO 1 profoundly alters vasculature architecture (Li, Hou et al. 2014, Ranade, Qiu et al. 2014). PIEZO 1 plays a key role during the arterial myogenic response, and it participates to arterial

remodeling in response to hypertension, by regulating arterial diameter and wall thickness. Its depletion in mice smooth muscle is associated with a deficit in arterial remodeling upon hypertension (Retailleau, Duprat et al. 2015). PIEZO 1 regulates cell volume in red blood cells. Mutations causing gain of function in PIEZO 1 is associated with xerocytosis, resulting in anemia in mice and humans. These mutations are associated with delayed inactivation of the PIEZO 1 mutant compared to WT PIEZO 1, leading to an increase in ion permeability which leads to the dehydration of erythrocytes that express mutant PIEZO 1. Knock down of PIEZO 1 in zebrafish is associated with anemia and an increase in erythrocyte volume. This suggests that PIEZO 1 is responsible for regulating cellular homeostasis and cell volume (Bae, Gnanasambandam et al. 2013, Ranade, Qiu et al. 2014, Faucherre, Kissa et al. 2016). In the heart, PIEZO 1 was reported to be upregulated in rat ventricular myocytes after heart failure caused by myocardial infarction. Mechanical stretch caused angiotensin II release from cardiac myocytes. The released angiotensin II will bind to the angiotensin receptor type I, which was proposed to increase the expression of Pezo1 during heart failure. Consequently, PIEZO 1 expression decreases following the inhibition of angiotensin receptor, results in an improvement of heart function after heart failure (Liang, Huang et al. 2017). PIEZO 1 was reported to be important for embryonic development. The homozygous expression of a truncated PIEZO 1 protein in embryonic endothelial cells is lethal; due to a defect of cardiovascular system development. Embryonic lethality was accompanied with poor heart function, and failure to develop proper vasculature (Ranade, Qiu et al. 2014). PIEZO 2 is expressed in lungs, primary sensory neurons, neurons in the dorsal root ganglion, nociceptive neurons, spinal cord, nerve fibers in the urinary bladder, colon, dura mater and skin (Coste, Mathur et al. 2010). PIEZO 2 is expressed in Merkel cells that constitute a component of the gentle touch complex in the skin

(Woo, Ranade et al. 2014). In zf, PIEZO 2 regulates light touch response, WT zf embryos respond normally to light touch stimuli. Although knocking down PIEZO 2 in zf embryos through PIEZO2 antisense oligomer morpholino injections results in an impaired response of these embryos, to light touch stimuli (Faucherre, Nargeot et al. 2013). PIEZO 2 plays an important role in the lungs. Patients with multiple distal contracture, lung disorder and pulmonary hypertension, have mutations in PIEZO 2 that cause a faster recovery from inactivation than WT PIEZO 2. (Gu and Gu 2014).

PIEZO 1 and PIEZO 2 are mechanosensitive cationic non selective ion channels that can be inhibited by unspecific inhibitors such as RR and Gd^{3+} . Spider toxin GsMTx4 inhibits PIEZO 1. The effect of GsMTx4 on PIEZO2 is unclear, it has been shown that this spider toxin fails to inhibit mechanosensitive current in DRG neurons generated mainly by PIEZO2 while its D enantiomer (D-GsMTx4) has the ability to inhibit PIEZO 2 currents in HEK cells transfected with PIEZO 2 (Drew, Rugiero et al. 2007, Alcaïno, Knutson et al. 2017)

3.3a.3_ Stretch-Activated Channels, K^+ -Selective (SAC_K):

SAC_K are potassium channels, known to have a large single channel conductance. SAC_K currents are recorded in atrial and ventricular myocytes from adult mammalian hearts (Kim 1992, Tan, Liu et al. 2002, Xian Tao, Dyachenko et al. 2006). Their reversal potential is around -80mV, close to the resting membrane potential of cardiac cells. This suggests that SAC_K activation, leads to membrane repolarization or hyperpolarization (Kohl, Bollensdorff et al. 2006). The major effectors of SAC_K are known to belong to the K_{2p} family.

TRAAK related arachidonic acid stimulated potassium channel (TRAAK) is a stretch activated potassium (K^+) channel that belongs to the K_{2p} family. TRAAK is expressed mainly in the central nervous system. It plays an important role in axon pathfinding and guidance, neurite elongation and cellular locomotion, by regulating intracellular calcium, and actin/myosin contraction. It also plays a role in touch and pain perception, and it was proposed to be a target for analgesia (Maingret, Fosset et al. 1999, Marion, Song et al. 2014). The deletion of TRAAK in the brain plays an important role against ischemia. After transient middle cerebral artery occlusion, mice that lack TRAAK (double negative TRAAK mice) show a small infarcted zone in the brain in response to ischemia compared to double positive TRAAK mice (Laigle, Confort-Gouny et al. 2012). It has been shown that TRAAK is expressed in the heart but its specific function in this organ is not yet known (Ozaita and Vega-Saenz de Miera 2002, Liu and Saint 2004).

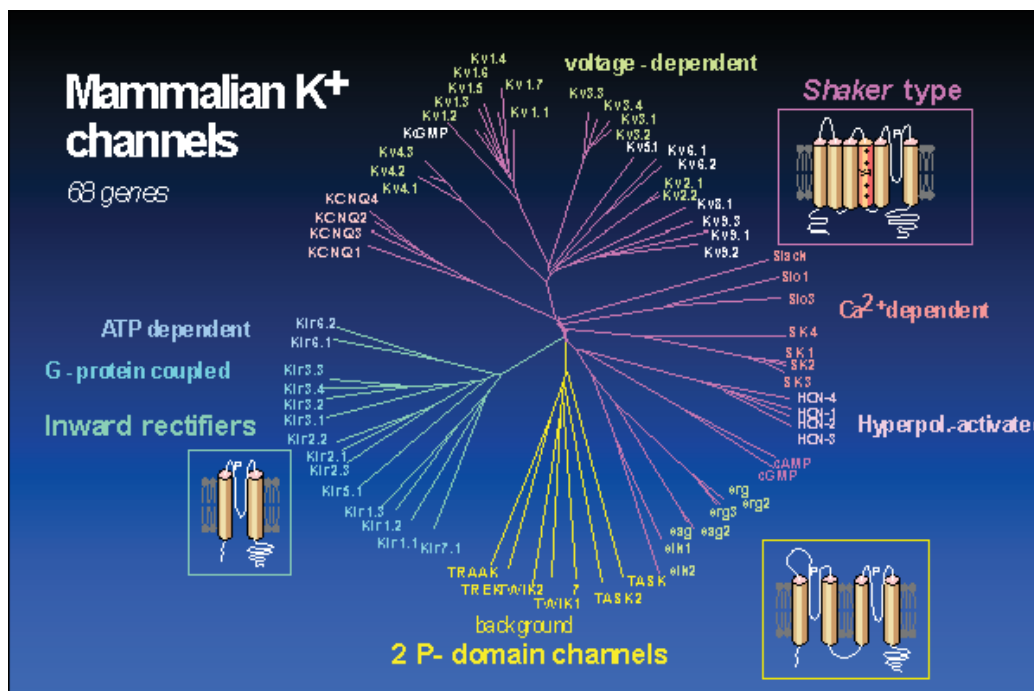
TWIK-Related K^+ Channel 2 (TREK-2) is a stretch activated potassium channel that belongs to the K_{2p} family. TREK-2 is expressed in the central nervous system, it stabilizes the resting membrane potential. It is implicated in pain perception and thermosensation (Kang, Choe et al. 2005, Kang, Choe et al. 2007). (Dong, Pike et al. 2015). It has been shown that TREK-2 is expressed in the heart but its specific function in this organ is not yet known (Ozaita and Vega-Saenz de Miera 2002, Liu and Saint 2004).

3.4_ Summary III:

Mechanotransduction is an important cellular mechanism in which mechanical stimuli are sensed by different cellular components, which transform mechanical signals into biochemical signals and transmit it into the cell. Mechanosensation is critical for tissue homeostasis, tissue

architecture, regeneration and development. Therefore, disruption of the mechanotransduction mechanisms can lead to pathologies such as cancer, muscular atrophy, deafness and many more. In the heart, mechanical transduction plays a key role not only in cardiac physiology, but also in pathophysiology. Different types of mechanical stimuli are present in the heart such as membrane tension related to pressure and shear stress related to blood flow. These stimuli can be sensed by mechanosensors present in the heart, such as mechanosensitive ion channels. These channels are divided in two major groups: stretch activated cationic non selective ion channels (SAC_{NS}) such as the TRPs and Piezo channels, and stretch activated potassium ion channels (SAC_K) such as K2p channels. Disturbance of SAC_{NS} and SAC_K expression and permeability can have severe consequences on heart function thus leading to pathologies.

4_ Potassium channels:



Potassium channels are highly conserved through evolution. They are expressed on the cell membrane, where they participate in a wide range of physiological and pathological mechanisms. These channels regulate membrane potential, cell growth and cell volume. They also regulate secretion, cell proliferation and migration. There are 3 major families of K⁺ channels classified in function of the structure of their α subunit: inward rectifier (Kir), voltage gated voltage-gated (Kv), and two-pore domain (K2P) channels. They differ by the number of transmembrane domains and pore P domains. The formation of functional K⁺ channels, requires the assembly of P domains (loops) in a set of 4 (O'Connell, Morton et al. 2002).

Inward rectifier family (K_{ir}): their α subunit is formed by 2 transmembrane domains and 1 P loop, they can form homo or heterodimers. These channels are regulated by G coupled protein receptors, they are ATP-sensitive and they are tightly linked to cellular metabolism (Hibino, Inanobe et al. 2010). K_{ir} channels are regulated by acetylcholine, intracellular magnesium, intracellular calcium and spermine. In the heart, under normal conditions, K_{ir} channels play a role in establishing resting membrane potentials in cardiac cells. Disruption of K_{ir} function may lead to arrhythmias.(Lopatin and Nichols 2001, Ishihara, Sarai et al. 2009).

Voltage gated potassium channels family (Kv): Shaker channels are voltage gated potassium channels, mutations in these channels that are localized in drosophila antennal nerve and mushroom bodies lead to behavioral changes in these animals. Each subunit is formed by 6 transmembrane domains and 1 P loop. They can form homo or heterodimers. Their voltage sensor is localized in the fourth transmembrane domain, it is made up of positively charged amino acids (arginine and lysine), (Dolly and Parcej 1996) which are sensitive to membrane potential changes. The resting membrane potential is between -80 mV and -90 mV.

Voltage gated potassium channels are typically closed, and they open when the membrane depolarizes. During an action potential, they play an important role in repolarization and return depolarized cells to a resting state (Kang, Huguenard et al. 2000). These channels are important for normal heart electrophysiological function and any disturbance in the conductance of these channels may lead to severe consequences on the heart function. Mutations in voltage gated channels like HERG channel that cause a loss of function of the channel, lead to long QT syndrome, characterized by an elongated QT interval and arrhythmias characterized by an irregular heart beat (January, Gong et al. 2000). However, mutations causing gain of function in voltage gated channels such as HERG and KCNQ1 lead to short QT-interval syndrome characterized by a short QT interval (Bellocq, van Ginneken et al. 2004). The gain of function in potassium channels, leads to an increase in the potassium current during the phase 2 of a cardiac action potential. This causes a shortening of the plateau phase (phase2) of an action potential, leading to a shortening of the overall action potential, causing a shortening of the QT interval. The loss of function of potassium channels leads to a reverse effect causing an elongation of the QT interval.

K_{2P} family: also known as the 2 P domain family. Each subunit is made out of 4 transmembrane domains and 2 P loops. This family is divided into 6 subgroups depending on their sequence homology as well as their properties: mechanogated (TREK-1, TREK-2 and TRAAK), alkaline activated (TALK2, TALK1 and TASK2), calcium activated (TRESK1), weak inward rectifiers (TWIK2, KCNK7), acid inhibited (TASK3, TASK1 and TASK5) and halothane inhibited (THIK1 and THIK2) (Honore 2007) (Fig 11).

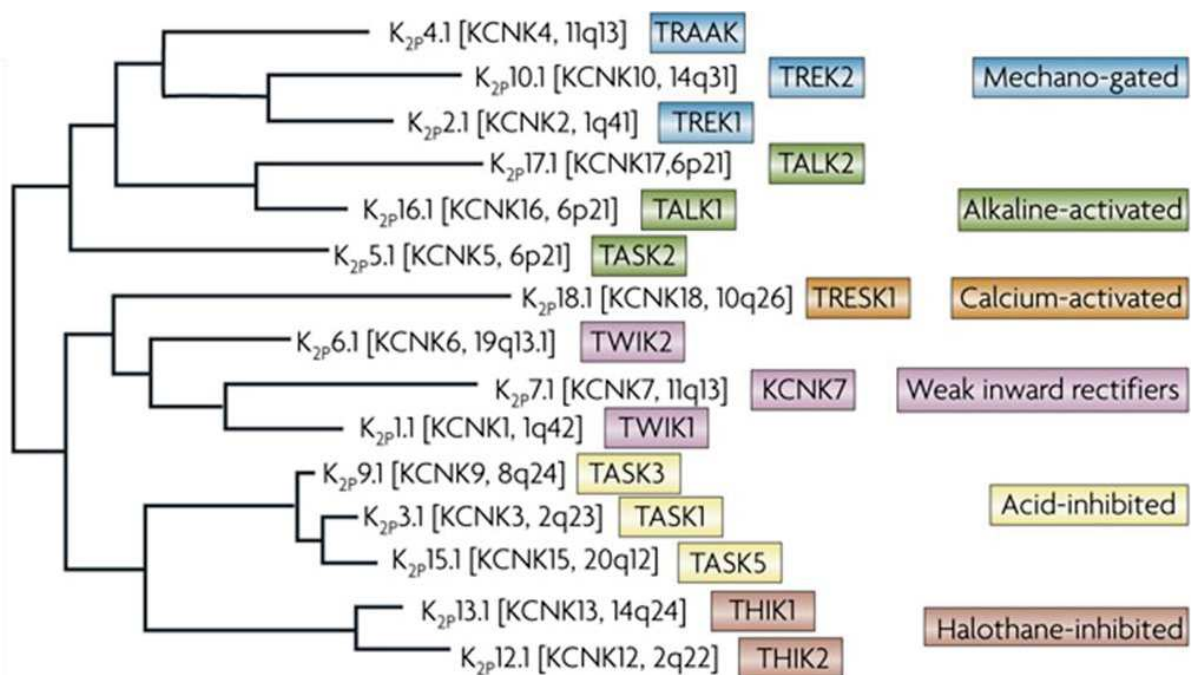


Figure 11: Honore E Nat Rev Neurosci. 2007: **Phylogenetic tree of K_{2p} channels.**

5_ TREK-1 channel:

Among the channels that belong to the K_{2p} family TREK-1 is known to be a mechano-gated potassium channel.

5.1_ TREK1 structure:

TREK-1 was cloned for the first time by Fink et al in 1996 (Fink et al 1996). It belongs to the K_{2p} family (Honore 2007), it is an outward rectifier potassium channel. Functional TREK-1 exists as dimers (homodimers or heterodimers). Each subunit forming a TREK-1 homodimer is made out of 2 intracellular domains (N and C terminus domains), 4 transmembrane domains (M1_M4), and 2 pore domains (P1_P2) (Fig7). In each pore there is a GFG motif which belongs

to the selectivity filter and it allows the dimerization between the loops P of other subunits in order to form homo/heterodimers (Honore 2007) (Fig 12).

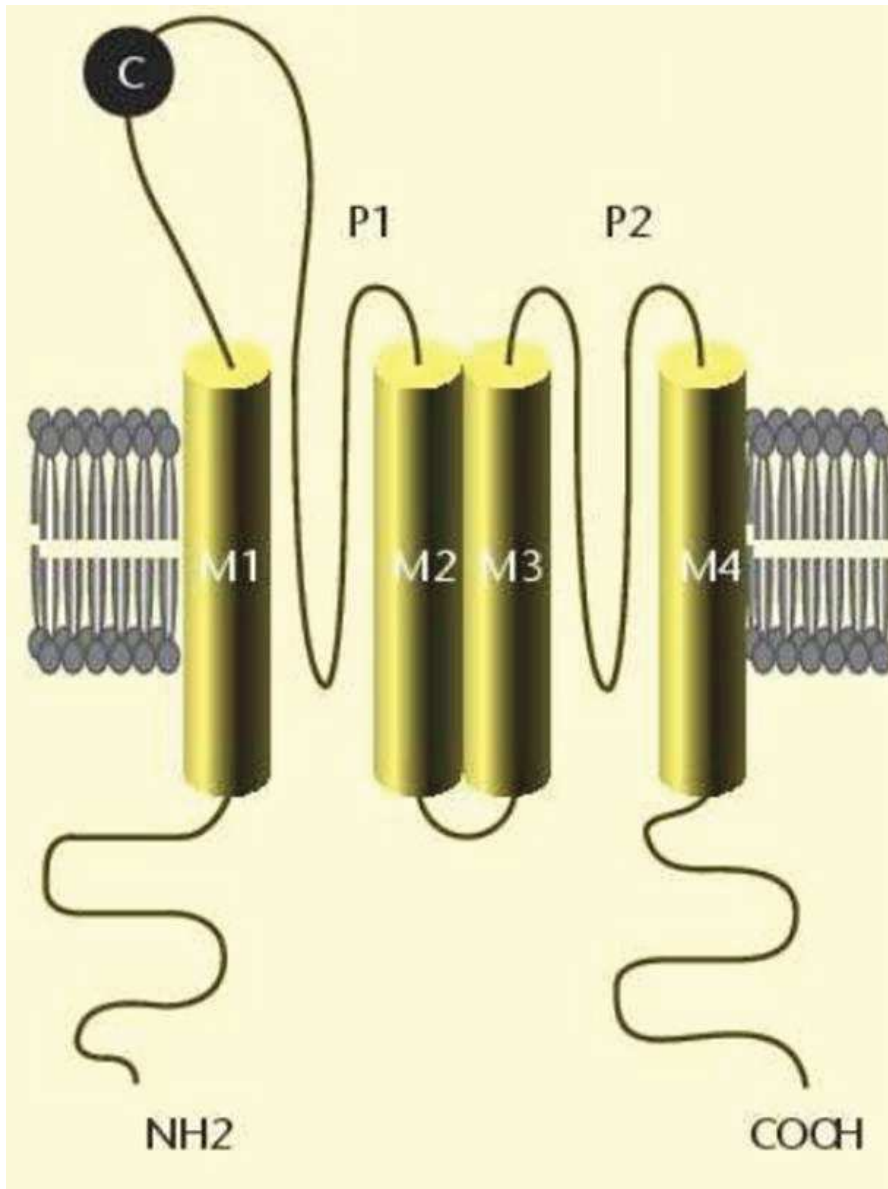


Figure 12: Honore E , Nat Rev Neurosci 2007: **A schematic presentation of TREK-1 subunit structure:** Each subunit is formed by 4 transmembrane domain and 2 loop P

5.2_ TREK-1 homodimers:

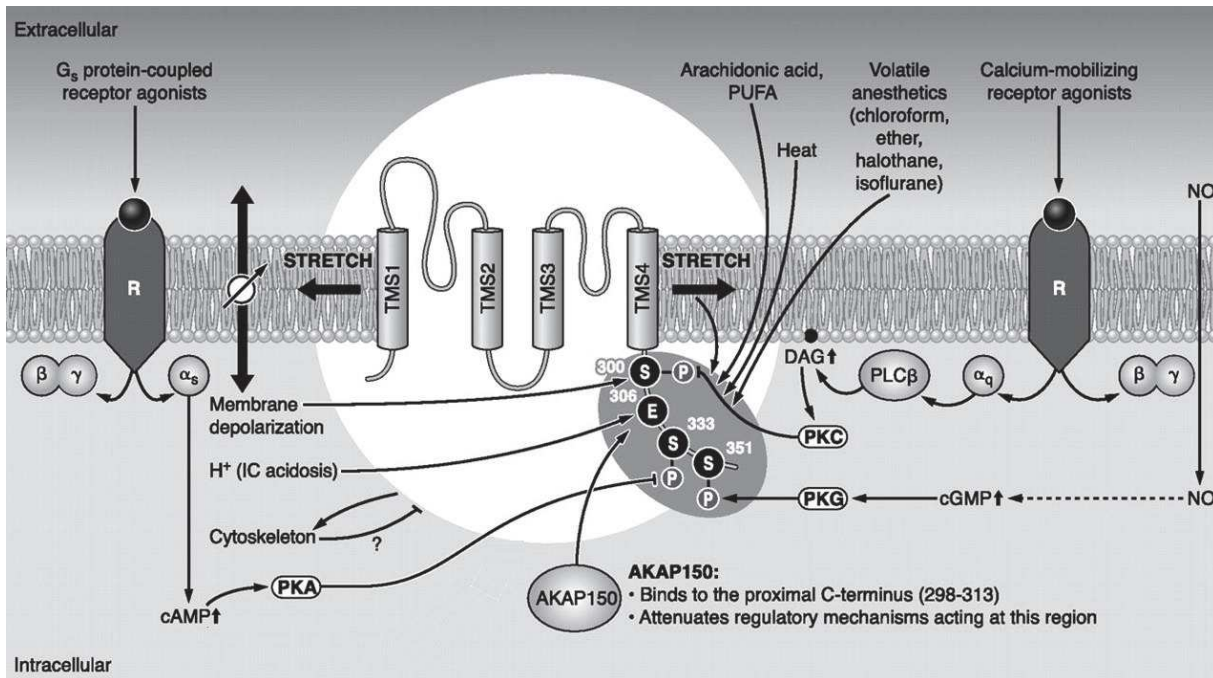


Figure 9: *Enyedi P and Czirják G. Physiol Rev. 2010.* A scheme representing the regulation sites of the mammalian TREK-1.

```

zTREK-1b -----MRWKTVL SVFLL VVL YL IL
hTREK-1 MAAPDLLDPKSAAQNSKPRL SFSTKPTVL ASRVE SDTTINVMKWKTVSTIFL VVVL YL II
mTREK-1 MAAPDLLDPKSAAQNSKPRL SFSSKPTVL ASRVE SDSAINVMKWKTVSTIFL VVVL YL II
zTREK-1a MAAPDLLDPKSATHNTPRL SFSSKPIVYNSGDCE SITTVMKWKTVL AIFLL VVL YL II
                                         *:**** :*:*****:

zTREK-1b GATVFKALEQPYETLQKL NIL MEKLEFLEQHPCVNSSDLENL VKQVVSAL RAGVNP SGNS
hTREK-1 GATVFKALEQPHEISQRTTIVIQKQTFISQHSVCVNSTEL DEL IQQIVAAINAGIIP LGNT
mTREK-1 GATVFKALEQPQEISQRTTIVIQKQTFIAQHACVNSTEL DEL IQQIVAAINAGIIP LGNS
zTREK-1a GATVFKALEQPEEGLQKYRIIQEKIDFL SMHTCVNTSELEDL VKQVVL AIRAGVNP SGHP
***** **** * *: *: :* *: * ****:::*****:*.**.* *:

zTREK-1b SNQSSLWDL SNSFFF SGTVITITIGFGNISPHTEVGRIF CIIYALLGIPLFGFLL AGVGDQ
hTREK-1 SNQISHWDLGSSFFFAGTVITITIGFGNISPRTEGGKIF CIIYALLGIPLFGFLL AGVGDQ
mTREK-1 SNQVSHWDLGSSFFFAGTVITITIGFGNISPRTEGGKIF CIIYALLGIPLFGFLL AGVGDQ
zTREK-1a SNESSMWDL SSSFFFAGTVITITIGFGNVSPHTEGGRIF CIIYALLGIPLFGFLL AGVGDQ
**:* * ***,.****:*****:***:** *:*:*****:*****:

zTREK-1b LGTIFGKAIKVEGMIDKWNVSQTKIRVISTLLF IL FGCLL FVTL PAVIFKHIEGWSALE
hTREK-1 LGTIFGKGIKVEDTF IKWNVSQTKIRIISTIIIF IL FGCVL FVAL PAIIFKHIEGWSALD
mTREK-1 LGTIFGKGIKVEDTF IKWNVSQTKIRIISTIIIF IL FGCVL FVAL PAVIFKHIEGWSALD
zTREK-1a LGTIFGKGIKVEKMFVKWNVSQTKIRVTSTVLF IL FGCLL FVAL PAL IFQHIEGWSALE
*****.***** : *****: **:*:*****:***:***:***:*****:

zTREK-1b SIYFVVITL TTIGFGDF VAGE AERRHHEE SSGGSQLEYL DYYKPL VWFVIL VGL AYF AAV
hTREK-1 AIYFVVITL TTIGFGDYVAG -----GSDIEYL DFYKPVVWFVIL VGL AYF AAV
mTREK-1 AIYFVVITL TTIGFGDYVAG -----GSDIEYL DFYKPVVWFVIL VGL AYF AAV
zTREK-1a SIYFVVITL TTIGFGDF VAG -----GSEIEYL DYYKPIVWFVIL VGL AYF AAV
:*****:*****:*** **:*:****:***:*****:

          293 298 300 306 311          333 335
zTREK-1b L SMIGDWRVVISKKTKEE VGEFRAHAAEWTANVSAEFKE TRRRLSVDIYDKFQRATSVKR
hTREK-1 L SMIGDWRVVISKKTKEE VGEFRAHAAEWTANVTAEFKE TRRRLSVEIYDKFQRATSIKR
mTREK-1 L SMIGDWRVVISKKTKEE VGEFRAHAAEWTANVTAEFKE TRRRLSVEIYDKFQRATSVKR
zTREK-1a L SMIGDWRVVISKKTKEE VGEFRAHAAEWTANVSAEFKE TRRRLSVEIYDKFQRAAYIKR
*****:*****:*****:*****:*****:*****:*****:*****:

          351          360
zTREK-1b KLSAEINL SPPINQOMTPGKRARSVNLGDRE A-YPYTL ARNGSL FLNSL IPDYADHRDM
hTREK-1 KLSAELAGN--HNC EL TPCRRTL SVNHL T-SERDVL PPLLKTESIYL NGL TPHCAGE -EI
mTREK-1 KLSAELAGN--HNC EL TPCRRTL SVNHL T-SEREVL PPLLKAEIYL NGL TPHCAGE -DI
zTREK-1a KLSSELGQN--PGCDMMPCRRTL SVNF TDELEKEGL PTL TKNGSLYL NGL TPDCPCSEI
*****:*. . *::* *:*** * * :*:***.* * . :

zTREK-1b TRIQTK-
hTREK-1 AVIENIK
mTREK-1 AVIENMK
zTREK-1a SIIHLK
: *:

```

Figure10: Sequence alignment of zebrafish TREK-1a (zTREK-1a) ([ENS DARG00000055123](#)) zebrafish TREK-1b (zTREK-1b) ([ENS DARG0000007151](#)), human TREK-1 (hTREK-1) (NP_055032.1) and mouse TREK-1 (mTREK-1) (NP_001153322.1).

TREK-1 is a leak potassium channel, it is active at all membrane potentials, it lacks of gating control, and it has an outward rectifying activity. One of the characteristics of TREK-1 channel is its polymodal regulation that allows it to respond to a wide range of stimuli (Lesage and Lazdunski 2000, Honore 2007) (Fig9).

2 TREK-1 isoforms are expressed in zebrafish: zebrafish TREK-1a (zTREK-1a) and zebrafish TREK-1b (zTREK-1b). Sequence alignment of zTREK-1a and zTREK-1b with human TREK-1 (hTREK-1) and mouse TREK-1 (mTREK-1) shows highly conserved regions among species. TREK-1 C terminal tail between G293 and Q360 where most of the regulation mechanisms take place is highly conserved between species (Fig 10). This suggests that zTREK-1a and zTREK-1b may have similar biophysical and pharmacological properties with human and mouse TREK-1.

Mammalian TREK-1 is activated by membrane stretch (negative and positive pressure) and cell swelling after exposure to a hypotonic solution, reflecting that cell volume is regulated by TREK-1. However, TREK-1 is more reactive to stretch stimuli in inside out (IO) configuration rather than in cell attached (CA) configuration. IO configuration consists of excising a membrane fragment from the rest of the cell, leading to a loss of interaction between the membrane proteins and the cytoskeleton. This suggests that TREK-1 is negatively regulated by the cytoskeleton (Patel, Honore et al. 1998, Moha ou Maati, Peyronnet et al. 2011, Fukasaku, Kimura et al. 2016). TREK-1 C terminal tail is implicated in the response to physical stimuli. Mutations in this region or its deletion lead to a loss of TREK-1 sensitivity towards membrane stretch (Honore, Maingret et al. 2002) (Fig9).

TREK-1 is activated by lysophospholipids (LP) including lysophosphatidylcholine (LPC). This activation is dependent on the size of the polar head and length of the acyl chain of LPs. LPs with large polar heads and long hydrophobic acyl chains have the ability to activate TREK-1. This activity is reversed in the presence of active protein kinase A (PKA) and protein kinase C (PKC). The activation of TREK-1 by LPs occurs in whole cell (WC) configuration, but not in inside out (IO) configuration, reflecting that the cell integrity is essential for LPs activity, (Maingret, Patel et al. 2000).

TREK-1 is activated by polyunsaturated fatty acids (PUFAs). This activation depends on PUFAs carbonyl chain's length. PUFAs with long carbonyl chains such as arachidonic acid (AA) and docosahexaenoic acid (DHA) are more efficient than the others. This activation occurs in cell attached (CA) and IO configuration. This suggests that the effect of PUFAs on TREK-1 may be due to a direct interaction between PUFAs and TREK-1, or through the integration of PUFAs into the lipid bilayer. The C terminus tail of TREK-1 is essential for activation by PUFAs and the loss of this region significantly reduces the sensitivity of TREK-1 to PUFAs. The replacement of the TREK-1 C terminal region by the TASK channel C terminal region through chimera formation, leads to a loss of TREK-1 activation by PUFAs. Activation of TREK-1 by PUFAs doesn't require cellular integrity consequently it can occur in excised patch. The TREK-1/TASK-1 chimera affect different TREK-1 properties: it impairs TREK-1 response to mechanical stimuli. And it decreases the sensitivity of TREK-1 to the heat. (Patel, Honore et al. 1998, Moha ou Maati, Peyronnet et al. 2011) (Fig9).

It has been shown that decreased intracellular pH activates TREK-1. Glutamic acid residue in the position 306 (E306) plays a key role in this activation (Fig9, 10). Its substitution

by another amino acid, strongly affects the sensitivity of TREK-1 towards intracellular acidification. This activation mode affects TREK-1 mechanosensitivity, shifts its activity towards positive pressure and makes it active at atmospheric pressure (Maingret, Patel et al. 1999, Honore, Maingret et al. 2002). It has been reported that extracellular acidification inhibits TREK-1 activity. Histidine in position 126 plays a key role in this inhibition. Its substitution by another amino acid drastically affects TREK-1 sensitivity towards extracellular acidification (Sandoz, Douguet et al. 2009).

TREK-1 is voltage dependent with an outward rectification activity. Its reversal potential is around -90 mV which is quite close to K^+ equilibrium potential (Fig9). It has been shown that the TREK-1 C terminal tail is important for voltage activation. The substitution of the serine in position 333 by alanine in mouse TREK-1, to mimic the dephosphorylated state of S333 doesn't affect the channel kinetics, while the substitution of the serine in position 348 by alanine in rat TREK-1 leads to a loss of TREK-1 voltage dependency. It has been shown that phosphorylation/dephosphorylation of serine at position 348 may be responsible for the interconversion between voltage dependent and leak state of rat TREK-1. (Bockenhauer, Zilberberg et al. 2001, Maingret, Honore et al. 2002).

It has also been shown that temperature can affect TREK1 activity. it reaches its maximal activation between 37°C and 42°C. TREK-1 loses its sensitivity to heat in excised patch. This demonstrates that TREK-1 plays a role in thermosensation and this activation requires the cell integrity, suggesting that a cytosolic factors might be involved in channel regulation. (Maingret, Lauritzen et al. 2000) (Fig9).

Volatile anesthetics such as chloroform, halothane and isoflurane activate TREK-1 in a dose dependent manner (Patel et al 1999). TREK-1 is also activated by gaseous anesthetics such as nitrous oxide, xenon, and cyclopropane (Gruss, Bushell et al. 2004). The C terminus tail of TREK-1 is important for its activation by either volatile or gaseous anesthetics. A truncation or deletion of TREK-1 C terminus region leads to a loss of its sensitivity towards these anesthetics. It was proposed the presence of potential binding sites for anesthetics in the C terminal tail of TREK-1, however these binding sites have not yet been identified (Fig9).

A-kinase anchor protein 150 (AKAP 150) is a scaffold protein that interacts with protein kinases such as PKA and PKC. PKC and PKA phosphorylate TREK-1 respectively on serine residue in position 300 and 333 which induce TREK-1 inhibition (Murbartian, Lei et al. 2005). AKAP 150 directly interacts with TREK-1 by binding its C terminal tail, leading to an increase of TREK-1 outward rectification and a loss TREK-1 sensitivity towards intracellular acidification, membrane stretch and PUFAs. AKAP150 brings PKA and PKC into close proximity to TREK-1, most likely the decrease of TREK-1 sensitivity towards PUFA, membrane stretch and intracellular acidification is caused by PKA. However PKC doesn't affect TREK-1 activity because its regulation site localized at the serine in position 300 is hidden by the interaction site of AKAP150 (Sandoz, Thummler et al. 2006) (Fig9, 10).

Phosphatidylinositol 4,5-bisphosphate (PIP₂) cooperates with TREK-1 by interacting with E residue at position 306 (E306), the protonation of E306 increases this interaction. TREK-1/PIP₂ interaction leads to an increase of the channel sensitivity to atmospheric pressure. It also increases the voltage dependency of the channel with an elimination of its outward rectifying activity (Chemin, Patel et al. 2005). Diacylglycerol (DAG) significantly downregulates TREK-1

activity. In the presence of DAG, TREK-1 displays a weak activity upon activation by arachidonic acid, intracellular acidification and membrane stretch. DAG activates Protein Kinase C (PKC) which will lead to an inhibition of TREK-1 through phosphorylation of S333. Gq coupled protein receptors in particular Gq/11 coupled to the glutamate receptor 1 (mGluR1) induces the activation of phospholipase C (PLC). PLC has the ability to hydrolyze the PIP₂ into DAG and inositol trisphosphate (IP₃) (Fig9). However, IP₃ has no effect on TREK-1 activity (Chemin, Girard et al. 2003)

Phospholipase D 2 (PLD 2) has the ability to interact with the TREK-1 C terminal tail, leading to an increase in its activity. However, phospholipase D1 (PLD 1) doesn't have the ability to directly interact with TREK-1(Comoglio, Levitz et al. 2014).

Gs protein induces the activation of adenylate cyclase which will catalyze the conversion of ATP to cyclic AMP (cAMP). cAMP inhibits TREK-1, it decreases TREK-1 basal current and it decreases TREK-1 sensitivity to voltage dependency. cAMP decreases channel sensitivity to heat. cAMP binds to PKA leading to PKA activation. PKA phosphorylates TREK-1 on serine at position 333 (S333) leading to TREK-1 inhibition (Fink, Duprat et al. 1996, Patel, Honore et al. 1998, Maingret, Lauritzen et al. 2000).

TREK-1 is activated indirectly by nitric oxide (NO). The increase of intracellular NO leads to an increase of cGMP which will activate protein kinase G (PKG). PKG phosphorylates TREK-1 on serine at position 351 (S351) leading to TREK-1 activation (Koh, Monaghan et al. 2001).

Popeye domain-containing (POPDC) gene family encodes membrane proteins containing cAMP binding sites. Human POPDC1 and mouse POPDC1 and 2 have interaction sites with

TREK-1 and they increase its membrane trafficking leading to an increase in TREK-1 current. However, increasing cAMP levels will lead to a loss of the effect of POPDC on TREK-1 trafficking to the plasma membrane resulting in a decrease of TREK-1 current (Schindler, Scotton et al. 2016).

TREK-1 is insensitive to classic potassium channel inhibitors. K⁺ voltage dependent inhibitors, such as 4-aminopyridine (4-AP) and tetraethylammonium (TEA), ATP sensitive K⁺ channel inhibitors such as glibenclamide and Ca²⁺ activated K⁺ channel inhibitors such as apamin and charybdotoxin (Moha ou Maati, Peyronnet et al. 2011). Most likely TREK-1 is insensitive to the classic potassium channel inhibitors because it lacks the interaction and regulation sites specific for these molecules.

The sortilin receptor regulates TREK-1. One step of sortilin receptor maturation consists of the cleavage of its N terminus tail by furin. This cleavage leads to the release of the 44 amino acid peptide (PE). PE has the ability to interact with the sortilin receptor and TREK-1. This will affect the channel activity by affecting its expression on the plasma since it has been shown that PE binding to TREK-1 promotes its endocytosis. Spadin has the ability to regulate TREK-1. Spadin is made out of the active site of PE. It has been shown that spadin interacts with TREK-1 by immunoprecipitation. Spadin negatively regulates TREK-1 sensitivity towards PUFAs, and membrane stretch (Mazella, Petrault et al. 2010, Moha ou Maati, Peyronnet et al. 2011, Gil, Gallego et al. 2012). In addition, spadin was reported to specifically inhibit TREK-1 among the K_{2p} family. The concentration of spadin that has the ability to inhibit 50% of human TREK-1 current is IC₅₀= 60.74 nM. For mouse TREK-1 IC₅₀=70.7 nM. Spadin has a short life

time its half life time is around 6 hours (Mazella, Petrault et al. 2010, Moha ou Maati, Peyronnet et al. 2011, Moha Ou Maati, Veyssiere et al. 2012).

Fluoxetine is a selective serotonin reuptake inhibitor (SSRI) antidepressant drug. Fluoxetine is commercialized under the name of Prozac. The active metabolite of fluoxetine is norfluoxetine. Fluoxetine has the ability to inhibit hTREK-1 after activation with AA with $IC_{50}=6.18 \mu M$ it also decreases the channel voltage dependency. Norfluoxetine also has the ability to inhibit TREK-1 and decreases its voltage dependency. However, fluoxetine is not specific to TREK-1, it has the ability to inhibit other channels that belong to K_{2p} family such as TASK-3 (Kennard, Chumbley et al. 2005, Moha ou Maati, Peyronnet et al. 2011). These drugs that inhibit TREK-1 represent a new drug category of analgesics, anesthetics, neuroprotectors and antidepressant.

Spadin retroinverso (RI) is an analog for spadin which has more efficiency for TREK-1 inhibition, more resistant for proteolysis and more stable *in vivo*. Spadin RI has an $IC_{50}=10nM$ around 6 fold higher than IC_{50} of spadin and its life time is 16 hours around 2.6 fold higher than spadin life time (6 hours).

5.3_ TREK-1 heterodimers:

TREK-1 forms heterodimers with other K_{2p} family members. TREK-1 forms heterodimers with TREK-2 (TREK-1/TREK-2). TREK-1/TREK-2 has a voltage dependency similar to TREK-1 with an outward rectification. In transfected HEK cells, the unitary conductance value of TREK-1/TREK-2 at +100 mV is 55.6 pS. The unitary conductance of TREK-1/TREK-2, is between the unitary conductance of TREK-1 (88.5pS) and the unitary conductance of TREK-2

(78.9 pS) (Blin et al 2016). In xenopus oocyte the heterodimer TREK-1/TREK-2 is inhibited by extracellular acidification. This inhibition is not significantly different from the inhibition of the TREK-1 homodimer by extracellular acidification. TREK-2 is significantly inhibited by RR, its inhibition is around 85% while the inhibition of TREK-1 by RR is modest it is around 10%. TREK-1/TREK-2 has a significant inhibition by RR is around 50%. This inhibition remains intermediate between TREK-1 and TREK-2 homodimers. In HEK cell the TREK-1/TREK-2 heterodimer has the same behaviors as in xenopus oocytes regarding its inhibition by extracellular acidification as well as by RR. Interestingly the heterodimer TREK-1/TREK-2 is significantly inhibited by 1 μ M of spadin, this inhibition is around 85% is similar to the inhibition of TREK-1 homodimer, while TREK-2 remains insensitive to spadin. This suggests that one TREK-1 subunit is sufficient to trigger the effect of spadin on the homodimers formed by TREK-1 (Lengyel, Czirjak et al. 2016).

TREK-1 forms heterodimers with TRAAK (TREK-1/TRAAK). TREK-1/TRAAK has current voltage activity similar to TRAAK. At +100mV the unitary conductance of TREK-1/TRAAK is 80pS while the unitary conductance of TRAAK is 65pS. Fluoxetine is able to inhibit TREK-1 while it doesn't have an effect on TRAAK. The TREK-1/TRAAK heterodimer is inhibited by fluoxetine, this inhibition is less than the one observed for TREK-1 homodimer. This suggests that one TREK-1 subunit is sufficient to trigger the effect of the fluoxetine on heterodimers formed by TREK-1. TREK-1 was reported to be inhibited by PKA and PKC while neither PKA nor PKC can affect TRAAK. The heterodimer TREK-1/TRAAK is inhibited by PKA, while PKC doesn't affect TREK-1/TRAAK activity. This suggests that the presence of one phosphorylation site for PKA (serine residue in TREK-1 at position 333) is sufficient to trigger the inhibition by PKA. Despite the presence of phosphorylation sites for PKC on both heterodimers subunits

(serine residue in TREK-1 at position 300 and serine residue in TRAAK at position 261), the absence of PKC effects on TREK-1/TRAAK remains complicated to explain and it suggests the presence of limited access of PKC to TREK-1/TRAAK heterodimer. TREK-1/TRAAK doesn't show any rectifying activity and has a linear current voltage activity (Blin et al 2016). PLD2 has the ability to activate TREK-1 channel, but it doesn't have an effect on TRAAK channel. TREK-1/TRAAK heterodimer is activated by PLD2, like TREK-1. This suggests that one TREK-1 C terminal domain is sufficient to bind PLD 2 and trigger the activation of TREK-1/TRAAK heterodimer. TREK-1 is activated by intracellular acidification while TRAAK is activated by intracellular alkalinization. Interestingly, TREK-1/TRAAK is activated by intracellular acidification as well as intracellular alkalinization. This suggests that the C termini of TREK-1 and TRAAK sense individually intracellular pH changes and influence the gating of TREK-1/TRAAK heterodimers.(Levitz, Royal et al. 2016).

TREK-1 can form a heterodimer with TWIK-1 (TREK-1/TWIK-1) by forming a disulphide bridge between cysteine residues in the first extracellular loop of each channel. TREK-1/TWIK-1 association has been reported to increase the passive current conductance (Hwang, Kim et al. 2014).

5.4_ TREK-1 between physiology and pathology:

TREK-1 is expressed in a wide range of tissues. It is expressed in the mammalian central nervous system such as brain and spinal cord and hippocampus, it is also expressed in skeletal muscle, heart and colon.

TREK-1 is important for cellular proliferation and it plays a crucial role in cell cycle progression. Overexpression of TREK-1 in CHO/hTREK-1 stable cell line, leads to G1 cell cycle arrest and a decrease of the level of cyclin D1 (Zhang, Yin et al. 2016). It has been also reported the implication of TREK-1 in neurogenesis. TREK-1 inhibition with spadin, spadin RI or fluoxetine results in an anti-depressant effect with an increase of neurogenesis. Spadin treatment, results in an increase of brain derived neurotrophic factor (BDNF). BDNF is responsible of promoting neurogenesis demonstrated by BrdU assay. This suggests that the presence of TREK-1 in the brain don't have an effect on neurogenesis. (Mazella, Petrault et al. 2010, Moha Ou Maati, Veyssiere et al. 2012, Zhang, Yin et al. 2016).

Researchers were interested to look for spadin analogs that have better stability in vivo and better affinity for TREK-1 with an increase of the action duration. Spadin RI has the ability to significantly inhibit hTREK-1: it crosses the blood brain barrier after intravenous injections, it reaches the hippocampus and it enhances neurogenesis like spadin (Veyssiere, Moha Ou Maati et al. 2015).

Recent studies have demonstrated that a short version of spadin (PE 22-28) containing only the last 7 amino acid of the original spadin sequence, has a better affinity for TREK-1 than spadin and spadin RI, its $IC_{50} = 0.10nM$. Like spadin, PE 22-28 is a specific inhibitor of TREK-1 and it doesn't have the ability to inhibit other channels that belong to K_{2p} family. PE 22-28 induces neurogenesis 4 days after treatment with an anti-depressant effect (Djillani, Pietri et al. 2017). In addition, other studies have shown that TREK-1 down regulation in mouse alveolar epithelial cells (MLE-12) upon exposure to hyperoxia, results in a decrease of cell proliferation. (Schwingshackl, Teng et al. 2012). TREK-1 is reported to be overexpressed

in several types of cancer such as prostate cancer. The level of TREK-1 expression is correlated with the grade of cancer progression. Its inhibition results in a decrease of cell proliferation as well as a decrease of the tumor growth (Voloshyna, Besana et al. 2008, Zhang, Wan et al. 2015). Recent studies showed that TREK-1 plays a crucial role in neuroprotection against brain ischemia. TREK-1 silencing by siRNA results in a decrease in cell viability by increasing apoptosis. This leads to an increase in the brain infarct area after ischemic injury. (Heurteaux, Guy et al. 2004, Tong, Cai et al. 2014). How TREK-1 regulates cell proliferation and cell cycle progression remains controversial. It depends on the environment in which TREK-1 is expressed. It depends also on TREK-1 downstream effectors that can activate different signalization pathways. On one hand the overexpression of TREK-1 promotes cell proliferation observed in several types of cancer and its inhibition lead to regression of the cancer state (Voloshyna, Besana et al. 2008, Innamaa, Jackson et al. 2013, Zhang, Wan et al. 2015, Sauter, Sorensen et al. 2016), on the other hand, overexpression of TREK-1 in different cell types leads to a cell cycle arrest (Zhang, Yin et al. 2016).

Another cellular process in which TREK-1 channel plays an important role is cell differentiation. It is overexpressed during differentiation to maintain cellular homeostasis, resting membrane potential and cellular excitability. Its inhibition by spadin leads to an inhibition of the differentiation of the mouse skeletal muscle cell line C2C12 (Afzali, Ruck et al. 2016) and it is associated with muscle dystrophy. Inhibition of TREK-1 during muscle differentiation leads to an impaired myoblast fusion and a downregulation in maturation markers which can be related to muscle dystrophy caused by increasing muscle breakdown and weakening. A point mutation in POPDC1 that consists of substituting serine at position 201 by phenylalanine (S201F) leads to a decrease of POPDC1^{S201F} affinity to cAMP. POPDC1^{S201F} interacts with

TREK-1 channels but it doesn't affect its membrane trafficking but it increases its outward current. This abnormal increase in outward TREK-1 current, was found in patients with limb-girdle muscular dystrophy and cardiac arrhythmia. Zebrafish transgenic line that express POPDC1^{S201F} shows muscular dystrophy and cardiac arrhythmias (Brand, Simrick et al. 2014, Schindler, Scotton et al. 2016).

TREK-1 was reported to be expressed in mammalian cardiomyocytes (Xian Tao, Dyachenko et al. 2006). TREK-1 is known to interact with the cytoskeleton and with the cytoskeleton associated protein such as β (IV)-Spectrin. β (IV)-Spectrin plays a key role in membrane trafficking of TREK-1 in the cardiomyocytes: loss of β (IV)-Spectrin activity results in a decrease of TREK-1 expression. This was associated with heart failure, arrhythmias and a long QT syndrome (Hund et al 2014). Under stress conditions, TREK-1 is important for heart automaticity. Under stress conditions or after an intensive exercise, the loss of TREK-1 expression leads to sino atrial node (SAN) dysfunction and abnormal pacemaker activity (Unudurthi, Wu et al. 2016).

Atrial fibrillation in animal models and patients is associated with arrhythmias, tachycardia phenotype, and an increase in collagen in the atrial tissue. Animals treated with an adenovirus that promotes TREK-1 expression in atrial tissue, leads to a decrease of atrial fibrillation with antiarrhythmic effect. This suggests that TREK-1 contributes to heart electrical remodeling and it controls the heart rhythm (Lugenbiel, Wenz et al. 2017).

TREK-1 has been reported to play an important role during cardiac hypertrophy. Cardiac hypertrophy is characterized by a prolonged action potential duration associated with a significant increase of TREK-1 expression in hypertrophic cardiomyocytes. The signalization

pathway proposed is complicated and suggests a disturbance in cellular calcium homeostasis related to potassium (Cheng, Su et al. 2006, Wang, Zhang et al. 2013). Different TREK-1 splice variants are detectable in different organs such as brain, kidney and adrenal gland. TREK-1 splice variants have a dominant negative effect on wild type TREK-1 (Veale, Rees et al. 2010, Rinne, Renigunta et al. 2014, Cowles, Wu et al. 2015). This leads to a decrease of TREK-1 current caused by a decrease of WT TREK-1 expression on the plasma membrane (Veale, Rees et al. 2010, Rinne, Renigunta et al. 2014, Cowles, Wu et al. 2015).

A single point mutation in the selective filter of TREK-1, which consists of a substituting isoleucine (I) by threonine (T) at position 267, results in permeability of TREK-1 to sodium rather than potassium. This mutation was associated with TREK-1 hypersensitivity to stretch activation. TREK-1^{I267T} is found in patients with right ventricle outflow tract tachycardia accompanied with arrhythmias. TREK-1^{I267T} causes intracellular sodium overload and depolarization of cardiac cells, which will trigger arrhythmias via secondary calcium overload (Decher, Ortiz-Bonnin et al. 2017).

5.4_ Summary IV:

TREK-1 belongs to the k_{2p} family. It can form homodimers or heterodimers with other channels from the k_{2p} family. TREK-1 homodimer has a polymodal activation (Fig 9). TREK-1 is inhibited by different pharmacological agents: fluoxetine, spadin, spain RI, and short version of spadin (PE 22-28).

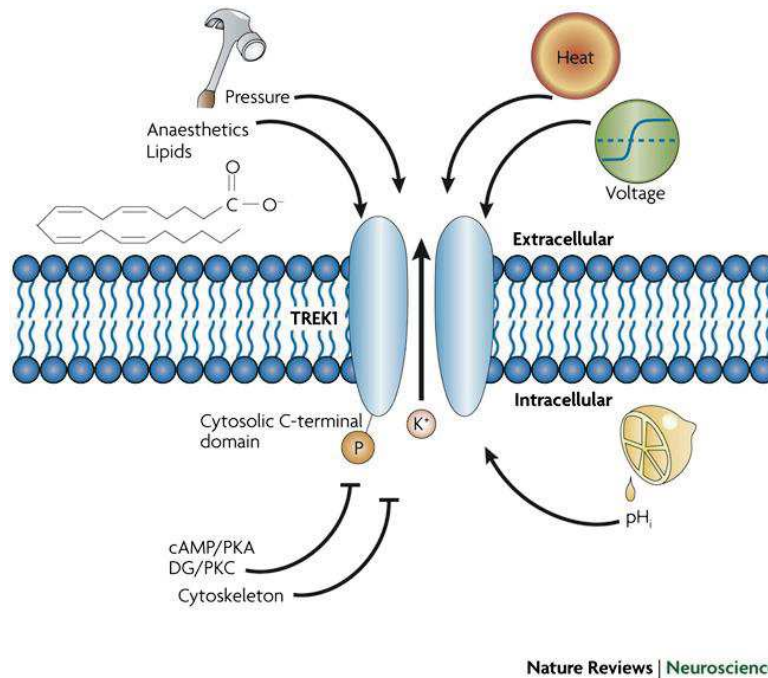


Figure 11: Honore E Nat Rev Neurosci. 2007: **Schematic presentation showing the Polymodal activation of TREK-1:** TREK-1 is activated by pressure, voltage, anaesthetics, lipids and intracellular acidification. It is inhibited by PKA, PKC, cAMP and the cytoskeleton.

TREK-1 is expressed in a wide range of tissues. It is implicated in several physiological and pathophysiological mechanisms, by regulating different cellular processes such as cellular hemostasis, cell proliferation and differentiation,

In the brain, TREK-1 has a protective effect against ischemia. However, TREK-1 is associated with depression disease and its inhibition, results in an anti-depressant effect with increasing in neurogenesis. TREK-1 was reported to regulate cellular proliferation and to be overexpressed in several types of cancer. Controversially, its overexpression in CHO leads to a cycle cell arrest. It also regulates cellular differentiation and its inhibition in muscles was associated with dystrophy.

TREK-1 is expressed in the heart. It promotes a normal heart activity and any disturbance in TREK-1 permeability leads to arrhythmias. Inhibition of TREK-1 expression in cardiomyocytes leads to arrhythmias under stress conditions. TREK-1 is associated with several heart diseases such as hypertrophy.

6_ Hypothesis:

In most species, soon after birth, cardiomyocytes switch from hyperplasia (increase in cell number) to hypertrophy (increase in cell size). Unlike adult zf, adult mammals fail to regenerate their heart after injury, they develop hypertrophic response leading to pathological hypertrophy. However, neonatal mice show a regenerative capacity after cardiac injury until 7 days after birth. Heart regeneration in zf and neonatal mice occurs through cardiomyocyte dedifferentiation followed by proliferation. The proliferative capacity of cardiomyocytes is observed in both species during embryonic development. This capacity is lost in mammals soon after birth, where they develop hypertrophy in response to stress. Adding to that, adult mammalian heart regeneration can be induced after cardiac injury by controlling environmental and molecular factors that promote cardiomyocyte dedifferentiation and proliferation to enhance heart regeneration. Hypoxia induces cardiomyocyte dedifferentiation and proliferation after myocardial infarction promoting heart regeneration. The introduction of extracellular matrix protein such as agrin or the stimulation of NGR/ERB2 receptor leads to cardiomyocyte dedifferentiation accompanied with the activation of ERK pathway to enhance cardiomyocyte proliferation ensuring by that heart regeneration in adult mice. These studies drive us to think that heart regeneration in adult mammals has been blocked/inhibited. Interestingly, recent studies showed that ventricular unloading to patients suffering from severe heart failure,

promotes cardiomyocyte proliferation leading to a reversal of their heart failure and improvement of their prognosis. This suggests that high blood pressure in humans prevents heart regeneration, supporting our hypothesis based on the implication of mechanosensors during adult mammalian hypertrophy and heart regeneration. During embryonic development, mechanical forces and mechanosensors are important for normal heart development. During zfish and mouse heart regeneration, adult cardiomyocytes dedifferentiate to an embryonic state allowing them to proliferate and redifferentiate into adult cardiomyocytes, to replace the damaged part of the heart. These studies suggest that pressure overload caused by cardiomyocyte loss, leads to cardiac hypertrophy in adult mammals. In contrast, it induces cardiac regeneration in neonatal mammals and zfish. The mechanism of mechanosensation and its different effectors play a key role during cardiac hypertrophy and cardiac regeneration.

Mechanosensitive ion channels play an important role in signal transduction after exposure to mechanical stimuli. Cardiac hypertrophy is caused by pressure overload and volume stress. Stretch activated potassium channels are proposed to play a key role during hypertrophy, cardiac remodeling and the response of cardiomyocytes to mechanical stress. TREK-1 is overexpressed in hypertrophic cardiomyocytes of rats suffering from left ventricular hypertrophy. It was suggested that mechanical stress that induces hypertrophic response causes changes in gene expression including changes in TREK-1 expression. During hypertrophy, the increase in mechanical stress and hemodynamic forces in the heart is associated with an increase of intracellular acidification, and changes in the amount of PUFAs and their metabolites (Tajima, Bartunek et al. 1998) (Zordoky, Aboutabl et al. 2008, Spector 2009). These studies suggest that TREK-1 may play a key role in pathological hypertrophy or heart regeneration depending on its downstream effectors. For that reason we will focus on zfish

TREK-1 isoforms (zebrafish TREK-1a and TREK-1b) to investigate their role during heart regeneration.

7_ Objectives:

The aims of my thesis are to directly address the role of zTREK-1a and zTREK-1b (zTREK-1a/b) during zebrafish heart regeneration and physiology. For that reason it is important to characterize the channels (zTREK-1a/b), to localize their tissue expression that allows us to investigate their role during zebrafish heart regeneration and function. Achieving my objectives will allow us to further investigate TREK-1 downstream effectors and the signaling pathways in which they are implicated during zebrafish heart physiology and pathophysiology.

7.1_ Characterization of zTREK-1a and zTREK-1b:

The characterization of zTREK-1a and zTREK-1b allows us to establish their biophysical and pharmacological properties. These properties are compared to those already described for mammalian TREK-1. This characterization, allows us also to test the efficiency of a DN form of the channel (DN TREK-1 del ex4 and DNTREK-1 del ex3). Knowing that no commercial antibodies are available from most zebrafish proteins, we will be able to screen the efficiency of antibodies used for other species. The validated antibody is used to investigate the expression of zTREK-1a and zTREK-1b proteins in zf hearts and cardiomyocytes. To support our results electrophysiological recordings are performed on freshly dissociated cardiomyocytes to validate the expression of functional zTREK-1a and zTRK-1b channels in these cells.

7.2_ The role of zTREK-1a and zTREK-1b during zebrafish heart regeneration:

This experiment allows us to establish if zTREK-1a and zTREK-1b are required for successful zebrafish heart regeneration. To achieve our goal we have used 2 approaches, the first approach consists of a pharmacological inhibition of the channels through spadin injections: (a pharmacological inhibitor of zTREK-1a and zTREK-1b) during 30days after heart amputation. The second approach consists of using a conditional DN fish line, based on the Cre/loxp system. This line expresses a 4-HT inducible CreER and a floxed red fluorescent protein (RFP) stop cassette that targets dominant negative (DN) TREK-1 del ex4 expression in the cardiomyocytes, under the control of the cardiomyocyte specific promoter (cmlc2a) upon tamoxifen treatment. Upon tamoxifen treatment, Cre recombinase induces the excision, of the loxp flanked stop sequence and permanently expresses the DN TREK-1 del ex4 in the cardiomyocytes. We use these 2 approaches to investigate the role of zTREK-1a and zTREK-1b during zebrafish heart regeneration.

7.3_ The role of zTREK-1a and zTREK-1b in physiological zebrafish heart function:

This experiment allows us to determine if zTREK-1a/b are required for normal/physiological zf heart function. To accomplish that, we have used 2 approaches. The first approach consists of recording heart rate on zf embryos.

We expressed DN TREK-1 del ex4 in zebrafish cardiomyocytes in vivo and determined whether this affected the heart rate of zf embryos.

The second approach consists of performing optical mapping experiment on adult WT zfish injected during 14 dpa with 800 μM of spadin or with E3 in order to inhibit zTREK-1a and zTREK-1b to see the effect on cardiac automatism and on conduction velocity.

Chapter 1

Electrophysiology

1_ Introduction:

Mammalian TREK-1 is a leak potassium channel with an outward rectifier activity. It belongs to the K_{2p} family and works as a dimer. Each subunit of TREK-1 homodimer contains a C terminal tail, N terminal tail, 4 transmembrane domains and 2 pore domains. The pore contains GFG motif responsible for the selectivity filter (Honore 2007).

Mammalian TREK-1 homodimer has a polymodal activation. It is a mechanosensitive ion channel, activated by membrane stretch and tension. It is also activated by negative and positive pressure as well as cell swelling. TREK-1 is known to interact with microtubule associated protein 2 (Mtap2) which increases its membrane trafficking and consequently its membrane expression. Interestingly, TREK-1 interacts with cytoskeleton, which has a negative regulatory effect on it. TREK-1 activation increases when it loses the interaction with cytoskeleton (Patel, Honore et al. 1998, Sandoz, Tardy et al. 2008, Moha ou Maati, Peyronnet et al. 2011, Fukasaku, Kimura et al. 2016). TREK-1 was shown to be activated by LPs, PUFAs, intracellular acidification while extracellular acidification inhibits TREK-1 (Patel, Honore et al. 1998, Maingret, Patel et al. 1999, Maingret, Patel et al. 2000, Honore, Maingret et al. 2002, Sandoz, Douguet et al. 2009, Moha ou Maati, Peyronnet et al. 2011). PKA and PKC interact with TREK-1 and they enhance TREK-1 phosphorylation, decreasing by that its activity. Activating G_q coupled protein receptor pathway or the G_s pathway results in TREK-1 inhibition through activation of PKC and PKA respectively (Fink, Duprat et al. 1996, Patel, Honore et al. 1998, Maingret, Patel et al. 2000, Chemin, Girard et al. 2003). Whoever, activation of PKG through NO/cGMP/PKG pathway results in TREK-1 activation (Koh, Monaghan et al. 2001). TREK-1 has a direct interaction with AKAP 150. The interaction between TREK-1 and AKAP

150 increases TREK-1 outward rectifying activity and decreases its sensitivity towards pH and stretch activation (Sandoz, Thummler et al. 2006). TREK-1 interacts with POPDC and β (IV) spectrin. These 2 proteins promote TREK-1 membrane trafficking and increase its membrane expression (Hund, Snyder et al. 2014, Schindler, Scotton et al. 2016). TREK-1 can also be activated by heat and a wide range of volatile and gaseous anesthetics (Patel, Honore et al. 1999, Gruss, Bushell et al. 2004).

Unlike other potassium channels, TREK-1 is insensitive to classic potassium channel inhibitors such as amphetamine, 4AP, TEA, tetrodotoxin, glibenclamide and K_{ATP} (Moha ou Maati, Peyronnet et al. 2011), most likely because it lacks of interaction sites with these inhibitors. TREK-1 is inhibited by spadin, and its analogs (short version of spadin and spadin RI) as well as fluoxetine commercialized under the name of Prozac (Kennard, Chumbley et al. 2005, Mazella, Petrault et al. 2010, Moha ou Maati, Peyronnet et al. 2011, Gil, Gallego et al. 2012, Veyssiere, Moha Ou Maati et al. 2015). However, the mechanism of action of these molecules is not well known. Interestingly, TREK-1 C terminus tail is important for most of the regulation mechanisms, such as activation by membrane stretch, intracellular acidification, PUFAs, PLs, and anesthetics. It also seems to play a role in the interaction between TREK-1/AKAP 150 and POPDC. The C terminus tail is also crucial for the inhibition of TREK-1 by PKA and PKC.

TREK-1 splice variants are found in different organs such as brain, kidney adrenal gland and endometrium. All the splice variants have a dominant negative effect on WT TREK-1, resulting in a decrease of TREK-1 current. TREK-1 splice variants decrease WT TREK-1 expression on the plasma membrane caused by the cytoplasmic retention of the heterodimer

formed by the DN and WT TREK-1 (Veale, Rees et al. 2010, Rinne, Renigunta et al. 2014, Cowles, Wu et al. 2015).

Mammalian TREK-1 is expressed in a wide range of tissue and organs. It is expressed in the central nervous system, DRG, cardiovascular system especially in the heart and the bladder. It plays a role in physiological and pathophysiological functions of these organs.

Our goal is to establish the biophysical and pharmacological properties of zTREK -1 isoforms (zTREK-1a/b) by using electrophysiological recordings based on the patch clamp technic. Establishing the properties of zTREK-1a/b allows us to investigate their functional expression in the cardiomyocytes. It also allows us to test the efficiency of a dominant negative form of zTREK-1a on both channels, as well as the efficiency of pharmacological agents, already described to have an effect on mammalian TREK-1.

2_ Materials and methods:

2.1_ Cloning:

To clone zTREK1a/b we have performed a nested Polymerase Chain Reaction (PCR) on 3 days post fertilization (dpf) cDNA library. 2 rounds of PCR are realized on library zebrafish cDNA. the first round of PCR is used to limit the non-specific products resulting from the DNA amplification. The primers used for this step for zTREK-1a/b are respectively Forward primer 5' AGCGAGAACAGCAGATCCCA 3' Reverse primer 5'GCTTACATTTTAGTATGTGC3' and Forward primer 5'GCTGCTGAAGCCTCCAGAGG3' Reverse primer 5'CAGCTTGTCCCTTTGAATTC3'. The remaining amplified DNA will be used as a target for the second run of PCR it should not amplify non-specific targets and the primers used during this round for zTREK-1a/b are respectively Forward primer 5'ATGGCTGCACCTGATCTTTT3' Reverse primer 5'TTATTTGAGATGTTCAATGA3' for and Forward primer 5'ATGCGCTGGAAGACCGTGCT3' Reverse primer 5'TCATTTTGTCTGTATTCTAG3'. The remaining products are introduced into PGEM vector for bacteria transformation and then they are transferred into PIRE5-2eGFP vector expression (Invitrogene).

2.2_ Cell culture and transfection:

Transformed human embryonic kidney (293) cell line stably expressing an SV40 temperature-sensitive T antigen (HEK TSA) are cultured in a Dulbecco's Modified Eagle Medium (DMEM) with 5% antibiotics (AB) and 10% fetal bovine serum (FBS) and maintained in 5% CO₂. After cloning zTREK-1a and zTREK-1b sequences in PIRE5-2eGFP plasmid, 1µg of DNA was used for transfection in HEK TSA using the JetPei (Ozyme) standard reaction that

serves to transfect 5 cell plates of 35 cm diameter. The DN TREK-1 deletion exon 4 (DN TREK-1 del exon 4) is cotransfected with zTREK-1a (ratio 1:1) or with zTREK-1b (ratio 1:1) in HEK TSA using the JetPei standard reaction. The transfection was done 24 hours after cell splitting and the experiments are done 48-96 hours post transfection.

2.3_ Adult zf cardiomyocyte's primary culture:

2.3.1_ Cardiomyocyte isolation:

Cardiomyocytes are cultured on plates coated with fibrin gel according to the protocol established by Sander.V et al (Sander, Sune et al. 2013). The fish are anesthetized in 0.5X tricaine solution, then their hearts are extracted and placed quickly in heparin solution. The heparin is replaced by a digestion buffer containing 5mg/l of collagenase II and IV. The digestion occurs at 32°C for 75 minutes (min). The digestion reaction is stopped by adding a solution with 12.5µM of Ca²⁺, the mix is spin at 4°C 1800 (rotation per minute) rpm for 5 min. Then 6 washes take place with solutions containing an increase Ca²⁺ concentrations from 12.5 µM to 1 mM. The pellet is dissolved in DMEM with 5% AB and 10% FBS. The dissolved pellet is plated in 2 dishes coated during the 3rd wash.

2.3.2_ Coating:

The plates are coated with fibrin gel following Sander's et al protocol (Sander, Sune et al. 2013). 500µl of fibrinogen (stock 20mg/ml) is diluted 1:10 in prewarmed DMEM then 25µl of thrombin (stock 50U/ml) is added to the diluted solution mixed and we quickly proceed for coating. The bottom of a 35cm dish is completely covered with 1.5ml of fibrinogen/thrombin mixture which will be incubated for 30min until the gel is formed then we proceed to plating.

2.4_ Electrophysiological recordings:

Electrophysiological recordings are performed on HEK cells transfected with 1 μ g of plasmid per 5 plates at 24-96 hours after transfection. Electrophysiological recordings are also performed on freshly dissociated cardiomyocytes.

2.4.1_ Stretch experiment:

2.4.1.1_ Inside out configuration:

The holding potential is maintained at 0mV potential and negative pressure is applied from 0 to -80 mmHg with a 10 mmHg step. During the first step a pressure of 0 mmHg is applied during 50 ms then the pressure changes are applied with 10 mmHg step each during 200 ms. At the end of each step the pressure was maintained at 0mmHg during 225 ms. The time between 2 steps is 15 s. The bath solution contains 155 mM of KCl, 3 mM of MgCl₂, 5 mM of EGTA and 10 mM of HEPES adjust to pH 7.2 with KOH. The pipette solution contains 150 mM of NaCl, 5 mM of KCl, 2 mM of CaCl₂, and 10 mM of HEPES adjust to pH7.4 with NaOH.

The stretch experiment in inside out configuration is performed to test the effect of spadin (10 μ M in the pipette medium) on zTREK-1a/b .This experiment is performed to test the effect of dominant negative TREK-1 deletion exon 4 (DN TREK-1 del ex4) as well as DN TREK-1 del ex3 on HEK co-transfected with zTREK-1a/b and the empty vector, or cotransfected with zTREK-1a/b and the DN forms of the channels, or transfected with the DN forms of the channels alone.

The average of the current amplitude for each step of pressure is analyzed and presented in a graph according to each pressure step.

2.4.1.2_ Cell attached configuration:

The holding potential is maintained at 0mV potential and negative pressure is applied from 0 to -80 mmHg with a 10 mmHg step. During the first step a pressure of 0 mmHg is applied during 50 ms than the pressure changes are applied with 10 mmHg step each during 200 ms. At the end of each step the pressure was maintained at 0mmHg during 225 ms. The time between 2 steps is 15 s. The bath solution contains 155 mM of KCl, 3 mM of MgCl₂, 5 mM of EGTA and 10 mM of HEPES adjust to pH 7.2 with KOH. The pipette solution contains 150 mM of NaCl, 5 mM of KCl, 2 mM of CaCl₂, and 10 mM of HEPES adjust to pH7.4 with NaOH.

The stretch experiment in cell attached configuration was performed on HEK cells transfected with zTREK-1a/b. This experiment was also performed on freshly dissociated cardiomyocyte in control condition and in the presence of spadin (10µM in the pipette medium).

The average of the current amplitude for each step of pressure is analyzed and presented in a graph according to each pressure step.

2.4.2_ Polyunsaturated fatty acids experiment:

zTREK-1a and zTREK-1b currents are measured using whole cell configuration, in the presence of cocktail inhibitor which allow the inhibition of a wide range endogenous potassium channels, voltage activated K⁺ blocker (3 mM of 4-aminopyridine (AP), 10 mM of tetraethylammonium (TEA), K_{ATP} blocker (10 µM of glibenclamide), and Ca²⁺ activated K⁺ channel blocker (100 nM of apamin, 50 nM charybdotoxin). The cells are clamped at -80 mV for 75 ms than voltage changes are applied to the cells are from -100 mV to +60 mV with 20 mV steps, the duration of the depolarization is 800 ms. At the end of each voltage changed step the voltage is maintained at -80 mV for 75 ms. The cells are perfused with the K⁺ cocktail

blockers followed by the K⁺ cocktail blockers combined with either 10 μM of arachidonic acid (AA) or 10 μM of docosahexaenoic acid (DHA). Currents amplitudes are expressed in currents densities (pA/pF). The holding potential is maintained at -80 mV potential. The time between 2 steps is 5 s. The changes of the perfused solution was done once we reach the channel's steady state. The bath solution contains 150 mM of NaCl, 5 mM of KCl, 3 mM of MgCl₂, 1 mM of CaCl₂ and 10 mM of HEPES adjust to pH7.4 with NaOH. The intracellular (pipette) solution contains 155 mM of KCl, 3 mM of MgCl₂, 5 mM of EGTA and 10 Mm of HEPES adjust to pH 7.2 with KOH.

The polyunsaturated fatty acids experiment is performed in whole cell configuration on HEK cells transfected with zTREK-1a/b.

The average of the current amplitude for each voltage is analyzed and presented in a graph according to each voltage step.

2.4.3 pH experiment:

This experiment is performed in inside out configuration. The holding potential is maintained at -80mV potential. The cells are perfused with intracellular solutions adjusted respectively to pH 7.2 then 6.2 and 5.2. A voltage ramp is applied from -120mV a +60mV for each perfused intracellular solution. Each voltage ramp has a duration time of 900 ms. The time between 2 steps is 5 s. The changes between of the intracellular perfusion is done once we reach the channel steady state. The bath solution contains 155 mM of KCl, 3 mM of MgCl₂, 5 mM of EGTA and 10 mM of HEPES adjust to pH 7.2 with KOH. The pipette solution contains

150 mM of NaCl, 5 mM of KCl, 2 mM of CaCl₂, and 10 mM of HEPES adjust to pH7.4 with NaOH.

The pH experiment is performed in inside out configuration on HEK cells transfected with zTREK-1a/b.

The average of the current amplitude at 0 mV potential is analyzed for each pH condition and presented in a graph according to pH solution.

2.4.4_ Statistical analysis:

We have presented our data by the mean \pm standard error of the mean (SEM). The difference between 2 groups was established using t test.

2.5_ Immunofluorescence and immunohistochemistry:

These technics will be detailed later in the next chapter.

3_ Results

3.1_ Characterization of zTREK-1a and zTREK-1b:

3.1.1_ Effect of membrane stretch on zTREK-1a and zTREK-1b:

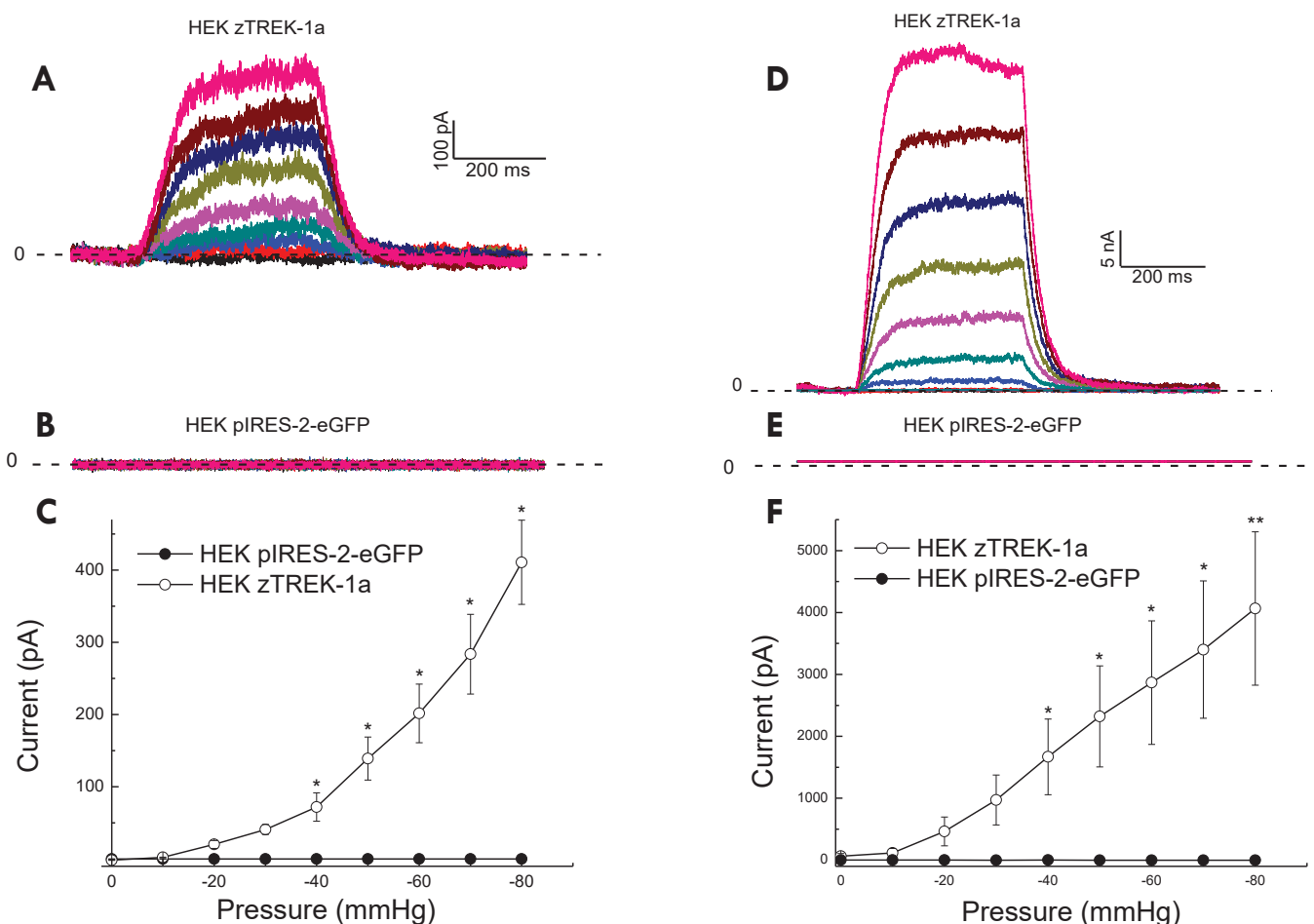


Figure 1: Effect of membrane stretch on zTREK-1a: recorded currents at 0mV potential by applying an increased negative pressure from 0 to -80 mmHg. Recorded currents on HEK cells transfected with zTREK-1a PIREs-2eGFP in CA configuration (n=3) (A) on HEK cells transfected with PIREs-2eGFP in CA (n=4) (B), and their corresponding current/pressure curves (C). Recorded currents on HEK cells transfected with zTREK-1a PIREs-2eGFP in IO configuration (n=7) (D) on HEK cells transfected with PIREs-2eGFP in IO configuration (n=4) (E) and their corresponding current/pressure curves (F). * P value < 0.05; ** P value < 0.01.

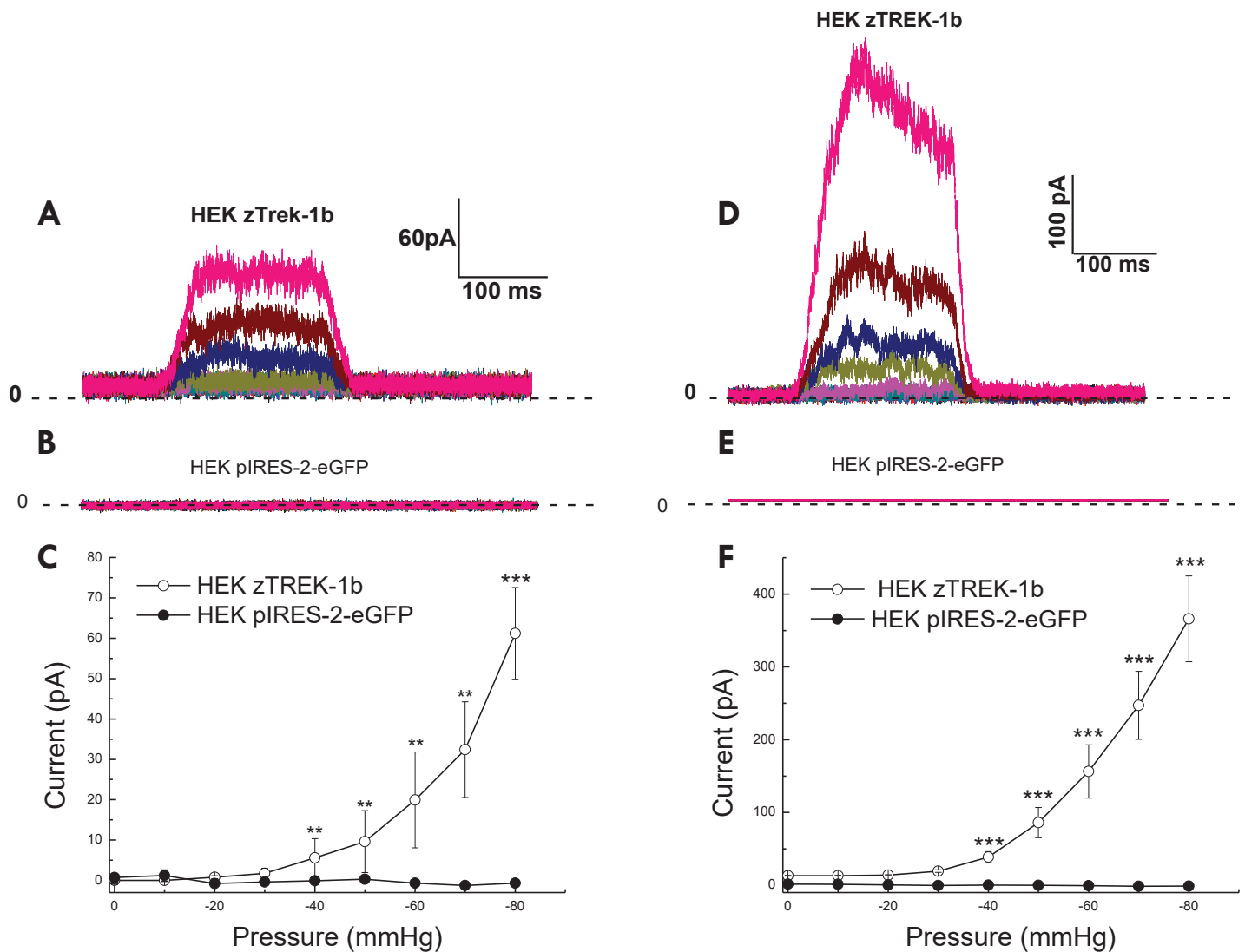


Figure 2: Effect of membrane stretch on zTREK-1b: recorded currents at 0mV potential by applying an increased negative pressure from 0 to -80 mmHg. Recorded currents on HEK cells transfected with zTREK-1b PIREs-2eGFP in CA configuration (n=8) (A) on HEK cells transfected with PIREs-2eGFP in CA (n=4) (B), and their corresponding current/pressure curves (C). Recorded currents on HEK cells transfected with zTREK-1b PIREs-2eGFP in IO configuration (n=19) (D) on HEK cells transfected with PIREs-2eGFP in IO configuration (n=4) (E) and their corresponding current/pressure curves (D). ** P value < 0.01, *** P value < 0.001

To test the effect of membrane stretch on zTREK-1a/b, a negative pressure protocol is applied on HEK cell transfected with either zTREK-1a PIRE5-2eGFP or zTREK-1b PIRE5-2eGFP.

We are able to record currents for zTREK-1a and zTREK-1b (zTREK-1a/b) in HEK cells transfected with zTREK-1a PIRE5-2eGFP or zTREK-1b PIRE5-2eGFP in CA configuration at 0mV potential. The current amplitudes for zTREK-1a/b increase from 0 to 201.7 ± 82.4 pA and 31.7 ± 11.9 pA respectively by increasing negative pressure applied on the cell membranes from 0 to -60 mmHg. At -80 mmHg zTREK-1a/b current amplitudes reach 410.8 ± 158.3 pA and 73 ± 11.4 pA respectively (Fig1 A,B_Fig2 A,C).

In IO configuration, the current amplitudes for zTREK-1a/b increase from 0 to 2867.6 ± 997.9 pA and 156.3 ± 36.5 pA respectively by increasing negative pressure applied on the cell membranes from 0 to -60 mmHg. At -80 mmHg their zTREK-1a/b current amplitudes reach 4064.6 ± 1239.4 pA and 366.1 ± 59.0 pA respectively (Fig1 C,D_Fig2 B,C).

No currents are recorded in the cell transfected with empty vector (PIRE5-2eGFP) neither in CA nor in IO configuration (Fig1 B, D, E, F_Fig2 C, D, E).

Electrophysiological recordings for this experiment are done at 0mV potential.

The significant increase of the current amplitudes for zTREK-1a/b in response to the increased negative pressure suggests that they are activated by membrane stretch. The significant increase of the current amplitudes of zTREK-1a/b between CA and IO configuration is due to the removal of interaction between the channels and the cytoskeleton.

3.1.2 Effect of polyunsaturated fatty acid on zTREK-1a and zTREK-1b:

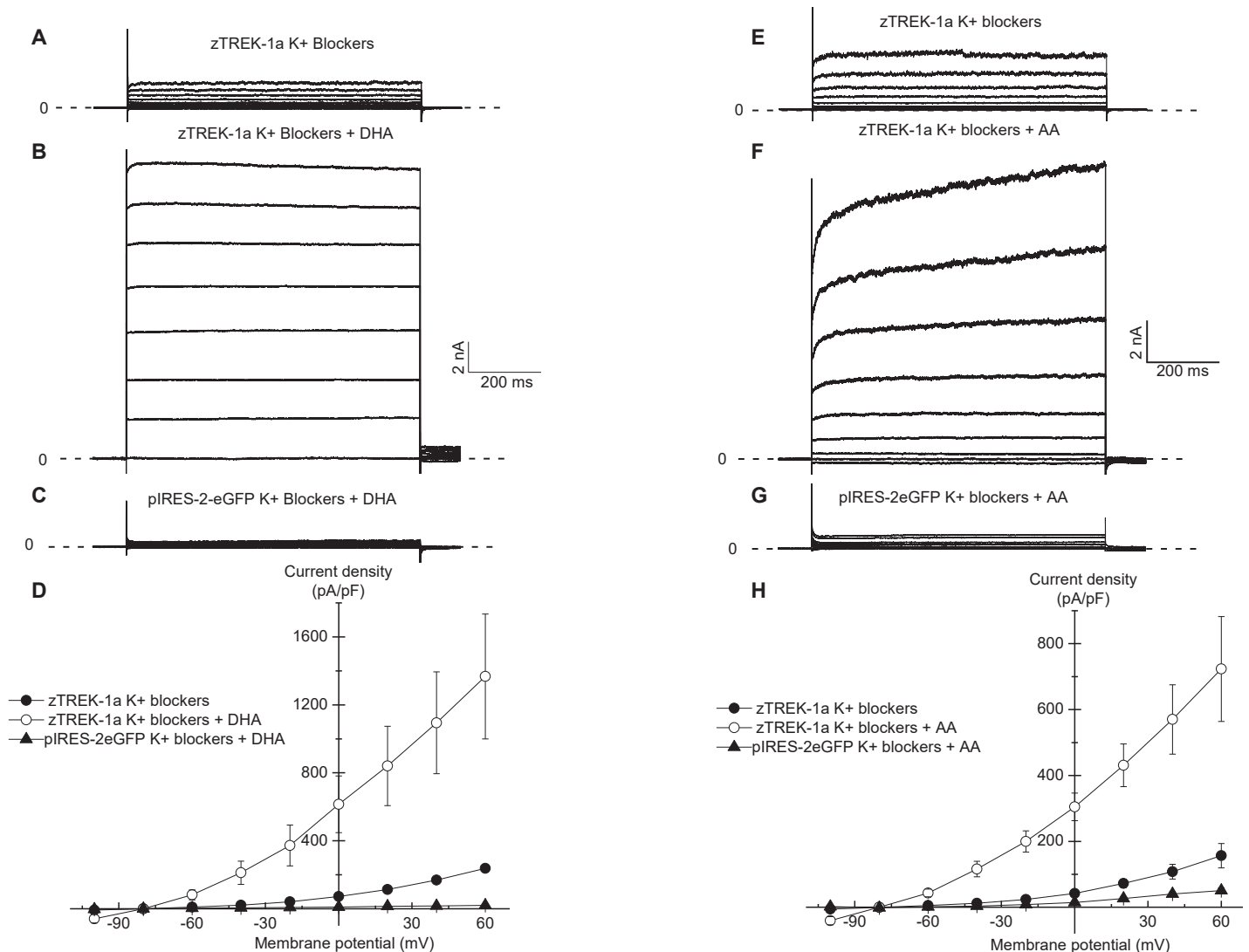


Figure 3: Effect of polyunsaturated fatty acids on zTREK-1a: Recorded currents in WC configuration by applying a voltage changes going from -100 to +60 mV. Recorded basal currents on HEK cells transfected with zTREK-1a PIREs-2eGFP in the presence of potassium cocktail blockers ($n=5$) (A) ($n=5$) (E), in the presence of potassium cocktail blockers and unsaturated fatty acid $10\mu\text{M}$ of Docosahexaenoic acid (DHA) ($n=5$) (B) or $10\mu\text{M}$ of arachidonic acid (AA) ($n=5$) (F). Recorded currents in transfected PIREs-2eGFP cells in presence of the potassium cocktail blockers and $10\mu\text{M}$ of each polyunsaturated fatty acid DHA ($n=5$) (C) or AA ($n=5$) (G) used as negative control. Corresponding Current/potential curves for each tested condition (D, H).

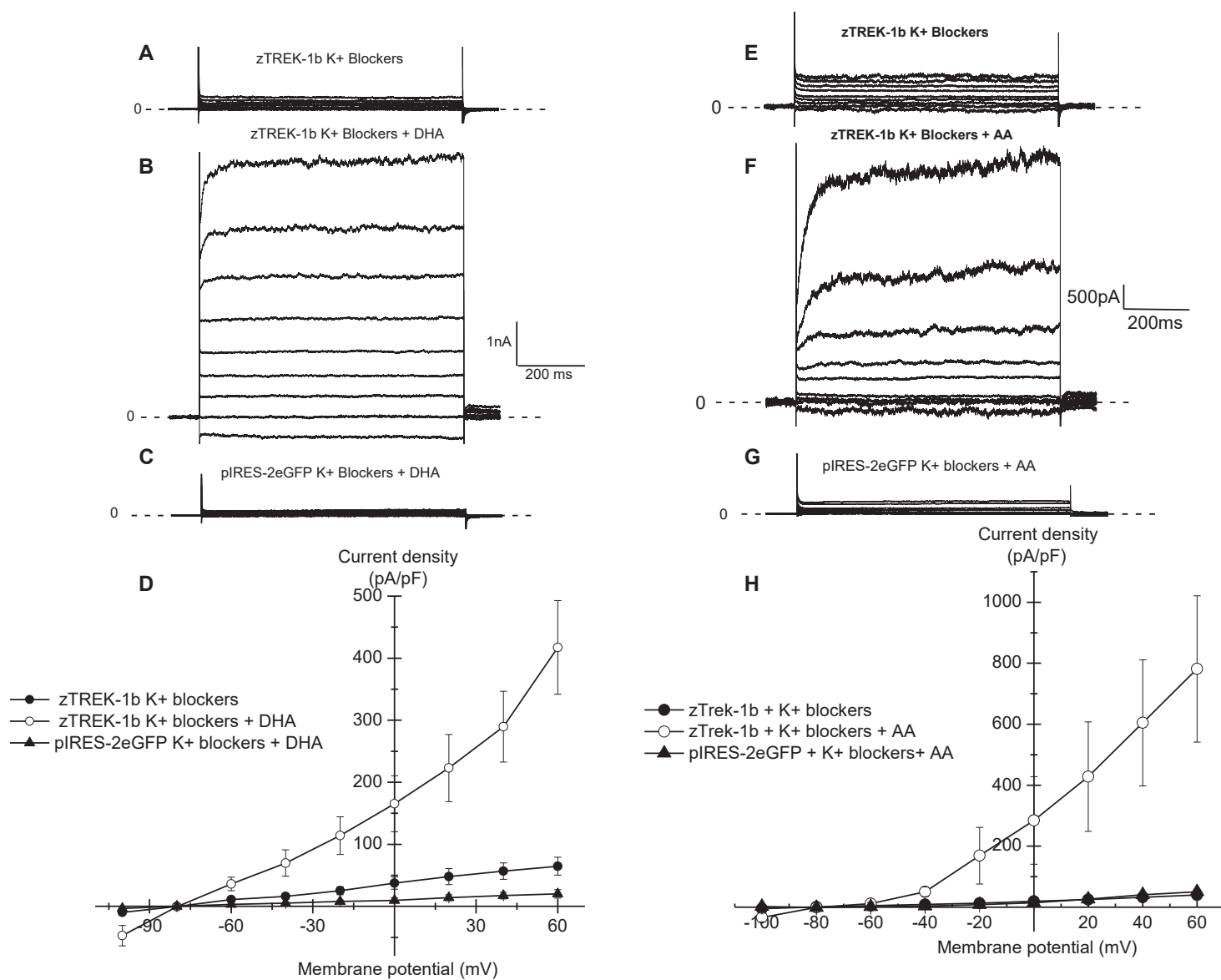


Figure 4: Effect of polyunsaturated fatty acids on zTREK-1b: Recorded currents in WC configuration by applying a voltage changes going from -100 to +60 mV. Recorded basal currents on HEK cells transfected with zTREK-1b PIREs-2eGFP in the presence of potassium cocktail blockers (n=7) (A) (n=5) (E), in the presence of potassium cocktail blockers and unsaturated fatty acid 10 μ M of Docosahexaenoic acid (DHA) (n=7) (B) or 10 μ M of arachidonic acid (AA) (n=5) (F). Recorded currents in transfected PIREs-2eGFP cells in presence of the potassium cocktail blockers and 10 μ M of each polyunsaturated fatty acid DHA (n=5) (C) or AA (n=5) (G) used as negative control. Corresponding Current/potential curves for each tested condition (D, H).

Polyunsaturated fatty acids are divided into 2 major groups: omega 3 and omega 6 fatty acids. These 2 groups are represented respectively by Docosahexaenoic acid (DHA) and arachidonic acid (AA).

We have tested the effect of 2 polyunsaturated fatty acids (PUFAs) AA and DHA on both channels zTREK-1a/b. The basal currents for zTREK-1a/b are respectively recorded by perfusing a cocktail of blockers (4-AP, TEA, glibenclamide, apamin, charybdotoxin) which inhibit a wide range of endogenous K⁺ channels, activated by PUFAs (Fig3 A,B,G,H_Fig4 A,B,G,H). Subsequently, we have perfused either AA or DHA. At 0mV potential, the current densities of zTREK-1a/b increase respectively by 8 fold (from 72.52 ± 3.48 pA/pF to 615.10 ± 166.87 pA/pF) and 4 fold (from 37.3 ± 9.8 pA/pF to 165.3 ± 45.1 pA/pF) in the presence of DHA (Fig3 C,G_Fig4 C,G). In the presence of AA at 0mV potential, the current densities of both channels (zTREK-1a/b) increase respectively 7 fold (from 42.35 ± 8.81 pA/pF to 304.70 ± 41.96 pA/pF) and 14 fold (from 19.7 ± 7.6 pA/pF to 284.7 ± 143.6 pA/pF) (Fig3 D,H_Fig4 D,H).

DHA and AA don't have an effect on the cells transfected with empty vector (PIERS_2eGFP). No increase of the recorded current densities of these cells in the presence of DHA and AA (Fig3 E,G,F,H_Fig4 E,G,F,H).

In the presence of AA and DHA, the significant increase of the current densities for zTREK-1a/b reflects their activation of the channels by PUFAs.

3.1.3 Effect of intracellular acidification on zTREK-1a and zTREK-1b:

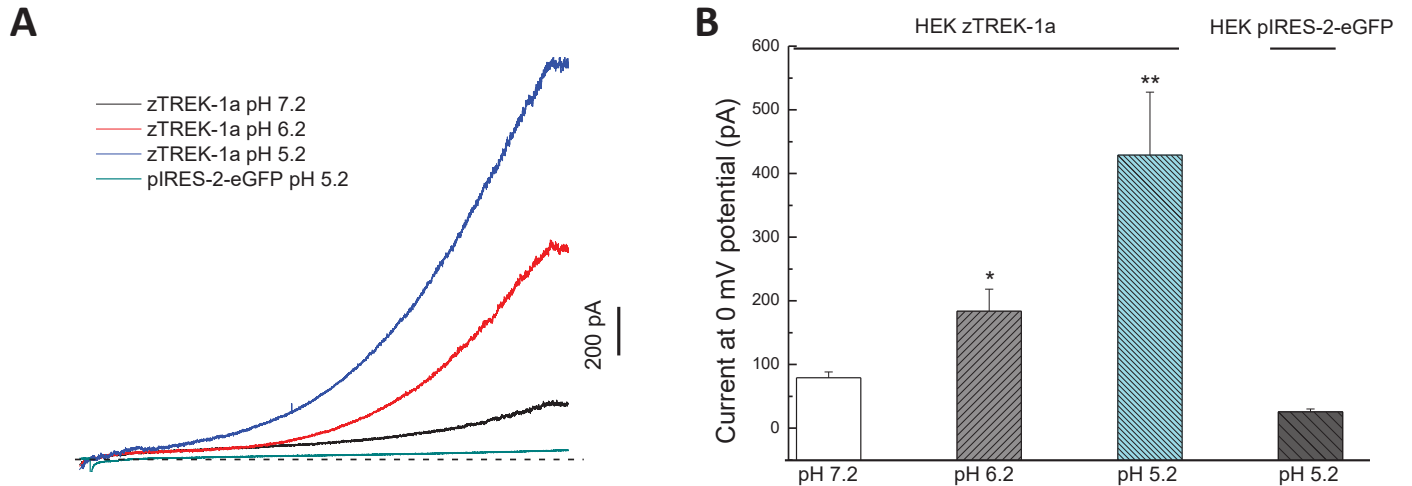


Figure 5: Effect of intracellular acidification on zTREK-1a: Recorded currents in IO configuration by applying a voltage ramp going from -100 to +100 mV. Recorded currents on HEK cells transfected with zTREK-1a PIREs-2eGFP at pH 7.2 (black line) at pH 6.2 (red line) at pH 5.2 (blue line) (A) (n=9) Recorded currents on HEK cells transfected with PIREs-2eGFP at pH 5.2 (green line) (A) (n=3). Corresponding potential graph at 0mV potential for each tested condition (B). * P value < 0.05, ** P value<0.01

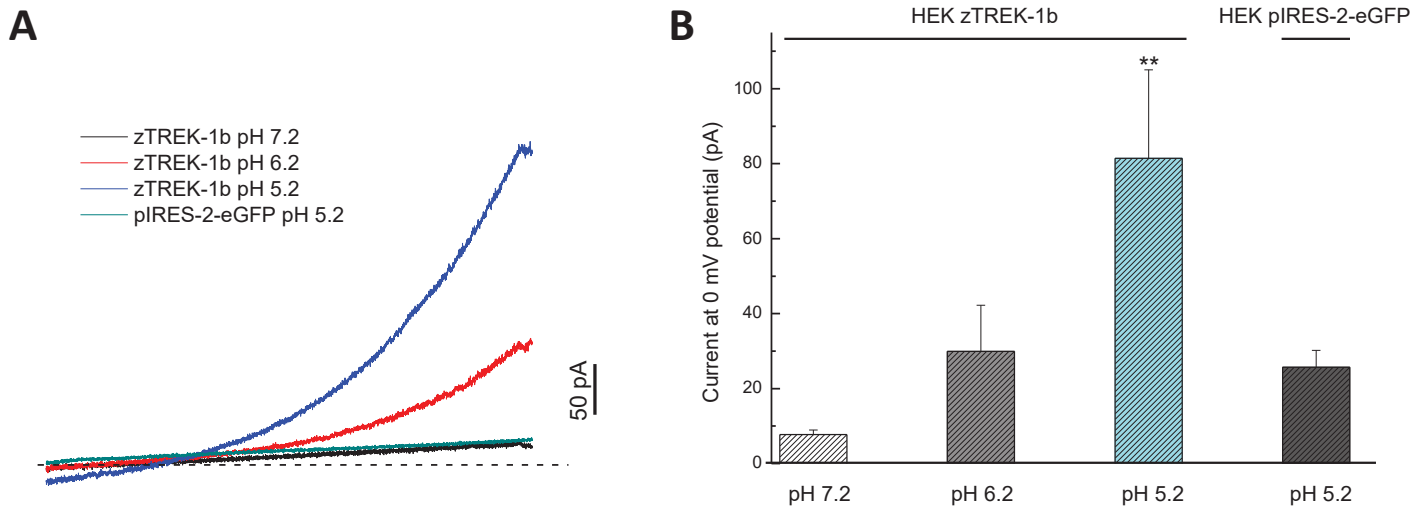


Figure 6: Effect of intracellular acidification on zTREK-1b: Recorded currents in IO configuration by applying a voltage ramp going from -100 to +100 mV. Recorded currents on HEK cells transfected with zTREK-1b PIREs-2eGFP at pH 7.2 (black line) at pH 6.2 (red line) at pH 5.2 (blue line) (A) (n=11) Recorded currents on HEK cells transfected with PIREs-2eGFP at pH 5.2 (green line) (A) (n=3). Corresponding potential graph at 0mV potential for each tested condition (B). ** P value<0.01.

To test the effect of intracellular acidification on zTREK-1a/b we have used IO configuration and we have decreased the pH of the perfused intracellular solution from pH7.2 to 6.2 then to 5.2.

An increase of the current amplitudes for both channels is reported by decreasing intracellular pH (Fig5 A, 6A). At 0mV potential, the current amplitudes for zTREK-1a increase from 79.1 ± 9.3 pA at pH 7.2 to 183.6 ± 34.7 pA at pH 6.2 and to 428.8 ± 99 pA at pH 5.2 while the control reach 25.7 ± 4.5 at pH 5.2 (Fig5 B) . At 0mV potential, the current amplitudes for zTREK-1b increase from 7.7 ± 1.2 pA at pH 7.2 to 29.9 ± 12.3 pA at pH 6.2 and to 81.5 ± 23.6 pA at pH 5.2 while the control reach 25.7 ± 4.5 at pH 5.2.

The significant increase of the current amplitudes for zTREK-1a/b by decreasing the intracellular pH reflects an activation of both channels by intracellular acidification.

3.1.4_ Effect of spadin on zTREK-1a and zTREK-1b:

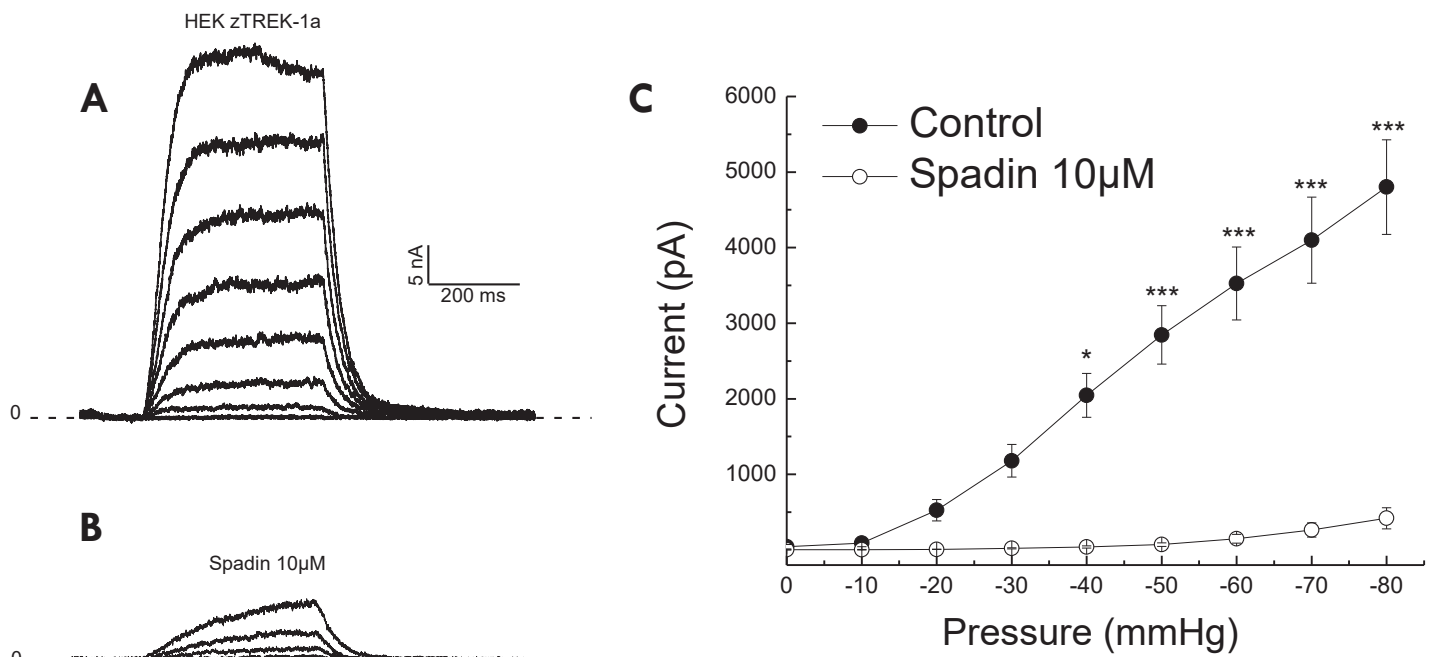


Figure 7: Effect of spadin on zTREK-1a: recorded currents in IO configuration by applying an increasing negative pressure protocol from 0 to -80 mmHg. Recorded currents on HEK cells transfected with zTREK-1a PIRE5-2eGFP (control condition) (n=7) (A), and in the presence of 10 μM of spadin (n=6) (B), their Corresponding current/pressure curves (C). * P value < 0.05, *** P value < 0.001.

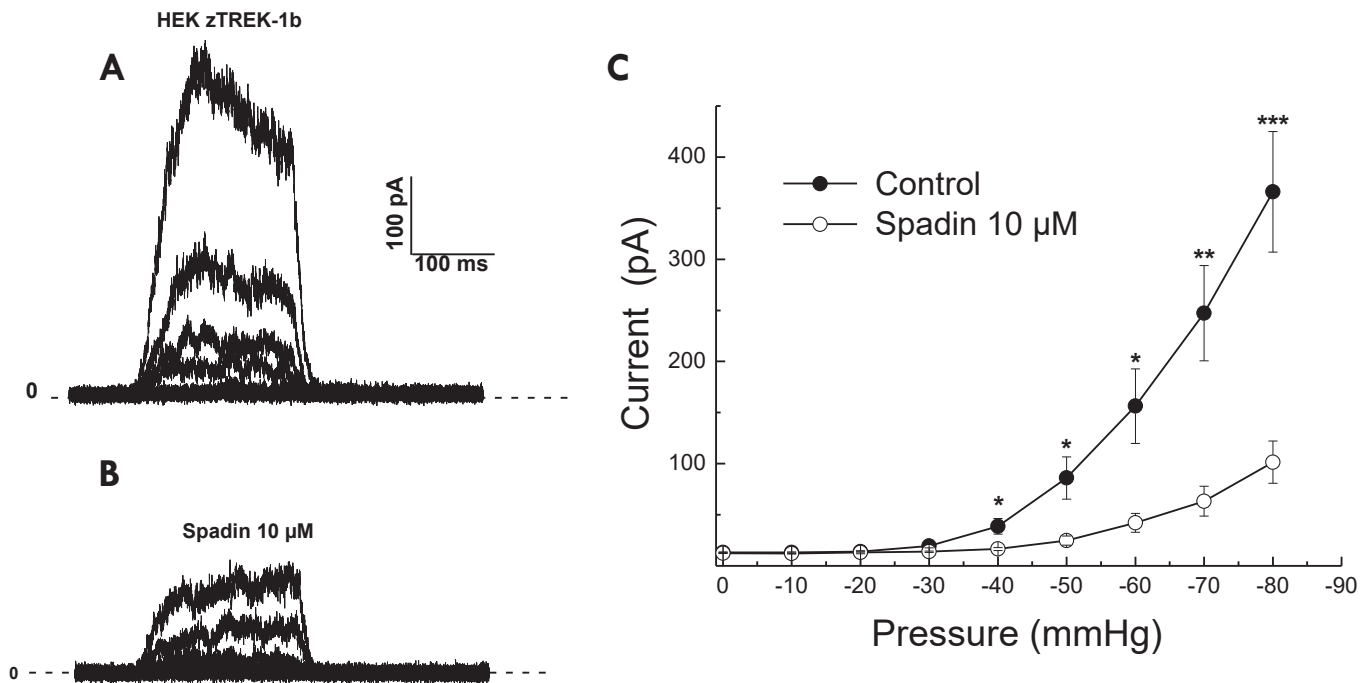


Figure 8: Effect of spadin on zTREK-1b: recorded currents in IO configuration by applying an increasing negative pressure protocol from 0 to -80 mmHg. Recorded currents on HEK cells transfected with zTREK-1b PIRE5-2eGFP (control condition) (n=19) (A) and in the presence of 10μM of spadin (n=18) (B), their Corresponding current/pressure curves (C). * Pvalue < 0.05, ** P value<0.01, *** P value < 0.001.

One of TREK-1 specific pharmacological inhibitor is spadin. The effect of this pharmacological agent is tested on both channels zTREK-1a/b.

Negative pressure protocol is applied at 0mV potential on HEK cells transfected with zTREK-1a/b in IO configuration in control conditions and in the presence of spadin (10 μM) in the extracellular compartment. The presence of spadin significantly decreases the current amplitudes for zTREK-1a/b at -60 mmHg respectively by 95% (from 3526 ± 482.4 pA to 148.4 ± 56.5 pA) and by 73% (from 156.3 ± 36.5 pA to 42 ± 9.2 pA). At -80 mmHg the significant

decrease of zTREK-1a/b current amplitudes reaches respectively 91% (from 4801.4 ± 624.9 pA to 419.2 ± 139.5 pA) and 72% (from 366.1 ± 59 pA to 101.5 ± 20.6 pA) (Fig7 A,B,D_Fig8 A,B,D).

The significant decrease of current amplitudes for zTREK-1a/b in the presence of spadin (10 μ M) suggests that this pharmacological agent has the ability to significantly inhibit both channels. Spadin will be efficient to be used for further experiments (*in vivo* and *ex vivo*).

3.2_ zTREK-1a and zTREK-1b expression in adult zf cardiomyocytes:

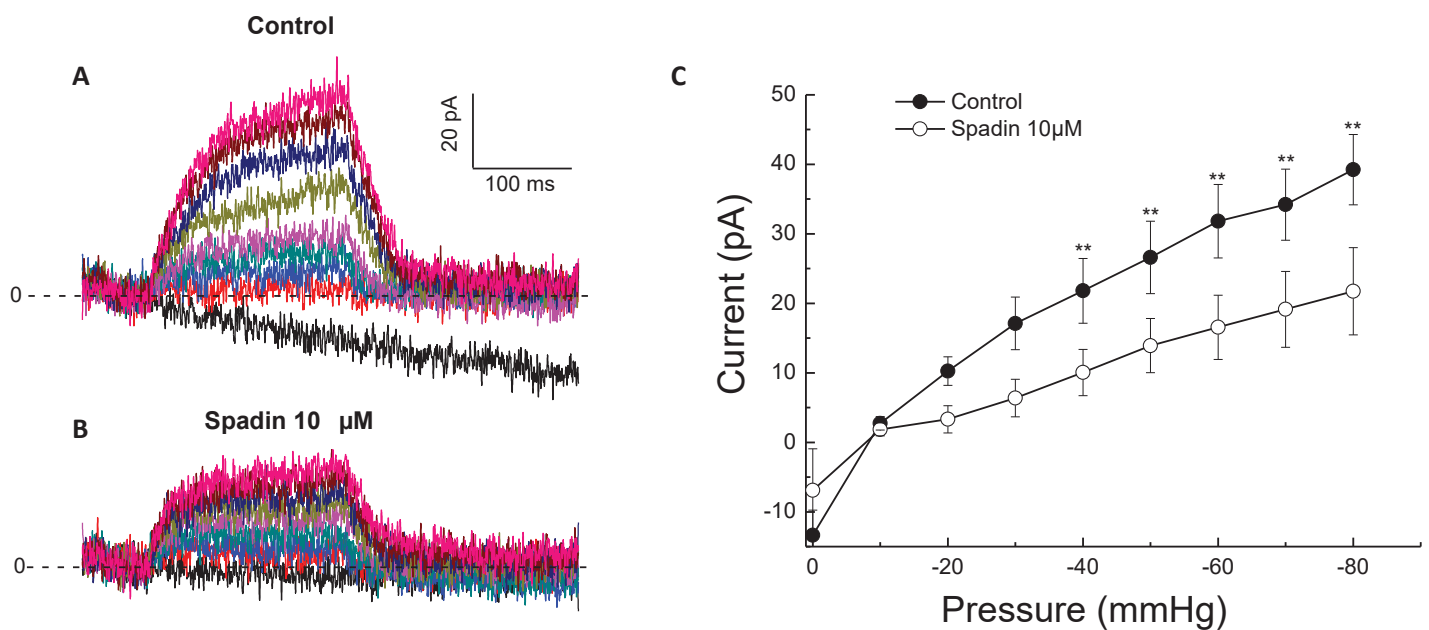


Figure 9: Effect of the membrane stretch and the spadin on zf cardiomyocytes primary culture: current traces recorded in CA configuration on zf cardiomyocytes by applying an increasing negative pressure protocol from 0 to-80 mmHg. Currents recorded in control condition (n=9) (A) in the presence of 10 μ M of spadin (n=9) (B). The corresponding current/pressure curves of all conditions (C). ** P value < 0.01.

We have established the biophysical and pharmacological properties of zTREK-1a/b: activation by membrane stretch, inhibition by spadin (10 μ M). We have used these properties to evaluate the expression of functional zTREK-1a/b channels in zf cardiomyocytes.

We are able to record currents in zf cardiomyocytes at 0mV potential using CA configuration and by applying a negative pressure protocol which goes from 0 to -80mmHg. The recorded current amplitudes increase by increasing negative pressure from -13.3 ± 3.6 pA at 0mmHg to 31.8 ± 5.3 pA at -60mmHg (39.2 ± 5.1 pA at -80mmHg) (Fig9 A,C). 10 μ M of spadin induces a significant inhibition of the recorded current amplitudes by 52% (16.5 ± 5.1 pA) at -60mmHg and by 45% (21.5 ± 6.9 pA) at -80mmHg (Fig9 B,C).

The presence of mechanically activated currents in zf cardiomyocytes which is significantly inhibited by spadin reflects the presence of zTREK-1 current. zTREK-1 current can be zTREK-1a or zTREK-1b or both.

3.3 Effect of the dominant negative zTREK-1 on zTREK-1a/b:

3.3.1 Effect of the dominant negative zTREK-1 deletion exon 4 (DN TREK-1 del ex4) on zTREK-1a and zTREK-1b:

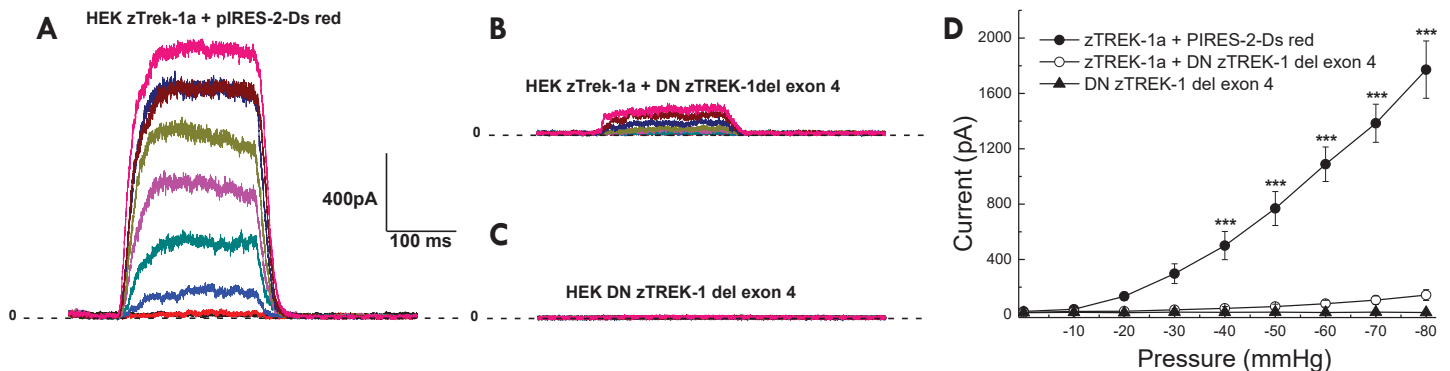


Figure 10: Effect of the DN zTREK-1 del ex4 on zTREK-1a: recorded currents in IO configuration by applying an increasing negative pressure protocol from 0 to -80 mmHg. Recorded currents on HEK cells cotransfected with zTREK-1a PIRES-2eGFP and PIRES Ds Red (n=6) (A) cotransfected with zTREK-1a PIRES-2eGFP and DN zTREK-1 del exon 4 PIRES Ds Red (n=15) (B), cells transfected only with DN TREK-1 del exon 4 PIRES Ds Red (n=6) (C). Their corresponding current/pressure curves (D). *** P value < 0.001.

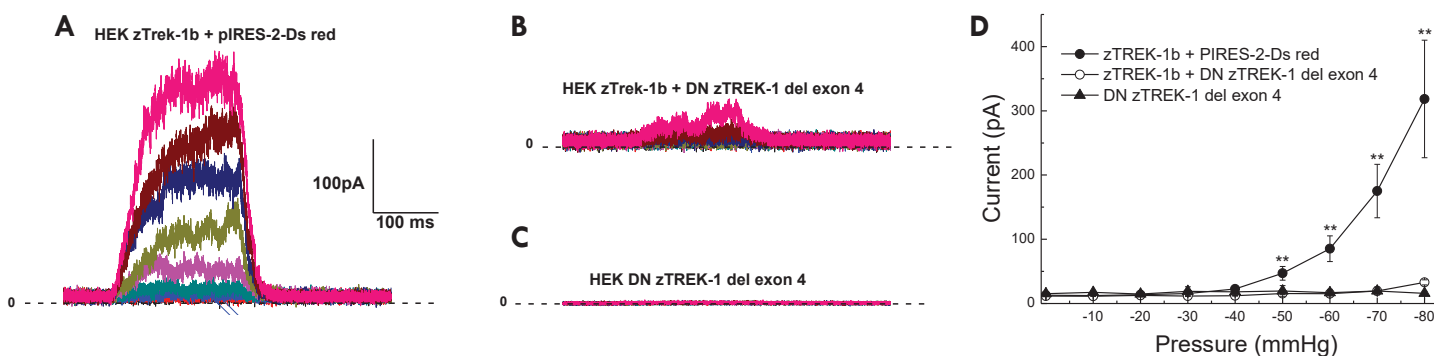


Figure 11: Effect of the DN zTREK-1 del ex4 on zTREK-1b: recorded currents in IO configuration by applying an increasing negative pressure protocol from 0 to -80 mmHg. Recorded currents on HEK cells cotransfected with zTREK-1b PIRES-2eGFP and PIRES Ds Red (n=10) (A) cotransfected with zTREK-1b PIRES-2eGFP and DN zTREK-1 del exon 4 PIRES Ds Red (n=7) (B), cells transfected only with DN TREK-1 del exon 4 PIRES Ds Red (n=6) (C). Their corresponding current/pressure curves (C). ** P value < 0.01.

In order to validate *in vivo* results that we will obtain on zf heart regeneration due to the pharmacological treatment, a genetic approach is important to realize. Genetic approach is based on using a conditional DN zf line that expresses a 4-HT inducible CreER and a floxed red fluorescent protein (RFP) stop cassette that targets dominant negative (DN) TREK-1 expression in the cardiomyocytes, under the cardiomyocyte specific promoter (*cmlc2a*) upon tamoxifen treatment. For that reason, we have generated a DN form of zTREK-1a/b (DN TREK-1 del ex4), as described by COWLES et al, by deleting the exon 4 from zTREK-1a WT sequence. exon 4 deletion, results in a reading frame shift leading to the generation of a premature stop codon, causing the formation of a truncated protein which contains only the first 3 exons (DN TREK-1 del ex4). The effect of DN TREK-1 del ex4 is tested by co-transfection with zTREK-1a/b

At 0mV potential, in IO configuration, the current amplitudes in cells co-transfected zTREK-1a/b + PIRE5 DsRed increase from 0 to 1087.7 ± 124.6 pA and 85.3 ± 20 pA respectively by increasing the negative pressure applied on the cell membranes from 0 to -60 mmHg. At -80 mmHg zTREK-1a/b current amplitudes reach 1771.6 ± 207.3 pA and 318.5 ± 91.5 pA respectively + PIRE5 Ds Red (Fig10 A,D_Fig11 A,D).

In the same conditions, co-transfection of zTREK-1a/b with the DN zTREK-1 del ex4 significantly decreases the current amplitudes for both channels respectively by 92% (from 1087.7 ± 124.6 to 80.1 ± 24.2 pA) and by 82% (from 85.3 ± 20 to 15.3 ± 0.90 pA) at -60mmHg. At -80mmHg this inhibition reaches 91% (from 1771.6 ± 207.3 to 142.2 ± 39 pA) for zTREK-1a + DN zTREK-1 del ex4, and 89% (from 318.5 ± 91.5 to 32.9 ± 3.85 pA) for zTREK-1b + DN zTREK-1 del ex4 (Fig10 B,D_Fig11 B,D).

We are not able to record currents in the cells transfected only with DN zTREK-1 del ex4 (Fig10 C,D_Fig11 C,D).

The significant decrease of the current amplitudes for zTREK-1a/b in the presence of the DN TREK-1 del ex4 suggests that this DN has the ability to significantly inhibit both channels.

The fact that we are not able to record currents in the cells transfected with DN TREK-1 del ex4 suggests that this DN doesn't form a functional channel on its own.

3.3.2 Effect of the dominant negative zTREK-1 deletion exon 3 (DN zTREK-1 del ex3) on zTREK-1a:

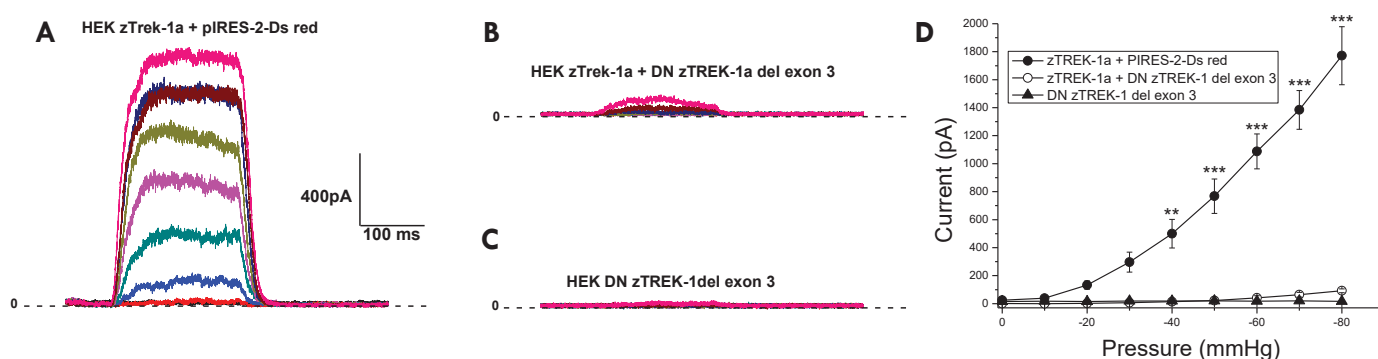


Figure 12: Effect of the DN zTREK-1 del ex3 on zTREK1a: currents traces recorded in IO configuration by applying an increasing negative pressure protocol from 0 to -80 mmHg. Current recorded in control condition HEK cells cotransfected with zTREK1a PIRES-2eGFP and PIRES Ds Red (A) with zTREK1a PIRES-2eGFP and DN zTREK1 del ex3 PIRES Ds Red (B), cells transfected only with DN TREK1 del ex3 PIRES Ds Red (C). The corresponding current/pressure curves of all conditions (D). ** P value < 0.01, *** P value < 0.001.

We have generated another DN form of zTREK-1a/b as described by COWLES et al by deleting exon 3 from zTREK-1a WT sequence. Deleting exon 3, results in reading frame shift leading to the generation of a premature stop codon, causing the formation of a truncated protein which contains only the first 2 exons (DN TREK-1 del ex3).

The DN TREK-1 del ex3 is tested by cotransfection with zTREK-1a/b. Cotransfection of the DN TREK-1 del ex3 with zTREK-1b may be toxic since the coexpression of both channels in cells results in cell death.

At 0mV potential, in IO configuration the current amplitudes in the cells cotransfected zTREK-1a + PIRE5 DsRed increase from 0 to 1087.7 ± 124.6 pA by increasing negative pressure applied on the cell membrane from 0 to -60 mmHg. At -80 mmHg current amplitudes reach 1771.6 ± 207.3 pA (Fig12 A, D).

In the same conditions, the co-transfection of zTREK-1a with the DN zTREK-1 del ex3 significantly decreases the current amplitudes by 96% (from 1087.7 ± 124.6 pA to 41.3 ± 15.7 pA) at -60mmHg. At -80mmHg this inhibition reaches 94% (from 1771.6 ± 207.3 pA to 92 ± 13.9 pA) (Fig12 B,D). We are not able to record currents in the cells transfected only with DN zTREK-1 del ex3 (Fig12 C, D). The significant decrease of zTREK-1a current amplitudes in the presence of the DNTREK-1 del ex3 suggests that this DN has the ability to significantly inhibit zTREK-1a channel. The fact that we are not able to record currents in the cells transfected with the DN TREK-1 del ex3 suggests that this DN doesn't form a functional channel on its own.

3.4_ Validation of mouse TREK-1 antibody:

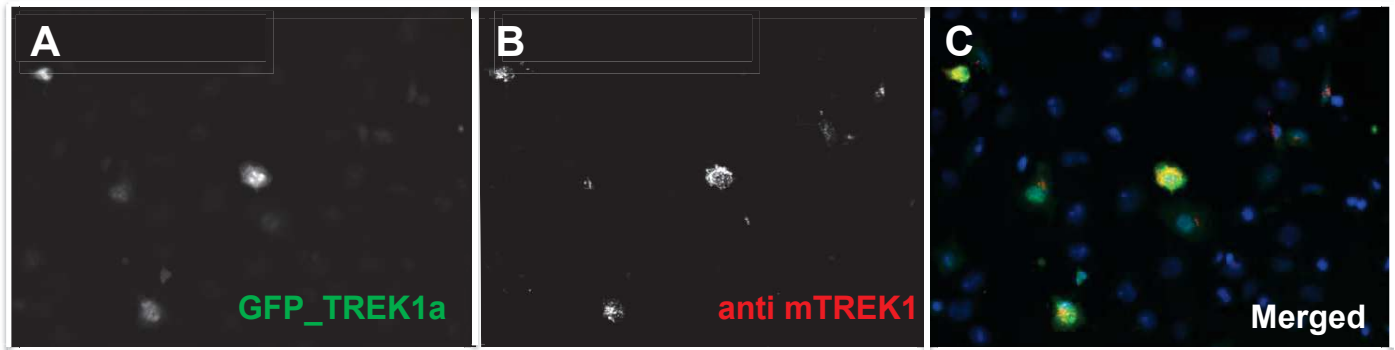


Figure 13: Validation of mouse TREK-1 antibody in U2OS cells transfected with zTREK-1a: using anti GFP antibody (green) (A) anti mouse TREK-1 (mTREK-1) antibody (red) (B). Merged anti GFP antibody (green) with mouse TREK-1 antibody (red) (C).

There is no commercial zebrafish TREK-1a/b antibody. For that reason, we wanted to test the efficiency of a mouse TREK-1 (mTREK-1) antibody. We have performed an immunofluorescence using mouse TREK-1 antibody on Human Bone Osteosarcoma Epithelial Cells (U2OS) transfected with either zTREK-1a or zTREK-1b. Our results show that mouse TREK-1 antibody recognizes the cells that express zTREK-1a (Fig13). However, mouse TREK-1 antibody doesn't recognize the cells transfected with zTREK-1b (data not shown). This suggests that mouse TREK-1 (mTREK-1) antibody recognizes specifically zTREK-1a.

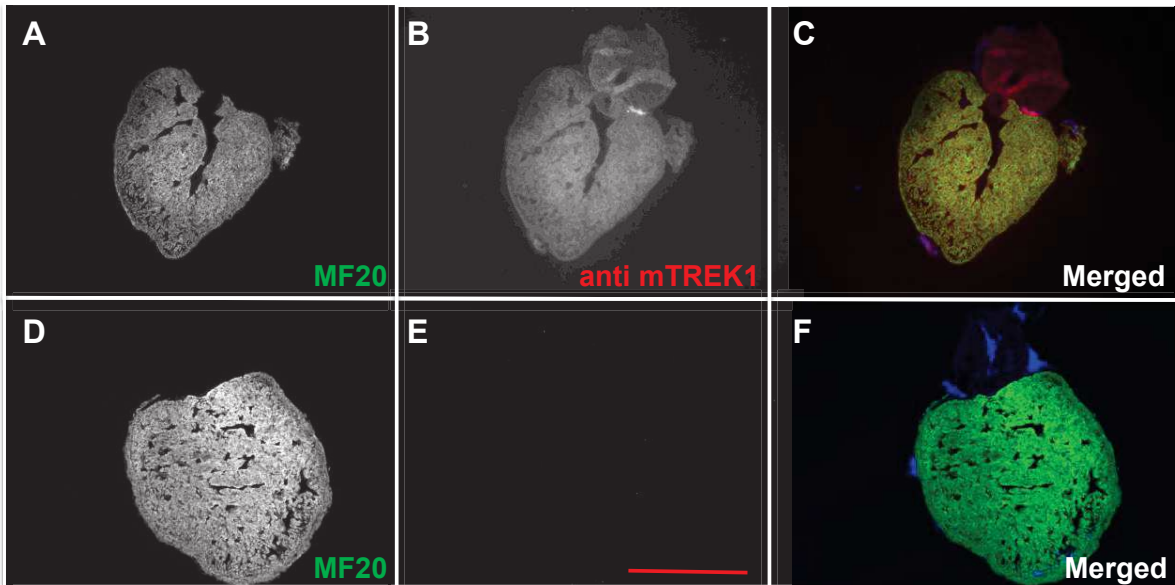


Figure 14: Validation of mouse TREK-1 antibody on zebrafish heart section: using the anti-myosin heavy chain antibody (MF20) (green) (A,D), anti-mouse TREK-1 (mTREK-1) antibody (red)(B), without anti mTREK-1 antibody (with secondary antibody anti mouse alexa 594) (E). Merged MF20/anti mTREK-1 (C), merged MF20/without mTREK-1(with secondary antibody anti mouse alexa 594) (F).

In order to validate mTREK-1 antibody on heart sections, we have realized an immunohistochemistry on zf heart sections using mouse TREK-1 antibody and anti MF-20 antibody which will label the cardiomyocytes. Our results show that mouse TREK-1 antibody labels the ventricle and the outflow tract (Fig 14 A, B, C). This suggests that zTREK-1a may be expressed in these tissues. In order to overcome the unspecific effect of the secondary antibody (anti mouse alexa 594), we have performed immunohistochemistry on zf heart sections using secondary antibody (anti mouse alexa 594) and anti MF-20 which will label the cardiomyocytes. Our results show that without mTREK-1 primary antibody, its secondary antibody doesn't have the ability to label the heart sections (Fig14 D, E, F). This suggests that mTREK-1 specifically recognizes zTREK-1a which is localized in the heart.

4_ Discussion:

We have characterized zTREK-1a/b in order to obtain their biophysical and pharmacological properties and to compare it to those already described in mammals. This characterization allows us to determine the properties of zTREK-1a/b which are used to determine whether those channels are a/b are expressed in zf heart, more precisely in a particular cell type which is cardiomyocytes. It will also allow us to test the efficiency of the pharmacological agents (spadin) as well as the efficiency of the DN forms of the channels.

Our data show that zTREK-1a/b are potassium channels, their reversal potential are around -70 mV which is quite close to the K^+ equilibrium potential. zTREK-1a/b share biophysical and pharmacological properties with the mammalian TREK-1. They are both activated by increased negative pressure eventually induced by membrane stretch. Our data show an increase of zTREK-1a/b current amplitudes between CA and IO configuration (in which the interaction channel/cytoskeleton is removed), this suggests that they are both inhibited by the cytoskeleton as described for mammalian TREK-1 (Patel, Honore et al. 1998, Maingret, Patel et al. 1999, Veale, Rees et al. 2010, Moha ou Maati, Peyronnet et al. 2011, Rinne, Renigunta et al. 2014, Cowles, Wu et al. 2015). Like mammalian TREK-1, zTREK-1a/b are both activated by intracellular acidification and by PUFAs. Adding to that, PUFAs are implicated in cardiovascular diseases accompanied with increase of ROS production as well as an increase of intracellular acidification (Ander, Dupasquier et al. 2003, Duffy, Ashton et al. 2004, Wang, Xiong et al. 2016). In addition, in most cardiovascular diseases, the balance between cardiomyocyte loss and renewal is disturbed leading to heart stiffness due to fluid overload in patients suffering from heart failure (Shotan, Dacca et al. 2005,

Cotter, Metra et al. 2008), suggesting that mechanical stress may have a key role in cardiovascular diseases.

We have demonstrated that zTREK-1a/b have polymodal activation. They are activated by membrane stretch, PUFAs and intracellular acidification. These parameters are modified in most cardiovascular diseases, and during heart regeneration after resection (Chao, Jin et al. 2002, Raya, Koth et al. 2003, Han, Zhou et al. 2014, Afzali, Ruck et al. 2016). This suggests that zTREK-1a/b may play an important role in pathophysiological state in zf heart especially during heart regeneration.

Like mammalian TREK-1, zTREK-1a/b appear to be significantly inhibited by pharmacological agents such as spadin (Mazella, Petrault et al. 2010, Moha ou Maati, Peyronnet et al. 2011, Veysiere, Moha Ou Maati et al. 2015, Djillani, Pietri et al. 2017). This suggests that spadin is efficient to be used *in vivo* to evaluate the implication of zTREK-1a/b during zf heart function, physiology and regeneration.

After we have established that zTREK-1a/b are activated by membrane stretch and they are both inhibited by spadin, we have used these two properties to check if they are expressed in zf cardiomyocytes. On freshly dissociated zf cardiomyocytes we are able to record a mechanosensitive current at 0mV, reflecting the presence of potassium mechanosensitive ion channel. In the presence of spadin (10 μ M), the mechanosensitive current in the cardiomyocytes significantly decreases by 50%. This suggests the presence of either zTREK-1a or zTREK-1b or both channels in zf cardiomyocytes. Like mammalian TREK-1, functional zTREK1-a/b channels are expressed in zf cardiomyocytes. The resident current corresponds to a mechanosensitive potassium ion channel which doesn't represent a target for spadin such as TREK-2 (Gierden, Hassel et al. 2012) because

it has been shown that spadin is specific inhibitor for TREK-1 among the K_{2p} family (Moha Ou Maati, Veyssiere et al. 2012).

In vivo experiments, in which we will use the pharmacological agent (spadin) need to be supported by a genetic approach. For that reason, we have generated a DN from of zTREK-1a/b (zTREK-1 del ex4) as described by Vaele EL et al et al. We have tested the effect of zTREK-1 del ex4 on zTREK-1a/b using electrophysiological approach. Our results show that zTREK-1a/b are significantly inhibited by DN TREK-1 del ex4 so it will be efficient to be used for the genetic approach.

DN TREK-1 del ex 4 was generated according to Veale EL et al, by deleting the ex4 from, zf WT zTREK-1a sequence which leads to the generation of a premature stop codon, resulting in a truncated protein containing only the first 3 exons. The effect of the DN TREK-1 del ex4 on zTREK-1a/b is due to a cytoplasmic retention of the heterodimers formed by WT zTREK-1a/b and DN TREK-1 del ex4, inhibiting their membrane trafficking, decreasing by then their membrane expression. This explains the decrease of their current amplitudes in the presence of the DN TREK-1 del ex4 as described in 2015 by Cowles CL et al. Cell death upon coexpression of the DN TREK-1 del ex3 and zTREK-1b may be due to the high cytotoxicity of DNTREK-1 del ex3/zTREK-1b heterodimers.

We have also validated mTREK-1 antibody as a TREK-1 antibody which specifically recognizes zTREK-1a and it will be efficient to be used for further experiments.

5_ Perspectives:

The sequence alignment of the C-terminal tail of zTREK-1a/b with human and mouse TREK-1 show that it is a highly conserved region. For that reason it will be interesting to investigate other signalization pathways by which zTREK-1a/b will be activated or inhibited, such as the effect of PKG, PKA, PKC, heat, and anesthetics. It will also be important to check protein interaction between zTREK-1a/b and POPDC, AKAP 150, as well as the different proteins especially the ones that form the cytoskeleton and different mechanosensors since they are implicated in the transmission of the mechanical signal into the cell.

It will be interesting to test the effect of the DN TREK-1 del ex4 on other biophysical and pharmacological properties of zTREK-1a/b.

It will also be interesting to check the inhibition of zTREK-1a/b by DN TREK-1 del ex4 *ex vivo*. This experiment should be performed on freshly dissociated cardiomyocytes coming from DN zf line treated with tamoxifen or ETOH (as a control).

It will be important to study the ability of zTREK-1a/b to heterodimerize together and within other channels that belong to K_{2p} family such as zf TREK-2 and zf TRAAK. This will allow us to further investigate the biophysical and pharmacological properties of heterodimers and compare it to mammalian heterodimers properties.

It will also be important to test the effect of antinociceptive drugs such as caffeine esters on zTREK-1a/b. These antinociceptive drugs are used as mammalian TREK-1 activator in order to inhibit pain.

Chapter 2

Implication of zTREK-1a/b during zebrafish heart regeneration

1_ Introduction:

Unlike neonatal mammals and other species like zf, adult mammals fail to naturally regenerate their heart after a massive cardiomyocyte loss. However, the mechanism of zf heart regeneration is quite similar to neonatal mammal heart regeneration. Lineage tracing for both species reveals that heart regeneration in both cases occurs through dedifferentiation of preexisting cardiomyocytes. Cardiomyocyte dedifferentiation is characterized by a disassembly of cardiomyocyte sarcomeres, allowing them to proliferate in order to redifferentiate and repair the damaged part of the heart (Jopling, Sleep et al. 2010, Chablais, Veit et al. 2011, Porrello, Mahmoud et al. 2011, Haubner, Adamowicz-Brice et al. 2012). Zf and neonatal mouse heart regeneration are regulated with similar mechanisms. In both species, hypoxia increases cardiomyocyte dedifferentiation and proliferation, promoting heart regeneration. Hypoxia induces the regulation of HIF-1 α expression, promoting cardiomyocytes proliferation. Inhibition of HIF-1 α results in a failure of both species to regenerate their heart (Kido, Du et al. 2005, Ziello, Jovin et al. 2007, Jopling, Sune et al. 2012, Puente, Kimura et al. 2014). Zebrafish heart regeneration and neonatal mouse heart regeneration is negatively regulated by p38 and its upstream effectors. Downregulation of p38 results in cardiomyocyte proliferation a crucial step for heart regeneration (Engel, Schebesta et al. 2005, Jopling, Sune et al. 2012).

However, when neonatal mice reach the age of 7days, like adult mammals, they fail to naturally regenerate their heart after MI (Haubner, Adamowicz-Brice et al. 2012). Interestingly, during mouse and zf embryonic development, cardiomyocytes are in hyperplastic phase, where they have the ability proliferate. Soon after birth, mammalian cardiomyocytes switch from hyperplasia to hypertrophy where they can't proliferate and they increase in size. After

cardiac injury, adult mammalian cardiomyocytes push their hypertrophic response leading to pathological hypertrophy. In parallel, under the same stress after heart amputation or resection, zebrafish and neonatal mouse cardiomyocytes have the ability to dedifferentiate and switch to hyperplastic phase. This mechanism allows cardiomyocyte dedifferentiation followed by proliferation, resulting in repairing the damaged part of the heart (Matrone, Tucker et al. 2017). In addition, recent studies showed that controlling environmental and molecular factors allows adult mammals to switch their hypertrophic response into hyperplastic response after cardiac injury enhancing their heart regeneration. This switch doesn't occur naturally, it requires the control of environmental factors and the stimulation of signalization pathways such as ERK pathway that allow cardiomyocyte proliferation to promote heart regeneration. This let us think that heart regeneration in adult mammals has been blocked/inhibited. Adding to that, recent studies showed that human ventricular unloading to patients suffering from severe heart failure by using a ventricular assist device, results in cardiomyocyte proliferation that will lead to an improvement of the heart patient's function, prognosis and life style (Zafeiridis, Jeevanandam et al. 1998, Birks, Tansley et al. 2006). For that reason we suspect that mechanical stress that will induce hypertrophy in adult mammals will induce heart regeneration in neonatal mammals and zebrafish. This strongly supports our hypothesis suggesting the implication mechanosensors during zf heart regeneration.

Without surgical intervention and without controlling environmental and molecular factors, adult mammals develop pathological hypertrophy after MI. However, it has been shown that mechanosensors are overregulated in mammalian cardiomyocytes after hypertrophy.

Among mechanosensors, TRPC6 was reported to be overexpressed in the cardiomyocytes after heart failure. Overexpression of TRPC6 leads to the activation of calcineurin NFAT pathway, enhancing the expression of hypertrophic genes causing hypertrophy. However, it has been shown that TRPC6 inactivation through its phosphorylation by PKG at Threonine 69 results in an inhibition of TRPC6. Inhibition of TRPC6 leads to an inhibition of calcineurin NFAT pathway, resulting in anti-hypertrophic activity (Kuwahara, Wang et al. 2006, Nishida, Watanabe et al. 2010).

Another mechanosensor that was shown to be overexpressed during pathological hypertrophy in adult mammalian cardiomyocytes is TREK-1. Interestingly, it has been shown an increase of mechanical stress on the heart during hypertrophy as well as an increase of cardiac output (Rossi and Carillo 1991, Ruwhof and van der Laarse 2000). In addition, an increase of intracellular acidification was reported in pressure overloaded hypertrophied hearts (Tajima, Bartunek et al. 1998). The increase of mechanical stress on the heart as well as the increase of heart intracellular acidification, present 2 potential activators for TREK-1, which is upregulated during hypertrophy in adult mammals. However, the signalization pathway in which TREK-1 is implicated during pathological hypertrophy is not well known (Cheng, Su et al. 2006, Wang, Zhang et al. 2013). Interestingly, similar mechanisms occur after zebrafish heart amputation: an increase of heart hemodynamic force and intracellular acidification are observed (Chao, Jin et al. 2002, Raya, Koth et al. 2003, Han, Zhou et al. 2014). Adding to that, TREK-1 is known to be a potassium channel, implicated in different cellular processes such as proliferation and differentiation, 2 important processes for heart regeneration. This suggests that TREK-1 may play a key role during heart regeneration, for that reason we will investigate the role of zTREK-1a/b during zebrafish heart regeneration.

2_ Materials and methods:

2.1_ Making an antisense RNA probes for *in situ* hybridization:

The plasmids containing zTREK-1a/b are linearized using the EcoRI enzyme. 1 µg of the linearized DNA was used to synthesize the antisense RNA probe using the DIG RNA labeling kit (SP6/T7) from Roche (Ref: 11175025910). The RNA probes are then checked on an electrophoresis gel (agarose gel 1%). The RNA probes concentration are established with the nanodrop.

2.2_ *In situ* hybridization:

Zf embryos are fixed at different developmental stages in 4% paraformaldehyde (PFA) in PBS overnight at 4°C. The next day the embryos are dehydrated through washes at RT with solutions with increased concentrations of methanol (MeOH) in PBS 1% tween 20 (PST) to reach 100% MeOH then the embryos are placed over night at -20°C in MeOH. The embryos are then rehydrated through washes with solutions with decreased concentrations of methanol (MeOH) in PBST to reach 100%PBST. The embryos are then permeabilized with the proteinase K (stock 10mg/ml; dilution 1:1000) at RT. The exposure time of the proteinase k depends on the age of the embryos: 20 min for 3 dpf embryos, 25 min for 3 dpf embryos, 30 min for 5 dpf embryos. The hybridization is then performed with the DIG labeled antisense RNA probe in hybridization solution at 65°C overnight. The next day the embryos are incubated for 3 hours at RT with blocking buffer then incubated overnight at 4°C with anti-DIG antibody diluted in blocking buffer (1:2000). The revelation is performed by a colorimetric reaction using the BM purple substrate in AP buffer.

2.3_ Zebrafish heart cDNA:

2.3.1_ Embryonic heart cDNA:

Embryonic hearts are extracted according to Lombardo et al (Lombardo.V et al 2015). The embryos are sacrificed in 1X tricaine solution and then they are put in a L15 medium with 10%FBS and 1X tricaine. The hearts from zebrafish embryos are dissected and collected manually through a 19G needle , this allow to separate the hearts from the rest of the embryos based on the differential adhesion properties of zebrafish embryonic hearts compared to the rest of the embryonic tissues. The total RNA are extracted from the collected hears using the Quiagen RNeasy Mini Kit. Library cDNA is made by reverse transcriptase (RT) PCR on the total heart RNA obtained previously.

2.3.2_ Adult heart cDNA:

The fish are sacrificed in 1X tricaine solution in fish medium (E3). The fish is placed in the groove of a sponge, the hearts are then extracted using forceps. The extracted hearts are homogenized and lysed in trizol using a 1 mL syringe with a 27G needle. The trizol was then separated from the rest of the homogenized tissue by adding chloroform. We took the transparent layer and we have proceeded to RNA precipitation through isopropanol treatment. The precipitated RNA was then washed with 70% ethanol (ETOH) and dissolved in RNAase free water. The RNA concentration was measured using the nanodrop. Then the heart's cDNA was made by RT PCR on heart's RNA obtained previously.

2.4 Zebrafish heart amputation:

The fish surgery will be done according to Joping.C et al 2010 (Jopling, Sleep et al. 2010). The fish are anesthetized in a 0.5X tricaine solution in fish medium (E3). The fish is placed in the groove of a sponge. The skin and the muscle are removed and the pericardial sac is cut then we push gently on the fish abdominal. Once the heart pops out, we cut it with iridectomy scissors (around 20% of the ventricular apex). After surgery the fish is reanimated for 1 min and then put back in the water system.

2.5 Zebrafish pharmacological treatment:

The fish are anesthetized in a 0.5X tricaine solution in fish medium (E3). The fish is placed in the groove of a sponge. The intraperitoneal injection on fish (with E3 or 800 μ M of spadin) is performed using a 27G needle. The injected volume is around 100 μ l. After injection the fish are put back in the system overnight. Injections are performed during 30 days post amputation (dpa). Then the hearts are extracted and prepared for sectioning.

2.6 Preparing hearts for sectioning:

At different times points, the hearts are extracted and fixed with 4% paraformaldehyde (PFA) overnight at 4°C followed by dehydration through washes with solutions with increased concentrations of methanol (MeOH) to reach 100% then the hearts are placed over night at -20°C in MeOH. The hearts are then rehydrated through washes with solutions with decreased concentrations of methanol (MeOH) then place 30% sucrose in PBS overnight at 4°C , afterwards they are imbedded in Optimal cutting temperature compound (OCT) and frozen at -20°C overnight for sectioning. The sections of 10 μ m each are done in the Institute for

neuroscience of Montpellier (INM) using a microtome. The slides are then stored at -20°C until we use them for experiments.

2.7_ Immunohistochemistry:

Immunohistochemistry (IHC) is done on 10µm zf heart sections. In order to permeabilize the slides and for more effectiveness the slides are placed in a DAKO antigen retrieval solution in a pressure cooker for 15 minutes (min). The slides are then cooled down and then washed 3 times in PBS for 5 min. To block the antibody's unspecific interactions, the slides are blocked with a blocking buffer (5% fetal bovine serum (FBS), 1% bovine serum albumin (BSA) in PBT for 1 hour. The slides are then incubated with the primary antibody diluted in blocking buffer at 4°C overnight (anti MF20 diluted 1:25). The slides are then washed 3 times with PBT for 5 min each and then incubated with the secondary antibody diluted in blocking buffer at 37°C for 3 hours (anti mouse alexa 488 diluted 1:200) . Afterwards the slides are washed 3 times with PBT for 5 min each. To decrease the fluorescence background the slides are treated with sudan black for 4 min then washed with PBT to get rid of the sudan black. Slides are then incubated for 10 min with 4',6-diamidino-2-phenylindole (DAPI) diluted 1:5000. The slides are then mounted in ProLong™ Diamond Antifade Mountant.

2.8_ AFOG staining:

After drying out the slides at room temperature, they are fixed in Bouin solution at 60 °C. The slides are then rinsed and incubated in 1% phosphomolybdic acid which will serve for binding between tissue structures. Afterwards the slides will be rinsed then incubated in AFOG staining solution. The AFOG staining solution (aniline blue, acid fuchsin and Orange G) will

serve to stain the different tissue compounds (Muscle will be in red, collagen in blue and the fibrin in red).

2.9_ Immunofluorescence:

Adult zf cardiomyocytes are cultured and coated as described previously. After 16 hours of incubation at 32°C, the cardiomyocytes are washed 3 quick times in PBS 1X than fixed in 4%PFA in PBS 1X for 2 hours at room temperature (RT) followed by 3 washes in PBS1X +0.5% triton for 10 minutes each for permeabilization. The cells are incubated with the primary antibody (anti MF20 (1:25) and anti-TRE K-1 (1:1000)) for 1hour and a half at RT followed by 3 washes in PBS1X +0.5% triton for 10 minutes each. Then the cells are incubated with the secondary antibody (anti mouse alexa 488 (1:200) and anti-rabbit alexa 495 (1:200)) followed by 3 washes in PBS1X +0.5% triton for 10 minutes each then the nuclei are stained with DAPI 20 minutes at RT the slide are then mounted with fluorosheild. We proceed to immunofluorescence directly after fixation.

2.10_ Imaging:

We used the xyt mode (2D) of the confocal microscope leica TCS SP-8 to perform images for fluorescence labelling. We used the 488 nm excitation laser with and emission of 505 nm to detect the green fluorescence obtained due to the secondary antibody coupled to alexa fluor 488, we also used the 561 nm excitation laser with and emission of 600 nm to detect the red fluorescence obtained due to the secondary antibody coupled to alexa fluor 594 with a 10 X and 20 X objectives for the imaging on heart section and a 100 X objective for imaging on cardiomyocyte primary culture.

2.11_ Generating a transgenic conditional dominant negative TREK-1 del ex4 fish line:

2.11.1_ Construct:

The construct is generated using tol2 kit based on site-specific recombination-based cloning (multisite Gateway technology). The gateway technology is based on the recombination between 3 entry vectors. The 3 entry clones are divided into 5' entry clone, the middle entry clone and the 3' entry clone.

The middle element (loxp_RFP/stop_loxp) is generated with att specific recombination sites. att B sites will be replaced by att P sites through recombination with a donor vector (p donor 221). By using a combination of enzymes, the construct will end up with att L site (BP clonase mix) (Fig 1a) which can be recombined with att R sites present in the 5' entry clone and 3' entry clone to introduce it into a destination vector (fig 1a, b).

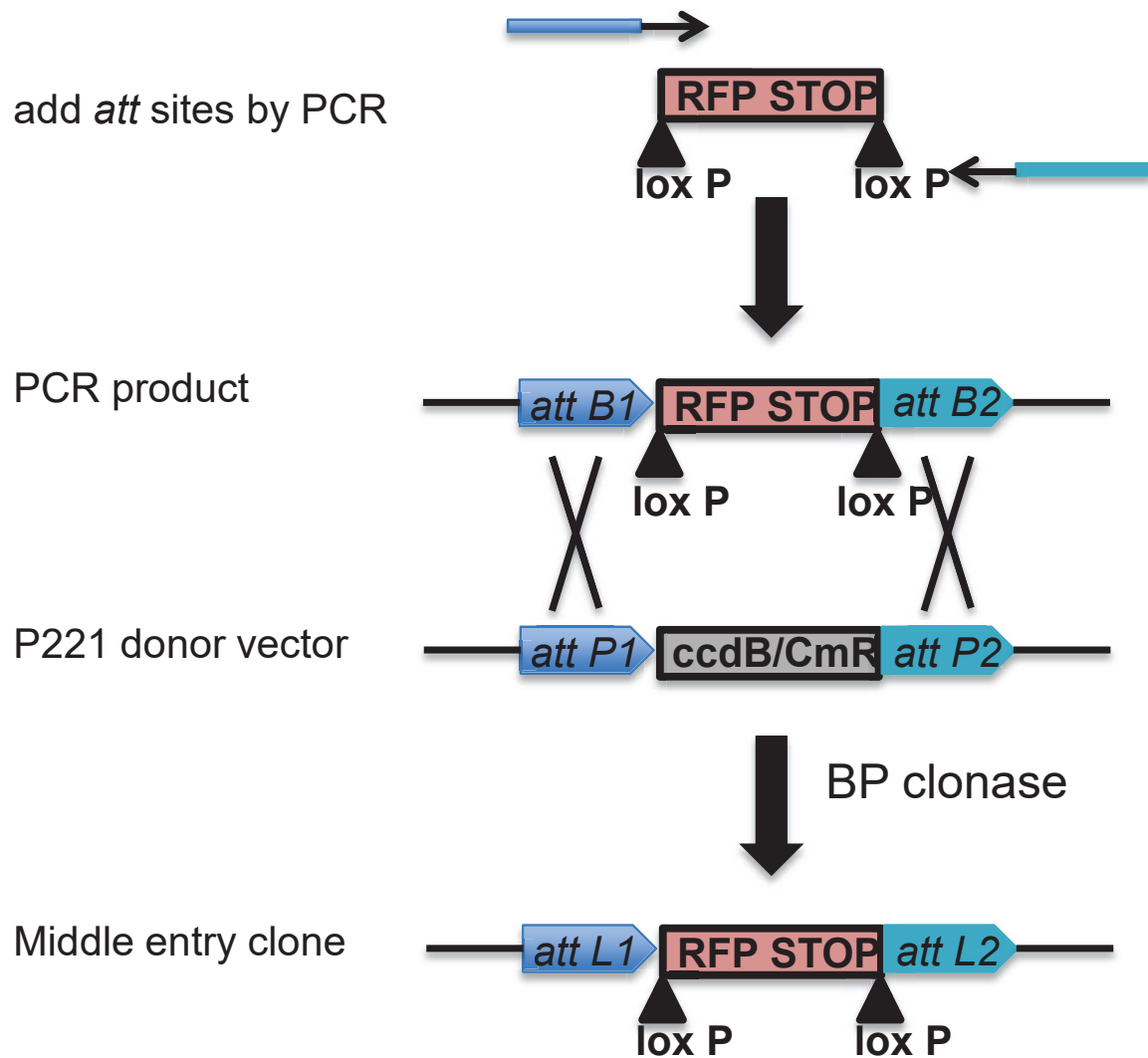


Figure 1a: BP reaction to create the donor vector

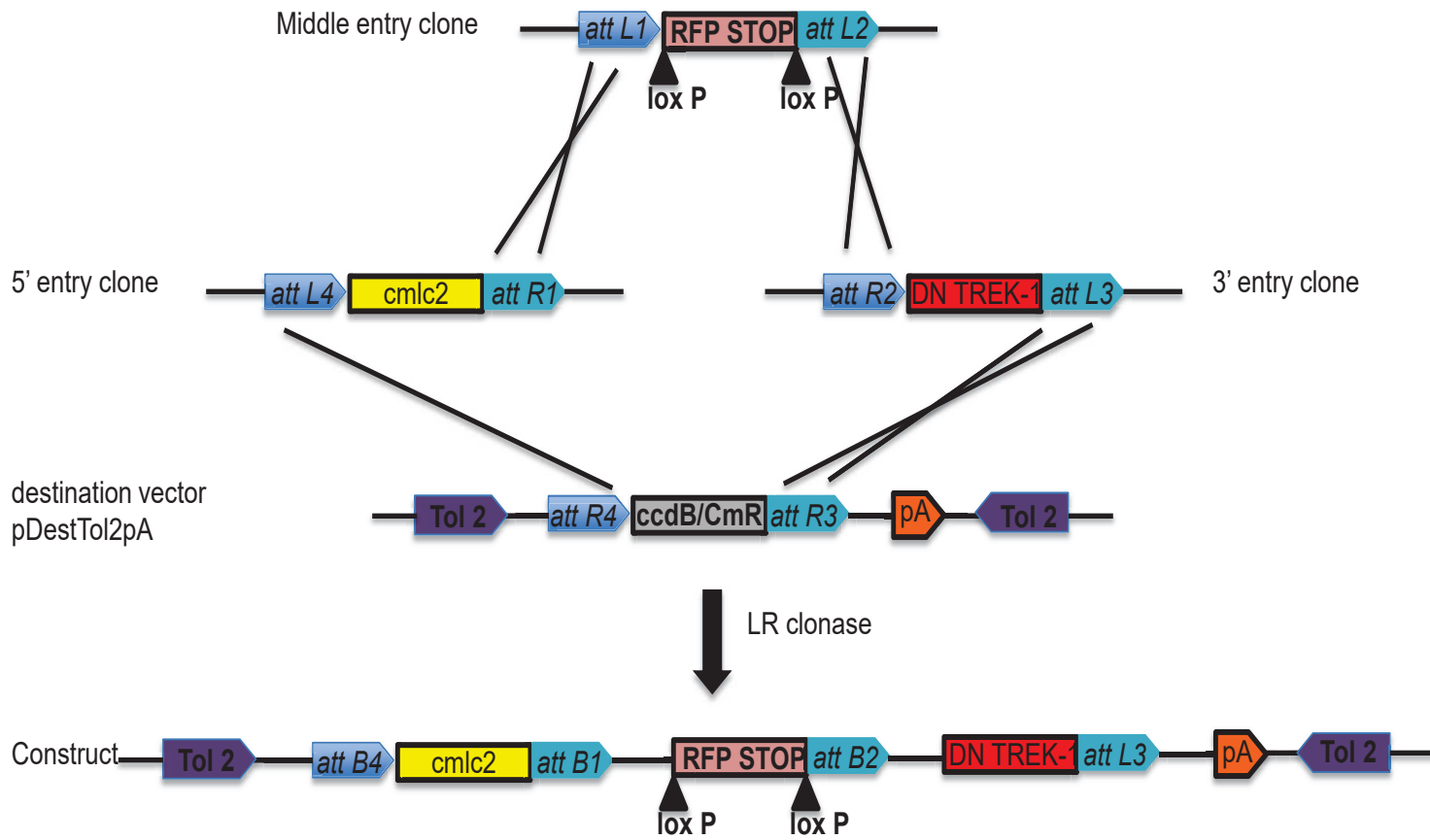


Figure 1b: LR reaction to create the construct with the destination vector

2.12.2_ Generating the conditional DN TREK-1 del ex4 line:

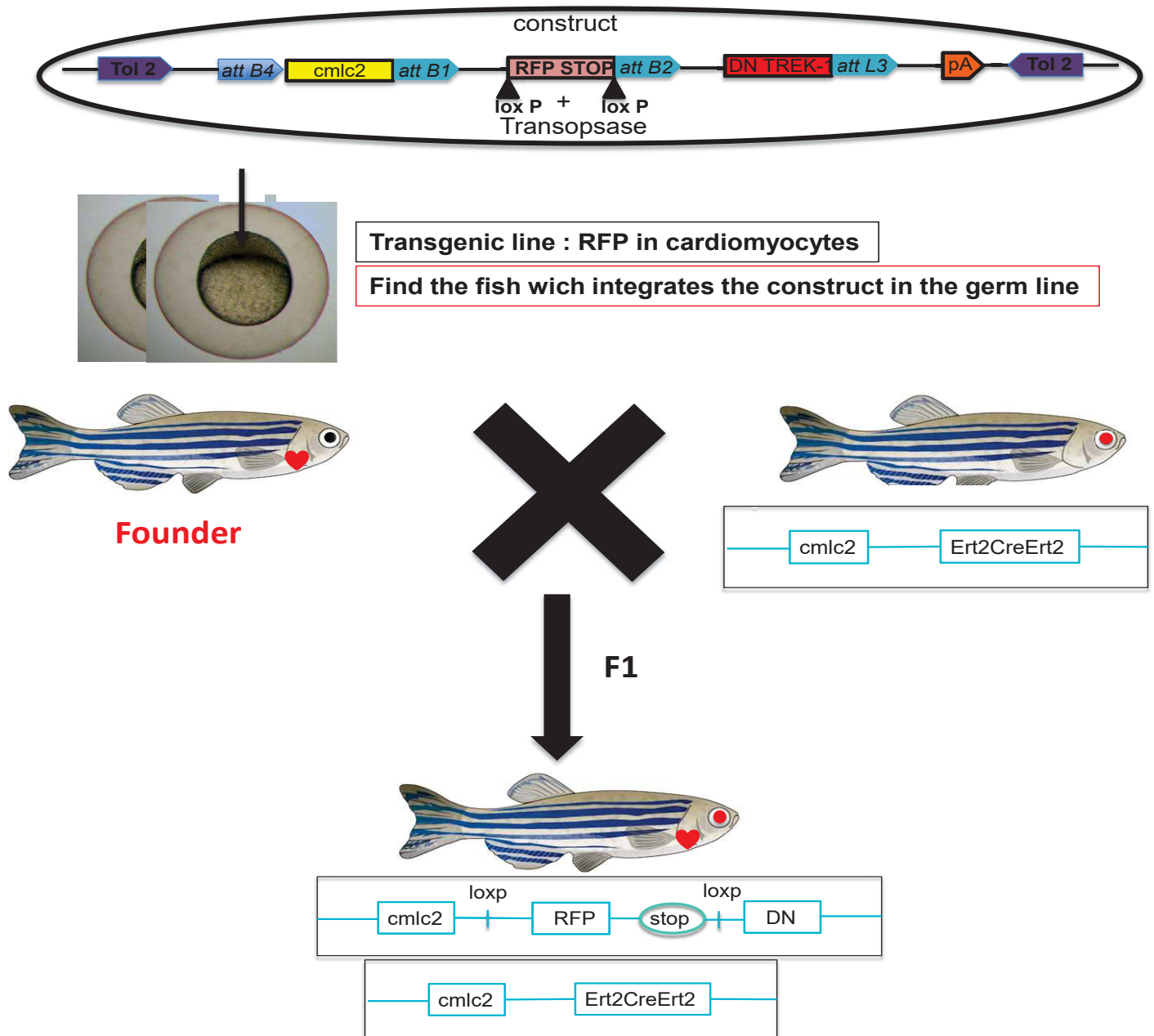


Figure 2: Transgenic DN TREK-1 del ex4 line creation: A scheme representing the generation of the conditional DN TREK-1 del ex4 transgenic fish line

The construct made previously is injected with transposase in one cell stage embryo. The transposase allows the integration of the construct in the embryo's genome. The construct integration in the genome is reflected by the embryos with red hearts. Once these embryos become adult we have screened of a founder that has integrated the construct in its germ line and has the ability to transmit the construct to its next generation. The founder is crossed with another transgenic fish line that expresses an inactive Cre in their cardiomyocytes under the control of the cardiomyocyte specific promoter (cmlc2) with a red gene reporter in the eyes. The outcome of this cross is the first generation (F1) that expresses the construct and the inactive Cre specifically in their cardiomyocytes under the control of the cardiomyocyte specific promoter (cmlc2) (Fig2).

2.13_ Cre/Tamoxifen induction:

2.13.1_ Embryos Cre/tamoxifen induction:

At 24hpf we add 3µl of tamoxifen (10µM) to 50mL of fish medium where we have put the embryos. We leave the tamoxifen in the medium during 6 days post fertilization.

2.13.2_ Adult Cre/tamoxifen induction:

In order to induce the activation of Cre, the transgenic fish are treated with tamoxifen 2 days before heart amputation. The fish are treated twice with tamoxifen (4-OHT) (10µM (100µl:500ml) with a waiting period of 2 days. Tamoxifen treatment is realized overnight.

3_ Results:

3.1_ Localization/expression of zTREK-1a and zTREK-1b:

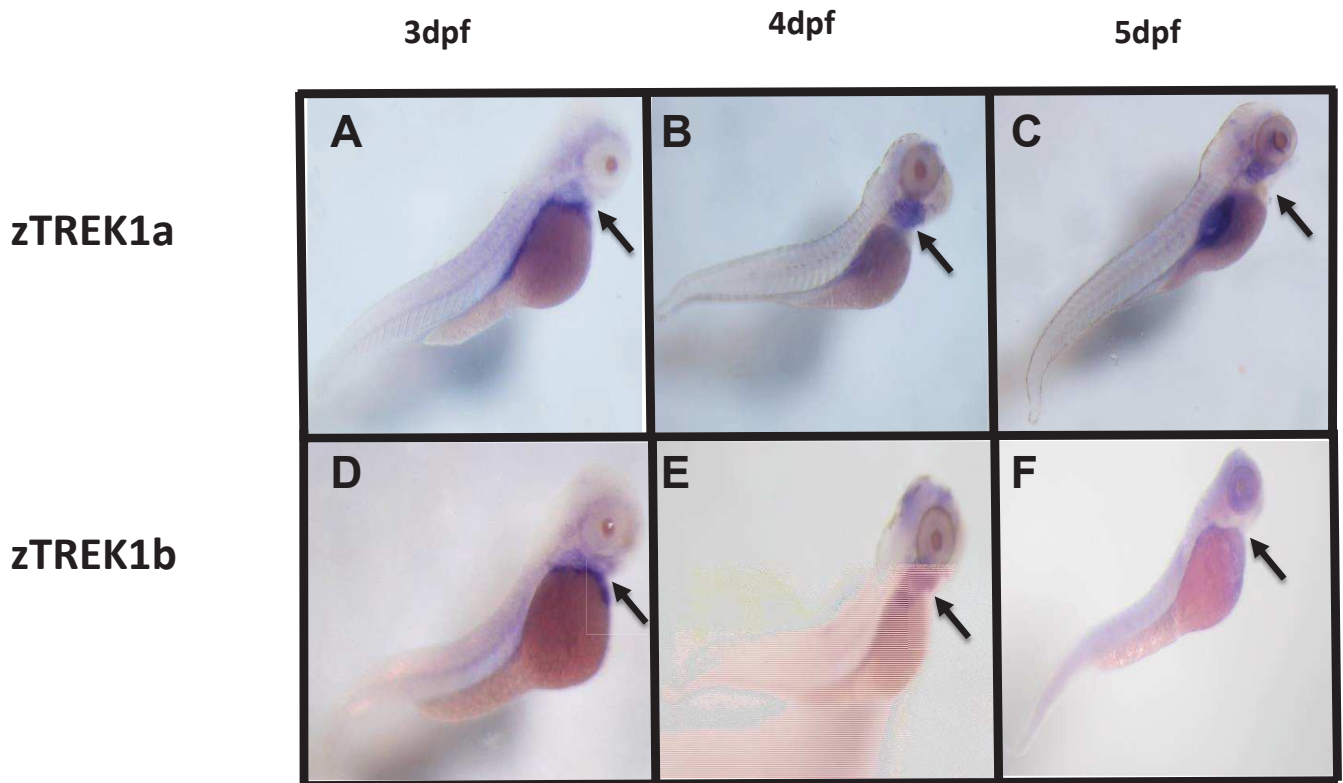


Figure 1: zTREK-1a/b expression through in situ hybridization: In situ hybridization for zTREK-1a/b respectively, on wild type (WT) zf embryos at 3 days post fertilization (dpf) (A, D), 4dpf (B,E) and 5dpf (C,F). Black arrows show the localization of the heart on the zf embryos.

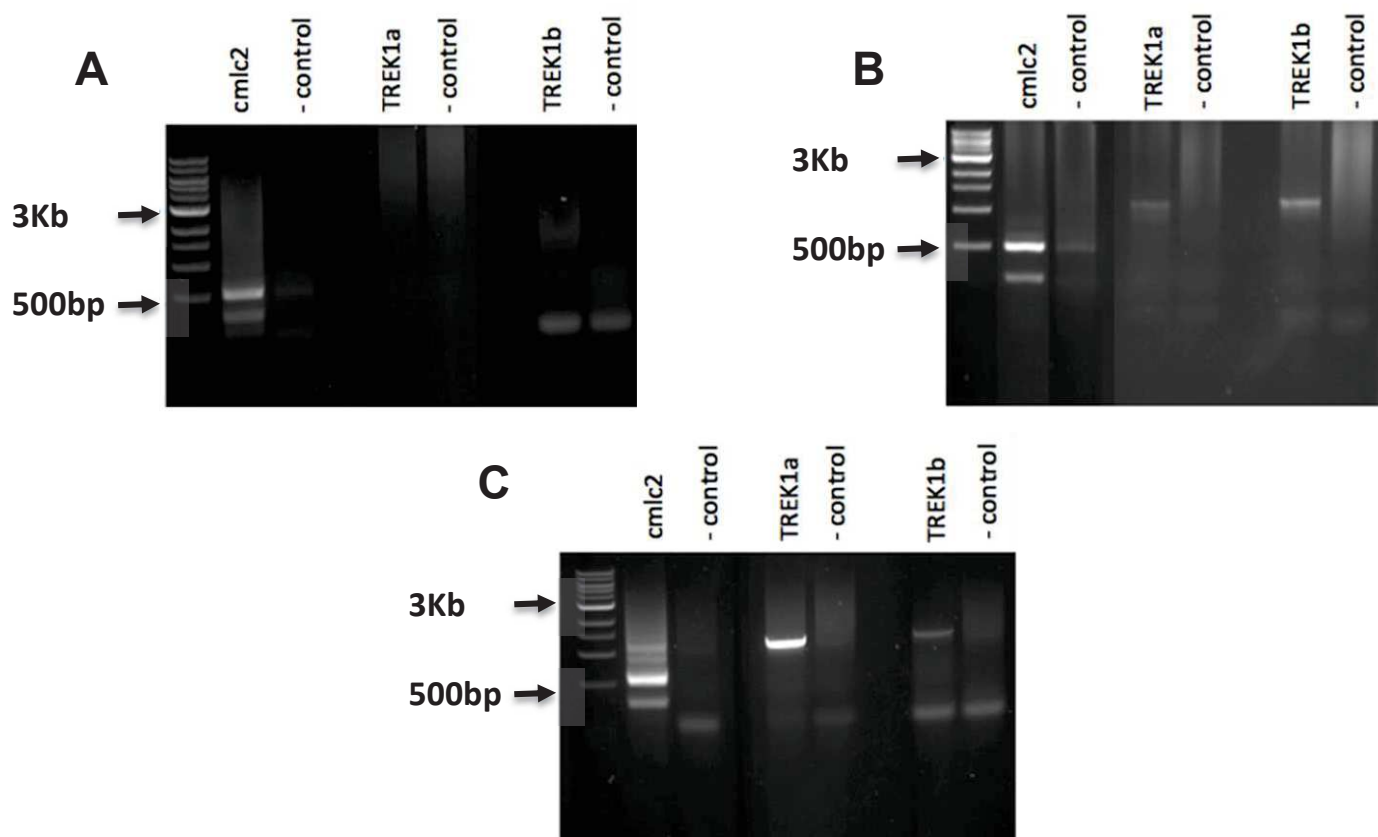


Figure 2: zTREK-1a/b expression in zf heart by using PCR on WT zf heart cDNA: at 3dpf (A), 4dpf (B), and on adult (C) WT zebrafish heart cDNA for zTREK1a/b and the cardiac myosin light chain 2 gene (cmlc2a). For the negative control (- control) we have used water as a template. The ladder used is 1Kb DNA ladder.

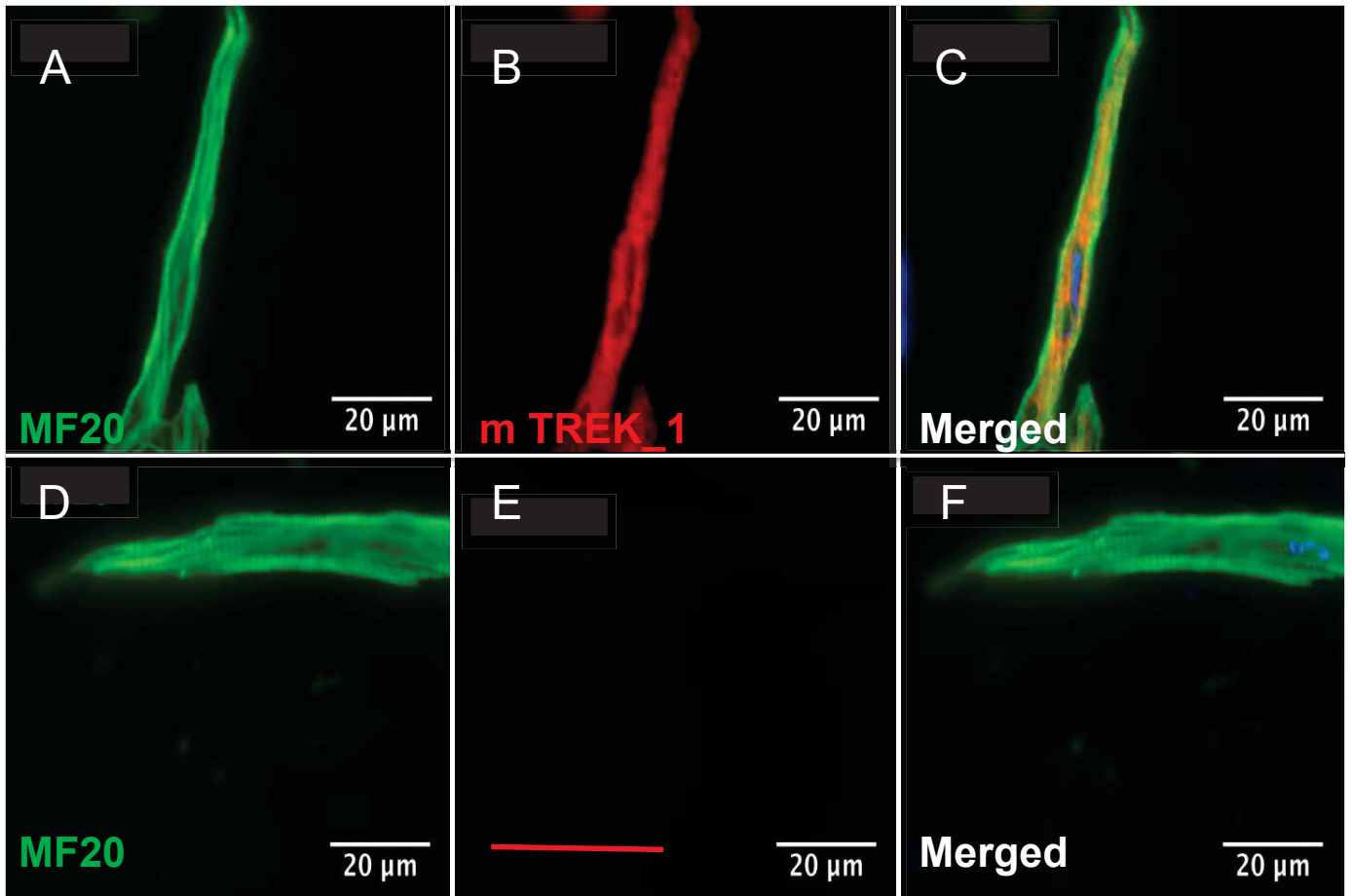


Figure 4: zTREK-1a/b expression in zf cardiomyocytes by immunofluorescence on adult zf cardiomyocytes: using anti myosin heavy chain antibody (green) (A, D) and anti- mouse TREK-1 antibody (red) (B), without anti mTREK-1 antibody (with secondary antibody anti mouse alexa 594) (E). Merged MF20/anti mTREK-1 (C), merged MF20/without mTREK-1(with secondary antibody anti mouse alexa 594) (F) . .

To check the expression of zTREK-1a/b in zf heart, an *in situ* hybridization is performed on WT zf embryos at different developmental stages: 3 days post fertilization (dpf), 4dpf and 5dpf, using an anti-sense RNA probe corresponding for each gene. We are not able to detect the expression of zTREK-1a nor zTREK-1b in WT zf embryos hearts (Fig1). However, *in situ* hybridization is not a sensitive technic to detect low messenger RNA level expression.

For that reason, we have performed Polymerase Chain Reaction (PCR) on WT zf heart cDNA at different developmental stages: 3dpf, 4dpf and on adult WT zf heart cDNA. *cmlc2a* was used as positive control since it is only expressed in the cardiomyocytes. The PCR reveals that zTREK-1a/b expression starts to appear in zf heart at 4dpf and then it increases during development to reach higher levels in adult (Fig2).

After we have determine that zTREK-1a/b mRNA are expressed in zf hearts, we suspect that they are present in the cardiomyocytes, where they may control cellular processes that may influence heart regeneration. For that reason, we have performed immunofluorescence (IF) on adult zf cardiomyocytes primary culture labeled with MF20 and with mTREK-1 antibody. Our IF reveals that zf cardiomyocytes are positive for TREK-1 where we see a colocalization of MF20 staining with TREK-1 staining (Fig4 A, B, C). However, no red staining corresponding to the presence of TREK-1 was detected in the condition where we have used only the secondary antibody coupled to RFP (red) without mTREK-1 antibody (Fig4 D, E, F). This Suggests that zTREK-1a is expressed in adult zf cardiomyocytes since we have showed in the previous chapter that the mTREK-1 antibody only recognizes zTREK-1a.

3.2 _ Validation of DN TREK-1 del ex4 transgenic line:

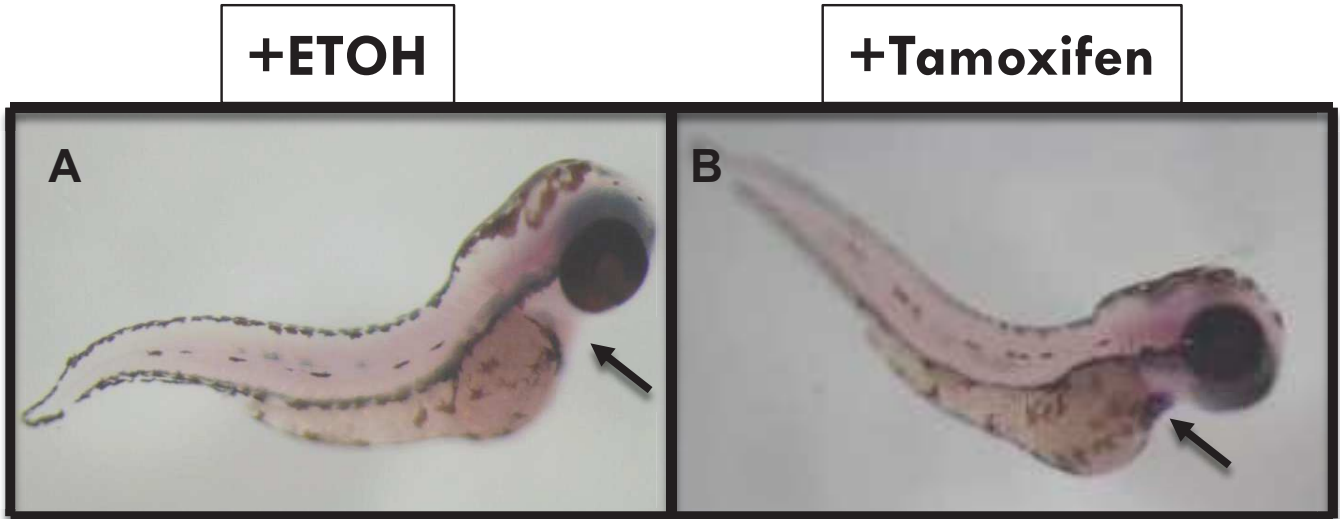


Figure 5: Effect of tamoxifen treatment on DN TREK-1 del ex4 line: In situ hybridization on F1 DN TREK-1 del ex4 treated with tamoxifen (B) or ETOH as a vehicle (A). Black arrows show the localization of the embryo heart.

In order to validate the conditional DN TREK-1 del ex4 transgenic line, an *in situ* hybridization was performed on F2 embryos at 3 dpf treated with ethanol (ETOH) as a vehicle (Fig5 A) or with tamoxifen (Fig5 B) at 24hpf, by using an anti-sense RNA probe corresponding for DN TREK-1 del ex4 .Unlike the embryos treated with tamoxifen, the embryos treated with ETOH don't express the DN TREK-1 del ex4 in their heart (Fig5). This suggests that our line is valid where the DN TREK-1 del ex4 is only expressed upon tamoxifen treatment.

3.3 Implication of zTREK-1a/b during zf heart regeneration:

3.3.1 Pharmacological inhibition of zTREK-1a/b during zf heart regeneration:

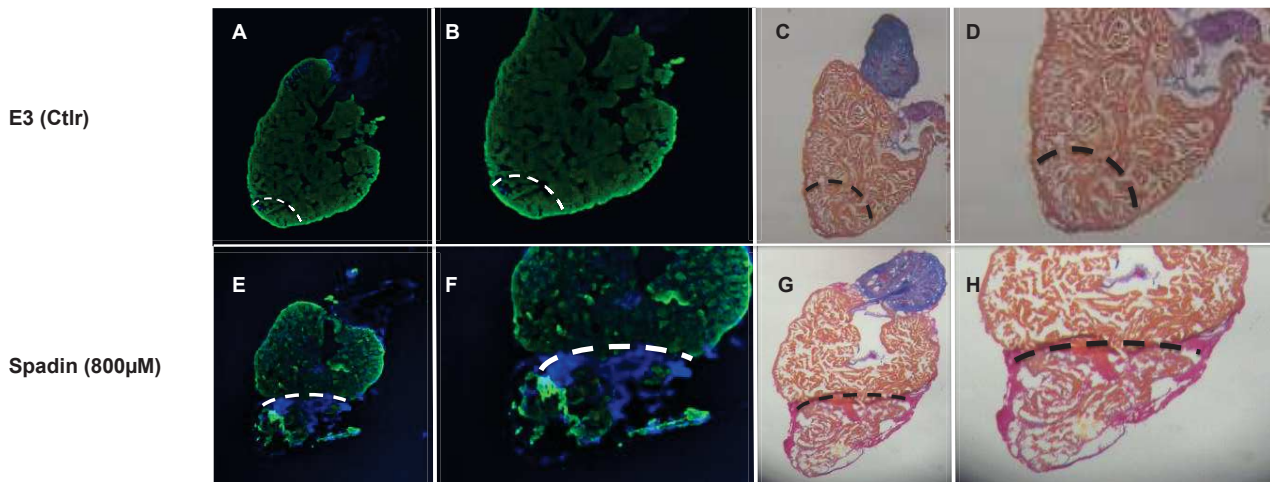


Figure 5: Effect of the spadin treatment on zf heart regeneration: Immunohistochemistry on heart sections after injection with E3 or with 800µM of spadin during 30 dpa (A, E), at higher magnification (B, F). Cardiomyocytes are labeled with MF20 in green and the nuclei are labeled with DAPI in blue. Dashed lines correspond to the amputation area. AFOG staining on the sections from the same conditions (C, G) at higher magnification (D, H).

In order to determine whether zTREK-1a/b are implicated during zebrafish heart regeneration, we have pharmacologically inhibited the channels during 30 dpa. After spadin treatment during 30 dpa through intraperitoneal injections, immunohistochemistry on heart sections shows a lack of cardiomyocytes in the amputation area compared to the control (Fig6 A, B, E, F). AFOG staining on heart sections from the same conditions reveals the presence of collagen staining in the amputation area upon spadin treatment compared to the control (Fig6 C, D, G, H). Spadin treatment, results in an inhibition of heart regeneration (30% of inhibition). This Suggests that zTREK-1a/b may play a role during zebrafish heart regeneration.

3.3.2 Effect of conditional transgenic zf line expressing a dominant form of zTREK-1a/b on zf heart regeneration:

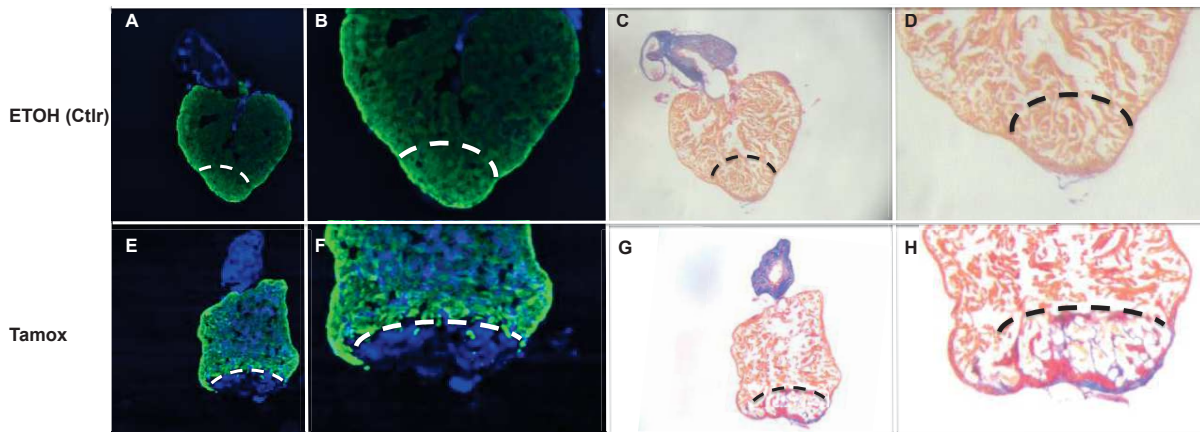


Figure 6: Effect of the induction of the DN TREK-1 del ex4 on zf heart regeneration: Immunohistochemistry on heart sections after treatment with ethanol (ETOH) or with 100 μ M of tamoxifen at 30 dpa (A, E), at higher magnification (B, F). Cardiomyocytes are labeled with MF20 in green, the nuclei are labeled with DAPI in blue. Dashed lines correspond to the amputation area. AFOG staining on the sections from the same conditions (C, G) at higher magnification (D, H).

To support our results obtained previously with the pharmacological inhibition of zTREK-1a/b, we have used a conditional dominant negative zf line that expresses under the control of the cardiomyocyte specific promoter (cmlc2a), a 4-hydroxytamoxifen (4-HT) inducible Cre recombinase (CreER) and a floxed stop cassette that targets the expression of the dominant negative form of the channels (DN TREK-1 del ex4) in the cardiomyocytes upon 4-HT treatment. 4-HT treatment leads to an irreversible expression of the DN TREK-1 del ex4 in zf cardiomyocytes. Immunohistochemistry on heart sections at 30dpa shows that the transgenic zf treated with 4-HT lack of cardiomyocytes in the amputation area compared to the control treated with ETOH (Fig7 A, B, E, F). AFOG staining on heart sections from the same conditions reveals the presence of collagen staining in the amputation area upon tamoxifen treatment

compared to the control where the muscle takes place over collagen in the amputation area (Fig7 C, D, G, H). The inhibition of zTREK-1a/b through induction of the DN TREK-1 del ex4 expression in the cardiomyocytes, results in an inhibition of zebrafish heart regeneration (43% of inhibition). This suggests that zTREK-1a/b play a crucial role during zebrafish heart regeneration.

4 Discussion:

Unlike adult mammals, neonatal mammals and adult zfish have the ability to regenerate their heart. Heart regeneration occurs due to cardiomyocyte dedifferentiation followed by proliferation (Jopling, Sleep et al. 2010, Porrello, Mahmoud et al. 2011). In all species during fetal/embryonic development, cardiomyocytes are in hyperplastic phase and they have proliferative capacities (Li, Wang et al. 1996). In adult stage, under stress, cardiomyocytes are in hypertrophic phase and they undergo hypertrophic response. Under extensive stress, adult mammals push cardiomyocyte hypertrophic response leading to pathological hypertrophy. Neonatal mammal and zebrafish cardiomyocyte dedifferentiate and return to hyperplastic phase with embryonic properties allowing them to proliferate and replace the lost cardiomyocytes. The loss of cardiomyocytes leads to an increase of ventricular loading. As described previously, the response of cardiomyocytes to the increase of ventricular loading is different between species. We suspect that adult mammalian heart regeneration has been blocked or inhibited for a protective mechanism. In fact we believe that adult mammals fail to regenerate their heart due to their high blood pressure. Cardiomyocyte dedifferentiation, is a crucial step for heart regeneration. During this step the tissue surrounding the wound area will be fragile due to the detachment of cardiomyocytes from the surrounding tissue. Increasing by that the risk of cardiac rupture in adult mammals due to their high blood pressure. For that reason, adult mammals develop cardiac hypertrophy rather than cardiac regeneration. We suspect the implication of mechanosensitive ion channels during zebrafish heart regeneration. It has been shown an upregulation of TREK-1 in the cardiomyocytes during adult mammalian pathological hypertrophy. In addition, different parameters that activate TREK-1 are present during

hypertrophy such as increase of intracellular acidification in the heart and increase in cardiac output, reflecting an increase in mechanical stress on the heart (Rossi and Carillo 1991, Tajima, Bartunek et al. 1998, Ruwhof and van der Laarse 2000).

Our data show that zTREK-1a/b expression start to appear at 4 dpf where the heart is fully developed and then it increases during development to reach higher levels in adult. This suggests that zTREK-1a/b may be important for heart regeneration rather than heart development. Immunofluorescence on zf cardiomyocyte primary culture, reveals the expression of zTREK-1a protein in these cells. We have already determined the expression of functional zTREK-1a/b channels in zf cardiomyocytes by using the patch clamp on freshly dissociated adult zf cardiomyocytes. Like mammalian TREK-1, zTREK-1a/b are expressed in the cardiomyocytes (Xian Tao, Dyachenko et al. 2006).

To investigate the role of zTREK-1a/b during heart regeneration, we have used 2 strategies. The first one consists of a pharmacological inhibition of zTREK-1a/b during 30 dpa, through spadin or fish medium E3 (as a control) intraperitoneal injections. For that reason, we have established a suboptimal concentration for spadin (800 μ M). The second one consists of using a conditional dominant negative zf line based on the Cre/lox system which will allow us to express the DN TREK-1 del ex4 specifically in zf cardiomyocytes, to study its effect on heart regeneration.

Our results show that upon spadin injections, zf don't regenerate their heart unlike the control. Adding to that AFOG staining reveals the presence of collagen staining in the amputation area upon spading injections reflecting the presence of a scar resulting in a blocked regeneration. This suggests that zTREK-1a/b inhibition prevents heart regeneration and they

may be important for this process by affecting either cardiomyocyte proliferation or cardiomyocyte dedifferentiation. However, the effect of spadin injections on heart regeneration is not specific due to the probability of zTREK-1a/b inhibition in other organs that can affect heart regeneration.

To overcome the unspecific effect that can occur due to pharmacological treatment, we have created a conditional dominant negative zf line based on the Cre/lox system. Inducing the translocation of CreER into the nucleus through tamoxifen treatment, leads to an irreversible expression of DN TREK-1 del ex 4 in zf cardiomyocytes. The induction of the DN TREK-1del ex4 expression in zf cardiomyocytes upon tamoxifen treatment inhibits heart regeneration compared to the control treated with ETOH. In addition AFOG staining reveals the presence of collagen in the amputation area reflecting the presence of a scar in resulting in a blocked/ inhibited regeneration in zf that express the DN TREK-1 del ex4 in their cardiomyocytes compared to the control. Our results show that the inhibition of zTREK-1a/b by inducing the expressing of their DN form (DN TREK-1 del ex4) in zf cardiomyocytes, results in an inhibition of heart regeneration. This suggests that zTREK-1a/b are important for heart regeneration by affecting either cardiomyocyte dedifferentiation, proliferation or cardiomyocyte differentiation.

After heart amputation in zf, it has been suggested an increase of hemodynamic forces (Raya, Koth et al. 2003). In addition, an increase of hydrogen peroxide (H₂O₂) in the heart was reported after heart amputation, caused by an increase in ROS production reflecting an increase of the heart intracellular acidification in zf after amputation (Chao, Jin et al. 2002, Han, Zhou et al. 2014). We have demonstrated in the previous chapter that zTREK-1a/b are activated by membrane stretch and intracellular acidification which are 2 important parameters that are

disturbed during zebrafish heart regeneration. zTREK-1a/b inhibition, results in a decrease of the heart ability to detect these changes which can explain the inability of zf to regenerate their hearts after a pharmacological or genetic inhibition of zTREK-1a/b.

The signalization pathway by which zTREK-1a/b control zebrafish heart regeneration remains unknown. However, TREK-1 regulates cell cycle progression where it has been shown to be highly expressed in proliferative endometrium through enhancing cell division (Patel, Jackson et al. 2013). It has been reported that TREK-1 was upregulated in different types of cancer such as ovarian cancer, prostate cancer (Voloshyna, Besana et al. 2008, Innamaa, Jackson et al. 2013). However, inhibition of TREK-1 was reported to enhance cell proliferation (Hughes S et al 2006). Controversially, recent studies show that overexpression of TREK-1 in CHO cells promotes cell cycle arrest, leading to a decrease of cell proliferative capacity (Zhang, Yin et al. 2016). These studies suggest that depending on the environment where TREK-1 is expressed as well as its downstream effectors it can enhance or inhibit cell cycle progression.

Heart regeneration occurs by cardiomyocyte dedifferentiation followed by proliferation. Inhibiting zTREK-1a/b using pharmacological agents or by expressing the DN TREK-1 del ex4 in zf cardiomyocytes inhibits zf heart regeneration decreasing the proliferative activity of the cardiomyocytes or by decreasing their capacity to dedifferentiate.

5 Perspectives:

We have demonstrated that zTREK-1a/b are important for zebrafish heart regeneration. Their pharmacological or genetic inhibition during zebrafish heart regeneration results in an inhibition of this mechanism. Knowing that heart regeneration occurs by cardiomyocyte dedifferentiation followed by proliferation, zTREK-1a/b will interfere during one of these steps to control heart regeneration.

We will study the effect of zTREK1-a/b on cardiomyocyte proliferation by using a BrdU assay on the DN TREK-.del ex4 zf line. After induction of the DN TREK-1 del ex4 expression upon tamoxifen treatment, following heart amputation, zf will be injected during 14 dpa with BrdU (2.5mg/ml). This will allow us to quantify the cardiomyocytes that have integrated the BrdU which will allow us to evaluate the number of cardiomyocytes that have re-entered the cell cycle in order to proliferate. To test if zTREK-1a/b inhibition has an effect on cardiomyocyte dedifferentiation, a dedifferentiation assay will be performed on cardiomyocyte primary culture, coming from DN TREK-.del ex4 zf line (after induction with tamoxifen). This will allow us to quantify the number of dedifferentiated cardiomyocytes by using specific markers (tropomyosin) which will label all cardiomyocytes and another marker alpha sarcomeric actin a specific marker which will highly label differentiated cardiomyocytes. Subsequently we will proceed for quantification of dedifferentiated cardiomyocytes that have conserved the tropomyosin marker and have lost the alpha sarcomeric marker

In order to determine if zTREK-1a/b reach their maximal activity during heart regeneration, it will be interesting to pharmacologically or genetically activate them. This will allow us to establish if stimulating the activation of these channels may lead to a more rapid heart

regeneration. Investigating the signalization pathways that can be implicated in this mechanism will be interesting.

The evaluation of zTREK-1a/b effect on cardiomyocyte dedifferentiation and proliferation can also be performed on zebrafish cardiomyocyte primary culture. It will be also interesting to investigate the effect of zTREK-1a/b activators such as PUFAs on cardiomyocyte dedifferentiation and proliferation. Cardiomyocyte primary culture will be treated with BrdU in different conditions (treated or not with spadin and treated with PUFAs). Immunohistochemistry will be performed to evaluate cardiomyocyte proliferation markers as well as dedifferentiation markers

It will be interesting to determine whether zTREK-1a/b are upregulated or there is only an increase in their activity after heart amputation. For that reason, a gene amplification from cDNA of amputated and non-amputated heart is important to be realized. This experiment will be accompanied by electrophysiological recordings on cardiomyocyte primary culture from amputated and non-amputated heart.

To further investigate signalization pathways and zTREK-1a/b downstream effectors that play a role during zebrafish heart regeneration, a microarray will be performed on 4 groups that belong to the conditional DN zf line (non amputated fish treated with tamoxifen and with ETOH as control and amputated fish treated with tamoxifen and with ETOH as control). A comparison of mRNA profile expression between the 4 groups will be realized in order to find the genes that are affected during regeneration upon tamoxifen treatment. In order to validate the results obtained by microarray a quantitative PCR in the same conditions is crucial to perform in order to figure out if the mRNA level expression changes fit with the results obtained by microarray.

Chapter 3

Implication of zTREK-1a/b in zebrafish normal cardiac physiology

1_ Introduction:

Zebrafish has been used as a model to study developmental and human diseases. The transparency and the clarity of zebrafish embryos allow to follow in real time, *in vivo* organs development. In addition, zebrafish embryos have the ability to receive oxygen from the water through passive diffusion and they can survive several days without a beating heart. This allows us to better understand several severe cardiac dysfunctions that can cause embryonic death for other laboratory models such as mice (Pelster and Burggren 1996, Sehnert and Stainier 2002). Zebrafish is described as a good model to study cardiovascular diseases. Drugs that cause QT prolongation and bradycardia in humans have similar effects on zebrafish embryonic hearts. (Milan, Peterson et al. 2003). Zebrafish mutant lines or zebrafish morphants are used to study genes that cause cardiovascular diseases in humans and to screen for different molecules that can have a potential therapeutic effect. Zebrafish deficient for homeodomain transcription factor *Shox2* are used to study human sick sinus syndrome (Blaschke, Hahurij et al. 2007, Hoffmann, Berger et al. 2013). *Shox2* knock out in mice leads to embryonic lethality caused by severe cardiac defects. *Shox2* knock down in zebrafish embryos, leads to severe sinus bradycardia. Nexilin mutations in zebrafish are used to study the role of this protein in human cardiomyopathy as well as during heart failure. Nexilin mutations detected in patients suffering from dilated cardiomyopathy, lead to the same Z disks pathologies in zebrafish. (Hassel, Dahme et al. 2009). These studies suggest that zebrafish is a good model to study human cardiovascular diseases.

Heart rate and calcium imaging are important parameters to evaluate cardiac function because the changes in the heart rhythm and calcium signaling are responsible of the pathological state of the heart. For that reason, different methods are been used to evaluate

heart parameters in zebrafish. For adult zebrafish, electrocardiogram is used to evaluate the heart rhythm, the action potentials that are correlated to their P wave, the QRS complex and the T wave component (Nemtsas, Wettwer et al. 2010). Optical mapping is used to evaluate zebrafish heart rate, action potential propagation and conduction velocity by using a voltage sensitive dye (Sabeh, Kekhia et al. 2012, Lin, Craig et al. 2015). Calcium imaging is performed on adult zebrafish heart as well as on zebrafish embryo heart by using calcium sensitive dye that will indicate the calcium signaling and dynamics (Hou, Kralj et al. 2014, Lin, Craig et al. 2015). To evaluate embryonic zebrafish heart rate, 2 main approaches can be used the counting of heart beats from slow motion video recordings and the automated zebrafish heart rate counting, which can be performed by using several existing software (Schwerte, Prem et al. 2006, Mikut, Dickmeis et al. 2013).

2_ Materials and methods:

2.1_ Embryonic heart rate recordings:

Embryonic heart rates are recorded using the viewpoint application manager software. The embryos used for recordings belong to the conditional DN fish line (F1). The embryos are treated at 24hpf with 5µl of 10 mM tamoxifen (in 50 mL of E3) or with 5µL of 100% ETOH (in 50 mL of E3). Tamoxifen and ETOH are leaved in the medium until the embryos reach 6 dpf (when we proceed for heart rate recordings). The embryos are placed in a concave slide containing 750 µl of E3 and then we have recorded their heart rate. The recordings are done until the heart rate of the embryos stabilizes.

2.2_ Optical mapping:

The hearts are extracted from zebrafish previously exposed for 14 days to pharmacological treatment: Spadin (800 µM) or E3 (control vehicle). The hearts are then placed for 20 min in a bath of voltage dye (Di-4-ANEPPS; 4 µM) prepared with tyrodesolution at room temperature (22-24 C°). Such dye is sensitive to voltage changes, allowing to record membrane potential by fluorescence. Then we placed zebrafish hearts for 10 min in a blebbistatin solution to stop heart contractions and to avoid fluorescence artifacts. A 150-W halogen light is used as an excitation source for the voltage dye. Excitation and emission light are filtered with a set included a 531/50-nm excitation filter, 580-nm dichroic mirror, and 580 long-pass emission filter. Objectives are combined to recorded fluorescence in a field of view of 1.26 x 1.26 mm. Recording are obtained with a sample rate of 1 to 2 ms per frame.

2.3_ Statistical analysis:

Data are presented by the mean \pm standard error of the mean (SEM). Differences between 2 groups are established using paired or unpaired t test.

2.4_ Zebrafish pharmacological treatment:

Animals are treated as described previously (in the previous chapter).

3_ Results:

3.1_ Effect of zTREK-1a/b on embryonic heart rate:

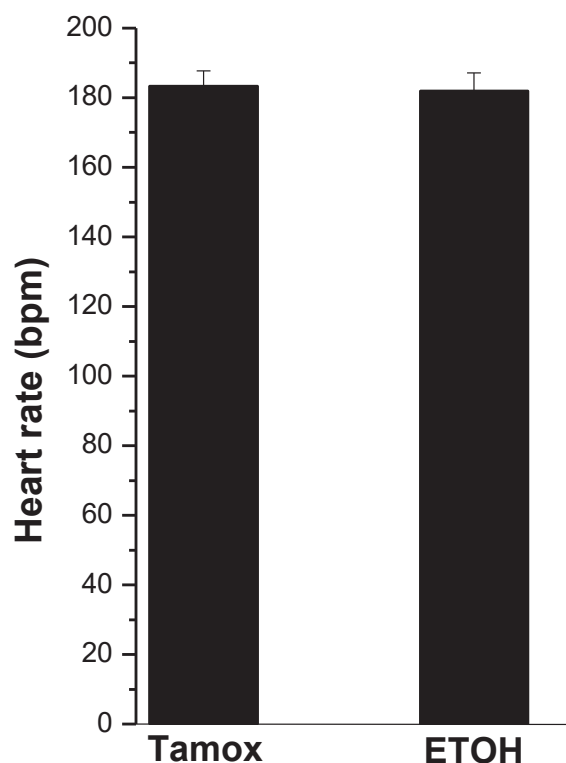


Figure 1: Effect of the induction of DN TREK-1 del ex4 on embryonic heart rate: Heart rate of the 6 dpf zf embryos expressing DN TREK-1 del ex4 treated with tamoxifen (n=7) or with a vehicle (100%ETOH) as a control (n=7).

Induction of the DN TREK-1 del ex4 expression in embryonic cardiomyocytes upon tamoxifen treatment, doesn't affect heart rate. No significant difference between heart rate of the embryos treated with tamoxifen 181.992 ± 5.197 beat per minute (bpm) compared to the embryos treated with 100% ETOH 183.376 ± 376 bpm. Suppressing the expression of zTREK-1a/b in zebrafish embryo heart doesn't affect their normal heart function. This suggests that zTREK-1a/b are not required for normal embryonic heart function and physiology.

3.2_ Effect of zTREK-1a/b on adult heart activity:

3.2.1_ Effect of zTREK-1a/b on adult heart rate:

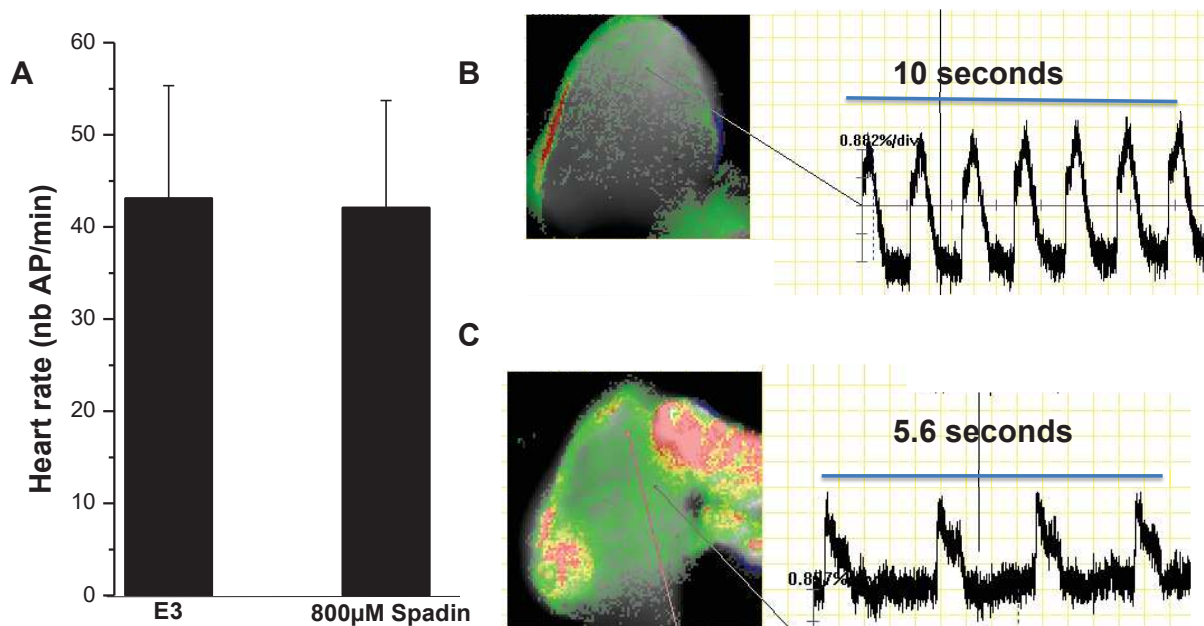


Figure 2: Effect of spadin treatment on adult heart rate: Heart rate of adult zf treated during 14 days with 800 µM of spadin $n=10$ (A, C) or with E3 as a control ($n=7$) (A, B).

We didn't observe a significant difference between the heart rate of zf injected with 800µM of spadin that have a heart rate of 42.17 ± 3.67 action potential per minute (AP/min) and the control injected with a vehicle (E3) that has a heart rate of 43.14 ± 5 AP/min.

3.2.2_ Effect of zTREK-1a/b on speed of conduction:

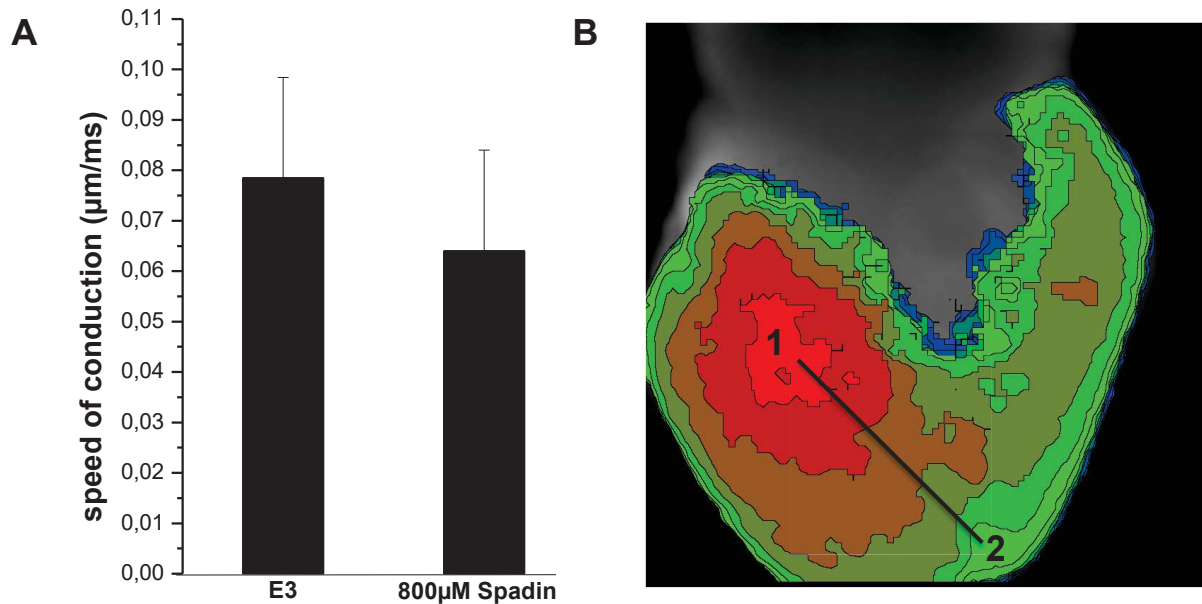


Figure 3: Effect of the spadin treatment on speed of conduction: Speed of conduction of adult zf treated during 14 days with 800 µM of spadin (n=10) or with E3 as a control (n=7) (A). A map showing the propagation of an action potential from the zone 1 to the zone 2 (B).

We have calculate the conduction velocity by calculating the distance corralated to the time that takes 1 action potential to propagat from the zone 1 where rises depolarization to reach the zone 2 (Fig3 B). We didn't observe a significant difference between the conduction velocity of the fish injected with 800µM of spadin that have a speed of conduction of 0.053 ± 0.012 µm/ms and the control injected with a vehicle (E3) that have a speed of conduction of 0.078 ± 0.010 µm/ms (Fig3 A).

4_ Discussion:

Suppression of zTREK-1a/b doesn't affect normal zebrafish heart function. Embryonic heart rate recordings are performed at 6 dpf, 2 days after the expression of zTREK-1a/b in the heart (see previous chapter). However, it has been shown that other mechanosensitive ion channels, that belong to the K_{2p} family start to appear early in zf development in the heart such as TREK-2 (Gierden, Hassel et al. 2012). This suggests that either TREK-2 doesn't affect normal embryonic heart function or the DN TREK-1 del ex4 doesn't have an effect on TREK-2 to influence normal embryonic heart function.

Our results show that embryonic heart rate is around 180 bpm/min (corresponding to a heart frequency of 3 hertz (Hz)). Adult heart rate is around 43 AP/min (corresponding to a heart frequency of 0.7 Hz). Knowing that adult zebrafish heart rate is between 120 and 130 bpm (corresponding to a heart frequency between 2 and 2.17 Hz)) (Verkerk and Remme 2012) this suggests that the difference of the heart frequencies between the embryonic state and the adult state is due to the experimental procedure. Adult heart recordings are realized on extracted heart, left outside the physiological environment. Adult hearts don't undergo sympathetic and parasympathetic stimulation, suggesting that adult zebrafish heart rate reflects zebrafish heart automatism.

The DN TREK-1 del ex4 has a dominant negative activity on zTREK-1a/b, our data suggest that these channels are not required for normal embryonic heart function and physiology. Most likely the DN TREK-1 del ex4 doesn't interact with other channels especially from K_{2p} family, which appear at early stages of development, to interfere with heart development or embryonic heart function.

Inhibiting zTREK-1a/b through spadin injections doesn't affect normal adult heart function. This suggests that zTREK-1a/b are not required for normal adult heart activity and that spadin injection doesn't have a side effect on normal cardiac function and physiology.

Our results coincide with the findings in adult transgenic mice that don't express TREK-1 in their cardiomyocytes. Under normal conditions these mice showed normal cardiac function characterized by normal echocardiography, normal fraction ejection and lack of cardiac remodeling. However, under stress conditions, caused by treadmill exercise and followed by stimulation of sympathetic nervous system through epinephrine injections, these mice showed prolonged QT intervals with increased susceptibility to stress-induced sinus pause (Unudurthi, Wu et al. 2016).

Despite, the lack of perfusion with physiological medium which reduces oxygenation in these experiments, and could impair normal heart activity, we have recorded relatively constant heart activity.

5_ Perspectives:

In order to validate our data, it will be interesting to perform optical mapping experiment using the conditional dominant negative fish line treated with tamoxifen or with ETOH (as a control). To overcome the limitation of this experiment we have to record electrocardiogram of zebrafish after spadin treatment or by using the conditional dominant negative fish line. This experiment will be performed under normal conditions.

In order to induce stress and increase ventricular overloading we have to record zebrafish electrocardiogram (Fig4) (fish will be either pharmacologically treated or express DN TREK-1 de ex4) after an exercise where the fish swim against the current in a zebrafish tunnel (Wang, Panakova et al. 2011) (Fig5). This experiment will give us an idea if like adult mammals zTREK-1a/b are required in physio pathological zebrafish heart function rather than normal cardiac activity.

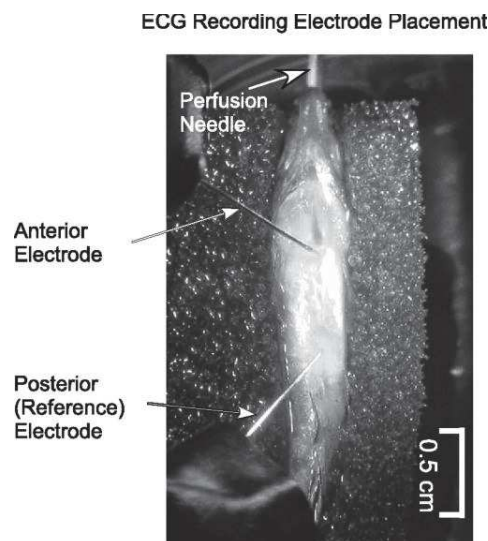


Figure 4: Milan DJ et al *Am J Physiol Heart Circ Physiol*. 2006. Picture representing the experimental set up to record zebrafish electrocardiogram.

It will be interesting to study the effect of zTREK-1a/b on physiological parameters of the heart, such as their effect on cardiomyocyte membrane potential, calcium homeostasis through calcium imaging using a fura-2. It will also be important to test the effect of zTREK-1 on heart contraction by using echocardiography.

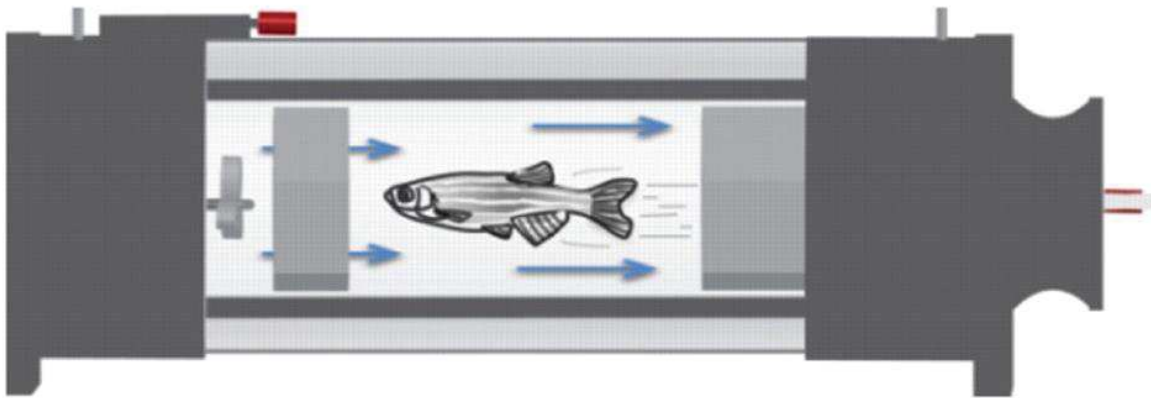


Figure 5: *Wang J et al Development 2011: A scheme representing a swimming tunnel. Zebrafish must swim in controlled current (indicated by blue arrows).*

General discussion

Zebrafish represents a model to study heart regeneration after cardiac injury. Zebrafish heart regeneration occurs with the same mechanism as neonatal mammal heart regeneration. Lineage tracing showed that heart regeneration in both species occurs through cardiomyocyte dedifferentiation followed by proliferation (Jopling, Sleep et al. 2010, Porrello, Mahmoud et al. 2011). Adult mammals lose their natural ability to regenerate their heart after cardiac injury where cardiomyocytes undergo hypertrophic response, rather than dedifferentiation leading to pathological hypertrophy. In addition, recent studies showed that pathological hypertrophy in adult mammals can be reversible after cardiac injury. Adult mammals can regenerate their heart by controlling environmental and molecular factors that can induce cardiomyocyte proliferation rather than cardiomyocyte hypertrophy (D'Uva, Aharonov et al. 2015, Bassat, Mutlak et al. 2017). Adding to that, interesting studies showed that ventricular unloading by using a ventricular assist device to patients suffering from severe heart failure, results in an improvement of their prognosis accompanied with cardiomyocyte proliferation (Birks, Tansley et al. 2006).

We believe that mechanosensation is an important mechanism in hypertrophy and heart regeneration. Cardiomyocyte proliferation has been blocked/ inhibited in adult mammals causing hypertrophy after cardiac injury. This drive to think that the mechanical stress that will induce cardiac hypertrophy in adult mammals will induce heart regeneration in zebrafish. Adding to, that different parameters change after cardiac injury in mammals as well as in zebrafish after heart amputation including heart pressure overload and increase in intracellular acidification (Chao, Jin et al. 2002, Raya, Koth et al. 2003, Han, Zhou et al. 2014).

It has been shown that TREK-1 is upregulated in cardiomyocytes during mammalian pathological hypertrophy (Cheng, Su et al. 2006). TREK-1 has a polymodal activation, suggests that it can be affected by several factors that are disturbed after cardiac injury. For that reason, we have focused on zTREK-1a/b to study their role during zf heart regeneration.

zTREK-1a/b are potassium channels, that have similar biophysical and pharmacological properties to those already described for mammalian TREK-1. Sequence alignment of zTREK-1a/b with human and mouse TREK-1 reveals that their C-terminal tail between G293 and Q360 where most of the regulation mechanisms take place is highly conserved between species (see introduction, page Fig9, 10). The first 28-30 amino acid are highly conserved in zTREK-1a/b which can explain their mechanoactivation and this sequence represent a potential direct interaction with PUFAs (Enyedi and Czirjak 2010). Glutamic acid in the position 306 (E306) is also conserved in zTREK-1a/b. E306 plays the role of pH sensor in mammalian TREK-1, its presence in zTREK-1a/b explains their activation by intracellular acidification (Honore, Maingret et al. 2002). Other amino acids that are conserved in zTREK-1a/b are S300 and S333 that can be potential targets for phosphorylation by PKC and PKA respectively. PKC and PKA may potentially have an inhibitory effect on zTREK-1a/b, while the conserved S351 may present a potential target for PKG rather than PKA and PKC which can potentially activate zTREK-1a/b (Fink, Duprat et al. 1996, Patel, Honore et al. 1998, Maingret, Patel et al. 2000, Koh, Monaghan et al. 2001). The proteins: AKAP 150 and Mtap2 have binding domains in mammalian TREK-1 between V298 and R311 and between E335 and Q360 which are conserved in zTREK-1a/b suggesting a potential interaction and regulation of zTREK-1a/b by these proteins (Sandoz, Thummler et al. 2006, Sandoz, Tardy et al. 2008). Like mammalian TREK-1, zTREK-1a/b are inhibited by the cytoskeleton, and spadin (Patel, Honore et al. 1998, Maingret, Patel et al. 1999,

Mazella, Petrault et al. 2010, Moha Ou Maati, Veyssiere et al. 2012). Spadin represents an efficient pharmacological agent to investigate the role of zTREK-1a/b in zf heart function and during heart regeneration.

After we established that zTREK-1a/b are activated by membrane stretch and they are inhibited by spadin, we have used these properties to demonstrate that these channels are expressed in zf cardiomyocyte, like the mammalian TREK-1 (Xian Tao, Dyachenko et al. 2006). Other mechanosensitive potassium channels may be present in zf cardiomyocytes. These potassium channels are not targeted by spadin.

We have then designed a DN form of zTREK-1a/b (DN TREK-1 del ex4) based on the DN already designed for mammalian TREK-1 (Veale, Rees et al. 2010). We showed the ability of the DN TREK-1 del ex4 to inhibit the mechanosensitive activity of both channels zTREK-1a/b. The DN TREK-1 del ex4 will be efficient to be used to study the role of zTREK-1a/b in zf heart function and during heart regeneration. This DN is used to develop a conditional DN zf line based on the Cre/lox system. This zf transgenic line expresses under the control of the cardiomyocyte specific promoter (cmlc2a), a 4-hydroxytamoxifen (4-HT) inducible Cre recombinase (CreER) and a floxed stop cassette that targets the expression of a dominant negative form of the channels (DN TREK-1 del ex4) in the cardiomyocytes upon 4-HT treatment, as described by Jopling et al 2012.

To investigate the effect of zTREK-1a/b on zf heart function, physiology and regeneration we have used two approaches. One of them consists of a pharmacological inhibition of zTREK-1a/b using spadin, and the other one consists of generating a conditional DN zf line based on the Cre lox system which will allow the expression of the DN TREK-1 del ex4 irreversibly in zf

cardiomyocytes. This experiment allows us to determine if zTREK-1a/b are important for zf heart function and regeneration. However, we didn't investigate further the signalization pathway in which they are implicated to ensure successful heart regeneration.

Different factors can play a role during zebrafish heart regeneration that can lead to zTREK-1a/b activation explaining their important role for successful heart regeneration. It has been suggested, an increase in hemodynamic forces after zebrafish heart amputation (Raya, Koth et al. 2003). zTREK-1a/b can sense these changes due to their mechanosensors activity which can be crucial for heart regeneration. Intracellular acidification also change in zf heart after amputation. It has been demonstrated an increase in zebrafish heart intracellular acidification after amputation, caused by an increase in the hydrogen peroxide (H_2O_2) concentration (Chao, Jin et al. 2002, Han, Zhou et al. 2014). zTREK-1a/b can detect the changes of intracellular acidification due to their proton sensor (showed by the sequence alignment chapter1 discussionFig1) leading to an increase of their activity which can also explain their role during heart regeneration. zTREK-1a/b implication during heart regeneration may not be due to simple fact of their mechanosensitive property, it may implicate different properties of the channels.

Investigating the implication of zTREK-1a/b in normal heart physiology and function is important. This allows us to determine whether these channels affect zebrafish heart regeneration due a defect in normal heart physiology. Under normal conditions, pharmacological inhibition of zTREK-1a/b doesn't affect adult zf normal heart function including heart rate and AP propagation. The inhibition of zTREK-1a/b by inducing the expression of their DN form in zf cardiomyocytes doesn't have an effect on normal embryonic function. However

pharmacological or genetic inhibition of zTREK-1a/b results in an inhibition of zf heart regeneration suggesting that these channels are important for a successful heart regeneration. This suggests that, like mammalian TREK-1, zTREK-1a/b play an important role in pathophysiological zf heart function rather than normal heart function (Unudurthi, Wu et al. 2016). Maintaining a normal heart function after zTREK-1a/b inhibition suggests that the inhibition of regeneration is directly associated with zTREK-1a/b and it is not a secondary effect of an abnormal heart function upon zTREK-1a/b inhibition.

In order to directly address the effect of mechanical stress on zebrafish heart regeneration, ventricular stretch and its ability of contraction should be evaluated after amputation by echocardiography. Recent studies showed that echocardiographic measurements in zebrafish using VEVO2100 imaging system allows to evaluate cardiac parameters (Hein, Lehmann et al. 2015), such as ventricular fractional shortening (The reduction of the length of the end-diastolic diameter that occurs by the end of systole), stroke volume (the volume of blood pumped from the left ventricle per beat), and ventricular outflow velocity (measure of cardiac systolic function and cardiac output). In order to validate our hypothesis based on the implication of mechanical stress during heart regeneration, zebrafish should be treated with hypotension drugs that are known to decrease the ventricular contractility to study their effect during heart regeneration.

In conclusion, zTREK-1a/b share biophysical and pharmacological properties with the mammalian TREK-1, they don't affect heart function under normal conditions, but they are required for successful heart regeneration. However the mechanism of mechanosensing required for heart regeneration as well as the signalization pathway in which zTREK-1a/b are

implicated should be investigated. This will allow us to identify genes that are important for successful heart regeneration which could be also implicated during mammalian pathological hypertrophy.

Our ultimate goal is to find therapeutic genes targets to treat hypertrophy in adult mammals. The massive loss of cardiomyocytes in adult mammals, leads to hypertrophy accompanied with an increase in TREK-1 expression and activity in hypertrophic cardiomyocytes. While inhibiting zTREK-1a/b during zf heart regeneration results in the inability of zf to regenerate their heart. We suspect that the downstream effector of zTREK-1a/b are activated during heart regeneration in zf to promote successful heart regeneration while these downstream effectors are inhibited in adult mammals during hypertrophy. Finding zTREK-1a/b downstream effectors that are activated during heart regeneration in zf and inhibited during hypertrophy in mammals represent potential therapeutic gene targets to treat cardiac hypertrophy. The drugs modulating the activity of TREK-1 provide a path to new category for cardio protective drugs.

French summary

Chez l'homme, les maladies cardiovasculaires représentent la première cause de décès mondiale. La majorité d'entre elles aboutissent à une destruction du tissu ventriculaire alors remplacé par de la fibrose à l'origine de troubles électromécaniques graves du muscle. Il s'en suit le développement d'une hypertrophie pathologique qui évoluera en insuffisance cardiaque nécessitant une greffe d'organe pour les patients. Certaines espèces tel que le poisson zèbre, possède l'extraordinaire capacité de régénération de nombreux organes y compris le muscle cardiaque. Cette capacité de régénération est également observée chez les mammifères dont l'homme mais uniquement à un stade néonatal avec disparition de cette dernière à l'âge adulte. Les mécanismes mis en jeu au cours de la régénération cardiaque chez le poisson zèbre adulte et les mammifères néonataux sont relativement similaires. En effet, le processus consiste en une dédifférenciation des cardiomyocytes associé à un phénotype fœtal pour leur permettre de proliférer. Une fois le nombre de cellules suffisant pour assurer une régénération du tissu atteint, une nouvelle différenciation des cellules est observée pour former des cardiomyocytes matures. Ce phénomène de régénération cardiaque est régulé de la même manière chez le poisson zèbre adulte et les mammifères néonataux. En effet, les conditions d'hypoxie vont réguler positivement la régénération à travers l'expression cardiomyocytaire du facteur HIF1 α (Hypoxia Inducible Factor 1 alpha). A l'opposé, la régénération est inhibée par l'activation de la voie de signalisation intracellulaire aboutissant à une augmentation de l'activité de la MAP Kinase p38 (Mitogen Activated Protein Kinase). L'ensemble de ces données conforte l'implication des mêmes mécanismes pour la régulation de la régénération cardiaque chez les espèces douées de ce phénomène à l'âge adulte et chez les mammifères néonataux.

Chez les mammifères, après sept jours post natal, la capacité de régénération disparaît au profit d'une hypertrophie ventriculaire pathologique suite à la destruction du tissu. De récentes études ont montrées que l'activation de la voie ERK dans les cardiomyocytes de mammifères adultes permettait de restaurer la capacité de régénération. De plus, l'utilisation en clinique humaine d'un dispositif d'assistance ventriculaire sur des patients souffrant d'insuffisance cardiaque sévère, permet d'améliorer leur pronostic. Chez ces patients, une prolifération des cardiomyocytes ventriculaires peut également être observée. L'ensemble de ces informations semble montrer que la capacité de régénération du tissu cardiaque est présente chez le mammifère adulte mais qu'elle semble être bloquée / inhibée. Cependant, au cours du développement embryonnaire, des similitudes entre les différentes espèces sont observées concernant la formation d'un organe adulte. En effet, les cardiomyocytes sont dans un premier temps dans une phase hyperplasique au cours de laquelle ils prolifèrent. Une fois le nombre de cellules nécessaires à la formation du muscle cardiaque atteint, les cardiomyocytes passent alors dans une phase hypertrophique au cours de laquelle ils augmentent leur taille et acquièrent leurs caractères de différenciation. C'est après ces deux étapes similaires que des divergences sont alors observées entre les espèces douées de

régénération à l'âge adulte ainsi que les mammifères néonataux et les mammifères adultes. En effet, chez le poisson zèbre et les mammifères néonataux, les conditions de stress vont provoquer la dédifférenciation des cardiomyocytes qui ré expriment alors un phénotype fœtal avec acquisition de la capacité de prolifération et par conséquent de régénération. En revanche, chez les mammifères adultes, ces mêmes conditions de stress vont alors déclencher des voies d'hypertrophies pathologiques avec une évolution en insuffisance cardiaque sévère et toutes les conséquences néfastes associées.

Au cours de ces deux phénomènes, à savoir la régénération et l'hypertrophie pathologique, de nombreux facteurs sont mis en jeu. Parmi ces différents, peuvent être citées les contraintes mécaniques, laissant ainsi supposer l'implication de mécano senseurs tels que les canaux ioniques. De nombreuses études ont montré que les forces mécaniques jouaient un rôle important dans le développement embryonnaire cardiaque, situation au cours de laquelle l'environnement cellulaire est similaire à celui observé au cours de la régénération. De plus, d'autres études révèlent l'implication de canaux ioniques mécano sensibles au cours de la mise en place de l'hypertrophie pathologique. En effet, le canal TRPC6 semble être un acteur essentiel de l'activation de la voie calcineurine NFAT3 dans ce processus. D'autres études montrent que le canal TREK-1 appartenant à la famille des canaux potassiques à deux domaines pores, est surexprimé au cours de l'hypertrophie pathologique et de l'ischémie cardiaque. Ce canal présente une activation qui est dite poly modale. En effet, le canal TREK-1 est activé par les stimuli mécaniques tels que la tension membranaire, la chaleur, les anesthésiques volatiles, les molécules à effet neuroprotecteur tel que le riluzole, les acides gras polyinsaturés ou encore l'acidification intracellulaire.

Lors de ces travaux sur la régénération cardiaque, un focus sur l'implication du canal TREK-1 a été réalisé pour différentes raisons. En effet, de nombreuses conditions d'activation du canal TREK-1 peuvent être observées, que ce soit au cours de la régénération sur le poisson zèbre adulte et les mammifères néonataux ou au cours du développement de l'hypertrophie pathologique chez le mammifère adulte. Durant la régénération, la dédifférenciation, l'individualisation et le changement de forme des cardiomyocytes pour permettre la prolifération laissent supposer de la présence de contraintes mécaniques. L'augmentation de la charge ventriculaire présente en post amputation va également dans ce sens. De plus, après une amputation cardiaque chez le poisson zèbre, une acidification du milieu intracellulaire est provoquée par une augmentation significative de peroxyde d'hydrogène H₂O₂. Enfin, la surexpression au cours de la régénération, des gènes permettant le contrôle des différents points de transition du cycle cellulaire, laisse penser à une implication potentielle de canaux potassiques dont le rôle dans la régulation de la prolifération a déjà été bien décrit. Durant le développement de l'hypertrophie pathologique, une surcharge ventriculaire avec des contraintes mécaniques associées, est également observée. L'augmentation de la taille des

cardiomyocytes est associée à des phénomènes de traction membranaire. L'ischémie cardiaque précédant l'hypertrophie, est accompagnée d'une acidification intracellulaire ainsi que d'une modification du ratio acides gras polyinsaturés / lipides membranaires totaux dans la membrane des cardiomyocytes. L'ensemble de ces données concernant ces deux voies opposées, à savoir la régénération et l'hypertrophie pathologique, fait du canal TREK-1, un candidat de choix pour l'étude de l'implication des canaux ioniques mécano sensibles dans la régénération cardiaque chez le poisson zèbre. Deux iso formes du canal TREK-1 sont exprimés sur le tissu cardiaque de poisson zèbre, à savoir les canaux zTREK-1a et zTREK-1b.

Dans un premier temps, l'expression des canaux TREK-1a et TREK-1b a été vérifiée par amplification de l'ADN complémentaire synthétisé à partir de l'ARN extrait du tissu cardiaque à différents stades de développement et adulte. Les résultats montrent alors que les canaux s'expriment seulement à partir de 4 jours de développement avec un niveau d'expression croissant jusqu'à l'âge adulte. En tenant compte du fait que le muscle cardiaque est entièrement formé à partir de 2 jours de développement, l'hypothèse que les canaux TREK-1a et TREK-1b ne semblent pas être impliqués dans ce processus, peut alors être faite. L'expression fonctionnelle des canaux sur le tissu cardiaque a par la suite été étudiée. Pour cela, différents outils pharmacologiques et de biologie moléculaires développés sur le canal TREK-1 humain ont été utilisés. Pour cette raison, cette étude de l'expression fonctionnelle a été précédée d'une caractérisation des canaux TREK-1a et TREK-1b. Cette dernière a consisté à déterminer les propriétés biophysiques et pharmacologiques des canaux TREK-1a et TREK-1b afin de les comparer avec celles décrites pour le canal TREK-1 humain dans la littérature, et à valider différents outils tels que les anticorps développés sur l'isoforme humaine.

Pour cela, les canaux TREK-1a et TREK-1b ont été clonés puis sous clonés dans un vecteur d'expression permettant de transfecter des cellules HEK. Des enregistrements de l'activité des canaux ont alors été réalisés par utilisation de la technique de patch clamp. Ces derniers ont permis de montrer que les canaux TREK-1a et TREK-1b possédaient des propriétés similaires à celles du canal TREK-1 humain. En effet, ils sont activés par l'étirement membranaire, par les acides gras polyinsaturés, et par l'acidification intracellulaire. En revanche, ils sont inhibés par le cytosquelette et par la spadine, un peptide inhibiteur spécifique de TREK-1. La caractérisation ainsi réalisée a, comme mentionné précédemment, été suivie d'une étude fonctionnelle des canaux TREK-1a et TREK-1b sur les cardiomyocytes adultes de poisson zèbre. Pour cela, une immunofluorescence a été réalisée sur des cardiomyocytes en culture primaire, ainsi que sur des sections de cœurs issus d'animaux sauvages adultes. Cette dernière permet de mettre en évidence la présence spécifique des canaux sur les cellules cardiaques. Des enregistrements de patch clamp avec applications de protocoles de pressions négatives ont également été effectués sur les cardiomyocytes adultes en culture primaire. Ces

enregistrements montrent la présence d'un courant caractéristique du courant TREK-1 avec une inhibition spécifique par la spadine observée.

L'objectif de cette étude a été d'étudier après clonage et caractérisation, l'implication des canaux TREK-1a et TREK-1b dans le phénomène de régénération cardiaque. Ainsi, deux stratégies ont été mise en place. La première de ces stratégies a consisté à réaliser une étude pharmacologique in vivo. Pour ce faire, des poissons sauvages ont été amputés puis séparés en deux groupes distincts. Le premier groupe a reçu un traitement véhicule par injection intrapéritonéale durant un mois, et le second groupe un traitement avec la spadine afin d'inhiber les canaux TREK-1a et TREK-1b. Après un mois de traitement, la régénération cardiaque a été évaluée sur les animaux de ces deux groupes. Pour cela, les cœurs ont été prélevés sur les animaux sacrifiés, et des sections ont été réalisées. Sur ces sections, des immunomarquages ont été effectués pour évaluer la présence ou l'absence de cardiomyocytes dans la zone d'amputation. Des tests AFOG (Acid Fuchsin Orange G) ont également été effectués afin de mettre en évidence la présence ou l'absence de collagène et de fibrine caractéristiques du caillot sanguin dans la zone d'amputation. Les résultats obtenus, montrent ainsi que les animaux traités avec le véhicule en post amputation, ont régénéré entièrement leur muscle cardiaque avec absence de marquage au collagène et à la fibrine donc de caillot sanguin dans la zone d'amputation. En revanche, pour les animaux traités avec la spadine, l'absence de régénération avec persistance du caillot sanguin dans la zone d'amputation, a été constatée, laissant supposer un rôle important pour la régénération des canaux TREK-1a et TREK-1b.

Pour valider plus spécifiquement ces résultats préliminaires, une seconde stratégie a été adoptée. Cette dernière a consisté à réaliser les mêmes expériences que celles décrites dans la première stratégie, mais sur des animaux transgéniques exprimant une forme dominante négative du canal TREK-1. Pour la réalisation de cette lignée transgénique, une délétion de l'exon 4 sur le gène codant le canal TREK-1 a été insérée. Cette dernière a été intégrée dans des embryons au stade une cellule sous la forme de deux constructions génétiques, avec un système inductible de type « CRE recombinase », permettant son expression à la demande par un simple traitement avec le tamoxifène. Le traitement avec le tamoxifène permet ainsi une expression irréversible de la forme dominante négative de TREK-1 dans les cardiomyocytes. Les embryons transgéniques obtenus sont alors développés jusqu'à obtention d'animaux adultes. Sur ces derniers, après une induction véhicule avec l'éthanol ne permettant pas l'expression de la forme dominante négative de TREK-1 ou une induction tamoxifène permettant l'expression de la forme dominante négative de TREK-1, une amputation cardiaque est réalisée. Après un mois, la régénération est alors évaluée par les mêmes expériences d'immunomarquages que celles décrites dans la première stratégie, à savoir des marquages permettant de mettre en évidence la présence ou l'absence de cardiomyocytes et la présence ou l'absence de collagène et de fibrine donc du caillot sanguin dans la zone d'amputation. Les

résultats obtenus pour ces expériences de régénération utilisant la lignée transgénique, montrent que l'induction véhicule avec l'éthanol n'empêche pas la régénération cardiaque puisque des cardiomyocytes sont présents dans la zone d'amputation et aucun marquage de collagène et de fibrine donc du caillot sanguin n'est détecté. En revanche, l'induction avec le tamoxifène empêche la régénération puisque aucun cardiomyocyte n'est détecté dans la zone d'amputation et une persistance du caillot sanguin est observée par un marquage positif pour le collagène et la fibrine. L'ensemble de ces résultats montre que les canaux TREK-1a et TREK-1b semblent être importants pour la régénération cardiaque chez le poisson zèbre et renforce les résultats qui ont été obtenus au cours de la première stratégie basée sur l'inhibition pharmacologique des canaux.

Dans le but de déterminer si les observations faites sur la régénération cardiaque suite à l'inhibition des canaux TREK-1a et TREK-1b ne résultent pas d'une perturbation de l'activité cardiaque normale, d'autres expériences complémentaires ont été réalisées. Pour cela, des enregistrements de fréquence cardiaque sur des embryons à 4 et 5 jours de développement ont été réalisés. Pour ces enregistrements, des embryons issus de la lignée transgénique exprimant la forme dominante négative de TREK-1 ont été induits avec l'éthanol pour le groupe contrôle et avec le tamoxifène pour le groupe expérimental. Les résultats ont montré qu'aucune différence n'est observée pour ces deux groupes d'embryons. Par la suite, des enregistrements de vitesse de propagation et de fréquence cardiaque ont été réalisés *in vitro*, sur des cœurs isolés issus de poissons sauvages traités avec un véhicule ou avec la spadine pour inhiber les canaux TREK-1a et TREK-1b. Une fois encore, aucune différence significative n'est observée entre les animaux contrôles et les animaux traités avec l'inhibiteur. L'ensemble de ces données semble montrer que les canaux TREK-1a et TREK-1b ne jouent pas de rôle prépondérant dans la physiologie cardiaque chez le poisson zèbre et que l'absence de régénération observée dans les expériences précédemment décrites, est bien une conséquence de leur inhibition.

Pour conclure sur l'ensemble de ce travail, l'expression des canaux TREK-1a et TREK-1b sur le tissu cardiaque de poisson zèbre peut-être mentionnée. Ces canaux présentent des propriétés biophysiques et pharmacologiques similaires à celles décrites précédemment sur le canal TREK-1 de mammifère. Les outils de biologie moléculaire tels que les anticorps anti TREK-1, développés sur le canal de mammifère sont également efficace sur les canaux TREK-1a et TREK-1b de poisson zèbre. Les expériences qui ont été réalisées pour évaluer le rôle des canaux TREK-1a et TREK-1b dans la physiologie cardiaque, ont montrés qu'aucune différence significative ne peut être mise en évidence concernant la fonction cardiaque suite à l'inhibition ou l'absence de ces canaux. En revanche, leur inhibition ou leur absence ne permet plus d'assurer une régénération du tissu cardiaque qui représente un phénomène naturel chez le poisson zèbre. Toutes ces données semblent suggérer que les canaux TREK-1a et TREK-1b ne sont pas impliqués dans des processus de régulation du développement cardiaque

embryonnaire et de physiologie mais qu'en revanche, ils jouent un rôle clé dans la régénération du tissu cardiaque avec donc une implication dans des processus physiopathologiques.

De nombreuses perspectives sont envisagées pour la suite de ces travaux évaluant l'implication des canaux TREK-1a et TREK-1b sur la régénération cardiaque chez le poisson zèbre. Parmi ces perspectives, une étude sur le rôle des canaux TREK-1a et TREK-1b sur le contrôle des différentes étapes de la régénération pourrait être faite. En effet, au cours de la régénération, les cardiomyocytes passent par des étapes de dédifférenciation, de prolifération et de re différenciation. Ainsi, il serait intéressant d'évaluer le rôle des canaux TREK-1a et TREK-1b sur le contrôle de chacune de ces étapes. Par la suite, des analyses de micro arrays pourraient être faites dans différentes conditions et au cours de la régénération. Ces analyses permettront de mettre en évidence des partenaires potentiels des canaux TREK-1a et TREK-1b et des voies de signalisations importantes pour la régénération cardiaque.

References

Afzali, A. M., T. Ruck, A. M. Herrmann, J. Iking, C. Sommer, C. Kleinschnitz, C. Preubetae, W. Stenzel, T. Budde, H. Wiendl, S. Bittner and S. G. Meuth (2016). "The potassium channels TASK2 and TREK1 regulate functional differentiation of murine skeletal muscle cells." *Am J Physiol Cell Physiol* **311**(4): C583-c595.

Alcaino, C., K. Knutson, P. A. Gottlieb, G. Farrugia and A. Beyder (2017). "Mechanosensitive ion channel Piezo2 is inhibited by D-GsMTx4." *Channels (Austin)* **11**(3): 245-253.

Amit, M., M. K. Carpenter, M. S. Inokuma, C. P. Chiu, C. P. Harris, M. A. Waknitz, J. Itskovitz-Eldor and J. A. Thomson (2000). "Clonally derived human embryonic stem cell lines maintain pluripotency and proliferative potential for prolonged periods of culture." *Dev Biol* **227**(2): 271-278.

Ander, B. P., C. M. Dupasquier, M. A. Prociuk and G. N. Pierce (2003). "Polyunsaturated fatty acids and their effects on cardiovascular disease." *Exp Clin Cardiol* **8**(4): 164-172.

Arnadottir, J. and M. Chalfie (2010). "Eukaryotic mechanosensitive channels." *Annu Rev Biophys* **39**: 111-137.

Avitabile, D., A. Crespi, C. Brioschi, V. Parente, G. Toietta, P. Devanna, M. Baruscotti, S. Truffa, A. Scavone, F. Rusconi, A. Biondi, Y. D'Alessandra, E. Vigna, D. Difrancesco, M. Pesce, M. C. Capogrossi and A. Barbuti (2011). "Human cord blood CD34+ progenitor cells acquire functional cardiac properties through a cell fusion process." *Am J Physiol Heart Circ Physiol* **300**(5): H1875-1884.

Bae, C., R. Gnanasambandam, C. Nicolai, F. Sachs and P. A. Gottlieb (2013). "Xerocytosis is caused by mutations that alter the kinetics of the mechanosensitive channel PIEZO1." *Proc Natl Acad Sci U S A* **110**(12): E1162-1168.

Barry, S. P., S. M. Davidson and P. A. Townsend (2008). "Molecular regulation of cardiac hypertrophy." *Int J Biochem Cell Biol* **40**(10): 2023-2039.

Bassat, E., Y. E. Mutlak, A. Genzelinakh, I. Y. Shadrin, K. Baruch Umansky, O. Yifa, D. Kain, D. Rajchman, J. Leach, D. Riabov Bassat, Y. Udi, R. Sarig, I. Sagi, J. F. Martin, N. Bursac, S. Cohen and E. Tzahor (2017). "The extracellular matrix protein agrin promotes heart regeneration in mice." *Nature* **547**(7662): 179-184.

Basson, M. D., B. Zeng, C. Downey, M. P. Sirivelu and J. J. Tepe (2015). "Increased extracellular pressure stimulates tumor proliferation by a mechanosensitive calcium channel and PKC-beta." *Mol Oncol* **9**(2): 513-526.

Belloq, C., A. C. van Ginneken, C. R. Bezzina, M. Alders, D. Escande, M. M. Mannens, I. Baro and A. A. Wilde (2004). "Mutation in the KCNQ1 gene leading to the short QT-interval syndrome." *Circulation* **109**(20): 2394-2397.

Bergmann, O., R. D. Bhardwaj, S. Bernard, S. Zdunek, F. Barnabe-Heider, S. Walsh, J. Zupicich, K. Alkass, B. A. Buchholz, H. Druid, S. Jovinge and J. Frisen (2009). "Evidence for cardiomyocyte renewal in humans." *Science* **324**(5923): 98-102.

Beyder, A., J. L. Rae, C. Bernard, P. R. Strege, F. Sachs and G. Farrugia (2010). "Mechanosensitivity of Nav1.5, a voltage-sensitive sodium channel." *J Physiol* **588**(Pt 24): 4969-4985.

Birks, E. J., P. D. Tansley, J. Hardy, R. S. George, C. T. Bowles, M. Burke, N. R. Banner, A. Khaghani and M. H. Yacoub (2006). "Left ventricular assist device and drug therapy for the reversal of heart failure." *N Engl J Med* **355**(18): 1873-1884.

Blaschke, R. J., N. D. Hahurij, S. Kuijper, S. Just, L. J. Wisse, K. Deissler, T. Maxelon, K. Anastassiadis, J. Spitzer, S. E. Hardt, H. Scholer, H. Feitsma, W. Rottbauer, M. Blum, F. Meijlink, G. Rappold and A. C. Gittenberger-de Groot (2007). "Targeted mutation reveals essential functions of the homeodomain transcription factor Shox2 in sinoatrial and pacemaker development." *Circulation* **115**(14): 1830-1838.

Blom, J. N., X. Lu, P. Arnold and Q. Feng (2016). "Myocardial Infarction in Neonatal Mice, A Model of Cardiac Regeneration." *J Vis Exp*(111).

Bockenauer, D., N. Zilberberg and S. A. Goldstein (2001). "KCNK2: reversible conversion of a hippocampal potassium leak into a voltage-dependent channel." *Nat Neurosci* **4**(5): 486-491.

Bowman, C. L., P. A. Gottlieb, T. M. Suchyna, Y. K. Murphy and F. Sachs (2007). "Mechanosensitive ion channels and the peptide inhibitor GsMTx-4: history, properties, mechanisms and pharmacology." *Toxicol* **49**(2): 249-270.

Boycott, H. E., C. S. Barbier, C. A. Eichel, K. D. Costa, R. P. Martins, F. Louault, G. Dilanian, A. Coulombe, S. N. Hatem and E. Balse (2013). "Shear stress triggers insertion of voltage-gated potassium channels from intracellular compartments in atrial myocytes." *Proc Natl Acad Sci U S A* **110**(41): E3955-3964.

Brand, T., S. L. Simrick, K. L. Poon and R. F. Schindler (2014). "The cAMP-binding Popdc proteins have a redundant function in the heart." *Biochem Soc Trans* **42**(2): 295-301.

Brendel, J. and S. Peukert (2003). "Blockers of the Kv1.5 channel for the treatment of atrial arrhythmias." *Curr Med Chem Cardiovasc Hematol Agents* **1**(3): 273-287.

Burger, E. H. and J. Klein-Nulend (1998). "Microgravity and bone cell mechanosensitivity." Bone **22**(5 Suppl): 127s-130s.

Bush, E. W., D. B. Hood, P. J. Papst, J. A. Chapo, W. Minobe, M. R. Bristow, E. N. Olson and T. A. McKinsey (2006). "Canonical transient receptor potential channels promote cardiomyocyte hypertrophy through activation of calcineurin signaling." J Biol Chem **281**(44): 33487-33496.

Canseco, D. C., W. Kimura, S. Garg, S. Mukherjee, S. Bhattacharya, S. Abdisalaam, S. Das, A. Asaithamby, P. P. Mammen and H. A. Sadek (2015). "Human ventricular unloading induces cardiomyocyte proliferation." J Am Coll Cardiol **65**(9): 892-900.

Chablais, F., J. Veit, G. Rainer and A. Jazwinska (2011). "The zebrafish heart regenerates after cryoinjury-induced myocardial infarction." BMC Dev Biol **11**: 21.

Chao, C. M., J. S. Jin, C. S. Tsai, Y. Tsai, W. H. Chen, C. C. Chung and S. H. Loh (2002). "Effect of hydrogen peroxide on intracellular pH in the human atrial myocardium." Chin J Physiol **45**(3): 123-129.

Chemin, J., C. Girard, F. Duprat, F. Lesage, G. Romey and M. Lazdunski (2003). "Mechanisms underlying excitatory effects of group I metabotropic glutamate receptors via inhibition of 2P domain K⁺ channels." Embo j **22**(20): 5403-5411.

Chemin, J., A. J. Patel, F. Duprat, I. Lauritzen, M. Lazdunski and E. Honore (2005). "A phospholipid sensor controls mechanogating of the K⁺ channel TREK-1." Embo j **24**(1): 44-53.

Chen, H., J. Wang, Z. Liu, H. Yang, Y. Zhu, M. Zhao, Y. Liu and M. Yan (2016). "Mitochondrial DNA depletion causes decreased ROS production and resistance to apoptosis." Int J Mol Med **38**(4): 1039-1046.

Cheng, L., F. Su, N. Ripen, H. Fan, K. Huang, M. Wang, H. Peng, C. Mei, F. Zhao and Y. Liao (2006). "Changes of expression of stretch-activated potassium channel TREK-1 mRNA and protein in hypertrophic myocardium." J Huazhong Univ Sci Technolog Med Sci **26**(1): 31-33.

Chiu, L. L., R. K. Iyer, L. A. Reis, S. S. Nunes and M. Radisic (2012). "Cardiac tissue engineering: current state and perspectives." Front Biosci (Landmark Ed) **17**: 1533-1550.

Clapham, D. E. (2003). "TRP channels as cellular sensors." Nature **426**(6966): 517-524.

Comoglio, Y., J. Levitz, M. A. Kienzler, F. Lesage, E. Y. Isacoff and G. Sandoz (2014). "Phospholipase D2 specifically regulates TREK potassium channels via direct interaction and local production of phosphatidic acid." Proc Natl Acad Sci U S A **111**(37): 13547-13552.

Coste, B., J. Mathur, M. Schmidt, T. J. Earley, S. Ranade, M. J. Petrus, A. E. Dubin and A. Patapoutian (2010). "Piezo1 and Piezo2 are essential components of distinct mechanically activated cation channels." Science **330**(6000): 55-60.

Cotter, G., M. Metra, O. Milo-Cotter, H. C. Dittrich and M. Gheorghiade (2008). "Fluid overload in acute heart failure—re-distribution and other mechanisms beyond fluid accumulation." Eur J Heart Fail **10**(2): 165-169.

Cowles, C. L., Y. Y. Wu, S. D. Barnett, M. T. Lee, H. R. Burkin and I. L. Buxton (2015). "Alternatively Spliced Human TREK-1 Variants Alter TREK-1 Channel Function and Localization." Biol Reprod **93**(5): 122.

Craelius, W., V. Chen and N. el-Sherif (1988). "Stretch activated ion channels in ventricular myocytes." Biosci Rep **8**(5): 407-414.

Cuadrado, A. and A. R. Nebreda (2010). "Mechanisms and functions of p38 MAPK signalling." Biochem J **429**(3): 403-417.

Curado, S., R. M. Anderson, B. Jungblut, J. Mumm, E. Schroeter and D. Y. Stainier (2007). "Conditional targeted cell ablation in zebrafish: a new tool for regeneration studies." Dev Dyn **236**(4): 1025-1035.

D'Uva, G., A. Aharonov, M. Lauriola, D. Kain, Y. Yahalom-Ronen, S. Carvalho, K. Weisinger, E. Bassat, D. Rajchman, O. Yifa, M. Lysenko, T. Konfino, J. Hegesh, O. Brenner, M. Neeman, Y. Yarden, J. Leor, R. Sarig, R. P. Harvey and E. Tzahor (2015). "ERBB2 triggers mammalian heart regeneration by promoting cardiomyocyte dedifferentiation and proliferation." Nat Cell Biol **17**(5): 627-638.

Darehzereshki, A., N. Rubin, L. Gamba, J. Kim, J. Fraser, Y. Huang, J. Billings, R. Mohammadzadeh, J. Wood, D. Warburton, V. Kaartinen and C. L. Lien (2015). "Differential regenerative capacity of neonatal mouse hearts after cryoinjury." Dev Biol **399**(1): 91-99.

Decher, N., B. Ortiz-Bonnin, C. Friedrich and M. Schewe (2017). "Sodium permeable and "hypersensitive" TREK-1 channels cause ventricular tachycardia." **9**(4): 403-414.

Delmas, P. and B. Coste (2013). "Mechano-gated ion channels in sensory systems." Cell **155**(2): 278-284.

Demion, M., J. Thireau, M. Gueffier, A. Finan, Z. Khoueiry, C. Cassan, N. Serafini, F. Aimond, M. Granier, J. L. Pasquie, P. Launay and S. Richard (2014). "Trpm4 gene invalidation leads to cardiac hypertrophy and electrophysiological alterations." *PLoS One* **9**(12): e115256.

Denzer, A. J., R. Brandenberger, M. Gesemann, M. Chiquet and M. A. Ruegg (1997). "Agrin binds to the nerve-muscle basal lamina via laminin." *J Cell Biol* **137**(3): 671-683.

Djillani, A., M. Pietri, S. Moreno, C. Heurteaux, J. Mazella and M. Borsotto (2017). "Shortened Spadin Analogs Display Better TREK-1 Inhibition, In Vivo Stability and Antidepressant Activity." *Front Pharmacol* **8**: 643.

Dolly, J. O. and D. N. Parcej (1996). "Molecular properties of voltage-gated K⁺ channels." *J Bioenerg Biomembr* **28**(3): 231-253.

Dong, Y. Y., A. C. Pike, A. Mackenzie, C. McClenaghan, P. Aryal, L. Dong, A. Quigley, M. Grieben, S. Goubin, S. Mukhopadhyay, G. F. Ruda, M. V. Clausen, L. Cao, P. E. Brennan, N. A. Burgess-Brown, M. S. Sansom, S. J. Tucker and E. P. Carpenter (2015). "K2P channel gating mechanisms revealed by structures of TREK-2 and a complex with Prozac." *Science* **347**(6227): 1256-1259.

Drew, L. J., F. Rugiero, P. Cesare, J. E. Gale, B. Abrahamsen, S. Bowden, S. Heinzmann, M. Robinson, A. Brust, B. Colless, R. J. Lewis and J. N. Wood (2007). "High-threshold mechanosensitive ion channels blocked by a novel conopeptide mediate pressure-evoked pain." *PLoS One* **2**(6): e515.

Duffy, H. S., A. W. Ashton, P. O'Donnell, W. Coombs, S. M. Taffet, M. Delmar and D. C. Spray (2004). "Regulation of connexin43 protein complexes by intracellular acidification." *Circ Res* **94**(2): 215-222.

Engel, F. B., M. Schebesta, M. T. Duong, G. Lu, S. Ren, J. B. Madwed, H. Jiang, Y. Wang and M. T. Keating (2005). "p38 MAP kinase inhibition enables proliferation of adult mammalian cardiomyocytes." *Genes Dev* **19**(10): 1175-1187.

Enyedi, P. and G. Czirjak (2010). "Molecular background of leak K⁺ currents: two-pore domain potassium channels." *Physiol Rev* **90**(2): 559-605.

Ernstrom, G. G. and M. Chalfie (2002). "Genetics of sensory mechanotransduction." *Annu Rev Genet* **36**: 411-453.

Evans, M. J. and M. H. Kaufman (1981). "Establishment in culture of pluripotential cells from mouse embryos." *Nature* **292**(5819): 154-156.

Faucherre, A. and C. Jopling (2013). "The heart's content-renewable resources." *Int J Cardiol* **167**(4): 1141-1146.

Faucherre, A., K. Kissa, J. Nargeot, M. E. Mangoni and C. Jopling (2016). "Comment on: 'Homozygous knockout of the piezo1 gene in the zebrafish is not associated with anemia'." *Haematologica* **101**(1): e38.

Faucherre, A., J. Nargeot, M. E. Mangoni and C. Jopling (2013). "piezo2b regulates vertebrate light touch response." *J Neurosci* **33**(43): 17089-17094.

Fink, M., F. Duprat, F. Lesage, R. Reyes, G. Romey, C. Heurteaux and M. Lazdunski (1996). "Cloning, functional expression and brain localization of a novel unconventional outward rectifier K⁺ channel." *Embo j* **15**(24): 6854-6862.

Flink, I. L. (2002). "Cell cycle reentry of ventricular and atrial cardiomyocytes and cells within the epicardium following amputation of the ventricular apex in the axolotl, *Amblystoma mexicanum*: confocal microscopic immunofluorescent image analysis of bromodeoxyuridine-labeled nuclei." *Anat Embryol (Berl)* **205**(3): 235-244.

Fruleux, A. and R. J. Hawkins (2016). "Physical role for the nucleus in cell migration." *J Phys Condens Matter* **28**(36): 363002.

Fukasaku, M., J. Kimura and O. Yamaguchi (2016). "Swelling-activated and arachidonic acid-induced currents are TREK-1 in rat bladder smooth muscle cells." *Fukushima J Med Sci* **62**(1): 18-26.

Garin, G. and B. C. Berk (2006). "Flow-mediated signaling modulates endothelial cell phenotype." *Endothelium* **13**(6): 375-384.

Geng, J., Q. Zhao, T. Zhang and B. Xiao (2017). "In Touch With the Mechanosensitive Piezo Channels: Structure, Ion Permeation, and Mechanotransduction." *Curr Top Membr* **79**: 159-195.

Gesemann, M., A. Brancaccio, B. Schumacher and M. A. Ruegg (1998). "Agrin is a high-affinity binding protein of dystroglycan in non-muscle tissue." *J Biol Chem* **273**(1): 600-605.

Gierten, J., D. Hassel, P. A. Schweizer, R. Becker, H. A. Katus and D. Thomas (2012). "Identification and functional characterization of zebrafish K(2P)10.1 (TREK2) two-pore-domain K(+) channels." *Biochim Biophys Acta* **1818**(1): 33-41.

Gil, V., D. Gallego, H. Moha Ou Maati, R. Peyronnet, M. Martinez-Cutillas, C. Heurteaux, M. Borsotto and M. Jimenez (2012). "Relative contribution of SKCa and TREK1 channels in purinergic and nitrergic neuromuscular transmission in the rat colon." *Am J Physiol Gastrointest Liver Physiol* **303**(3): G412-423.

Gnecchi, M., Z. Zhang, A. Ni and V. J. Dzau (2008). "Paracrine mechanisms in adult stem cell signaling and therapy." *Circ Res* **103**(11): 1204-1219.

Gruss, M., T. J. Bushell, D. P. Bright, W. R. Lieb, A. Mathie and N. P. Franks (2004). "Two-pore-domain K⁺ channels are a novel target for the anesthetic gases xenon, nitrous oxide, and cyclopropane." *Mol Pharmacol* **65**(2): 443-452.

Gu, Y. and C. Gu (2014). "Physiological and pathological functions of mechanosensitive ion channels." *Mol Neurobiol* **50**(2): 339-347.

Guilluy, C., L. D. Osborne, L. Van Landeghem, L. Sharek, R. Superfine, R. Garcia-Mata and K. Burrige (2014). "Isolated nuclei adapt to force and reveal a mechanotransduction pathway in the nucleus." *Nat Cell Biol* **16**(4): 376-381.

Gutierrez-Aranda, I., V. Ramos-Mejia, C. Bueno, M. Munoz-Lopez, P. J. Real, A. Macia, L. Sanchez, G. Ligerio, J. L. Garcia-Perez and P. Menendez (2010). "Human induced pluripotent stem cells develop teratoma more efficiently and faster than human embryonic stem cells regardless the site of injection." *Stem Cells* **28**(9): 1568-1570.

Han, P., X. H. Zhou, N. Chang, C. L. Xiao, S. Yan, H. Ren, X. Z. Yang, M. L. Zhang, Q. Wu, B. Tang, J. P. Diao, X. Zhu, C. Zhang, C. Y. Li, H. Cheng and J. W. Xiong (2014). "Hydrogen peroxide primes heart regeneration with a derepression mechanism." *Cell Res* **24**(9): 1091-1107.

Hassel, D., T. Dahme, J. Erdmann, B. Meder, A. Hüge, M. Stoll, S. Just, A. Hess, P. Ehlermann, D. Weichenhan, M. Grimmmler, H. Liptau, R. Hetzer, V. Regitz-Zagrosek, C. Fischer, P. Nurnberg, H. Schunkert, H. A. Katus and W. Rottbauer (2009). "Nexilin mutations destabilize cardiac Z-disks and lead to dilated cardiomyopathy." *Nat Med* **15**(11): 1281-1288.

Haubner, B. J., M. Adamowicz-Brice, S. Khadayate, V. Tiefenthaler, B. Metzler, T. Aitman and J. M. Penninger (2012). "Complete cardiac regeneration in a mouse model of myocardial infarction." *Aging (Albany NY)* **4**(12): 966-977.

Hein, S. J., L. H. Lehmann, M. Kossack, L. Juergensen, D. Fuchs, H. A. Katus and D. Hassel (2015). "Advanced echocardiography in adult zebrafish reveals delayed recovery of heart function after myocardial cryoinjury." *PLoS One* **10**(4): e0122665.

Heurteaux, C., N. Guy, C. Laigle, N. Blondeau, F. Duprat, M. Mazzuca, L. Lang-Lazdunski, C. Widmann, M. Zanzouri, G. Romey and M. Lazdunski (2004). "TREK-1, a K⁺ channel involved in neuroprotection and general anesthesia." *Embo j* **23**(13): 2684-2695.

Hibino, H., A. Inanobe, K. Furutani, S. Murakami, I. Findlay and Y. Kurachi (2010). "Inwardly rectifying potassium channels: their structure, function, and physiological roles." *Physiol Rev* **90**(1): 291-366.

Hoffmann, S., I. M. Berger, A. Glaser, C. Bacon, L. Li, N. Gretz, H. Steinbeisser, W. Rottbauer, S. Just and G. Rappold (2013). "Islet1 is a direct transcriptional target of the homeodomain transcription factor Shox2 and rescues the Shox2-mediated bradycardia." *Basic Res Cardiol* **108**(2): 339.

Honore, E. (2007). "The neuronal background K₂P channels: focus on TREK1." *Nat Rev Neurosci* **8**(4): 251-261.

Honore, E., F. Maingret, M. Lazdunski and A. J. Patel (2002). "An intracellular proton sensor commands lipid- and mechano-gating of the K(+) channel TREK-1." *Embo j* **21**(12): 2968-2976.

Hou, J. H., J. M. Kralj, A. D. Douglass, F. Engert and A. E. Cohen (2014). "Simultaneous mapping of membrane voltage and calcium in zebrafish heart in vivo reveals chamber-specific developmental transitions in ionic currents." *Front Physiol* **5**: 344.

Hund, T. J., J. S. Snyder, X. Wu, P. Glynn, O. M. Koval, B. Onal, N. D. Leymaster, S. D. Unudurthi, J. Curran, C. Camardo, P. J. Wright, P. F. Binkley, M. E. Anderson and P. J. Mohler (2014). "beta(IV)-Spectrin regulates TREK-1 membrane targeting in the heart." *Cardiovasc Res* **102**(1): 166-175.

Hwang, E. M., E. Kim, O. Yarishkin, D. H. Woo, K. S. Han, N. Park, Y. Bae, J. Woo, D. Kim, M. Park, C. J. Lee and J. Y. Park (2014). "A disulphide-linked heterodimer of TWIK-1 and TREK-1 mediates passive conductance in astrocytes." *Nat Commun* **5**: 3227.

Innamaa, A., L. Jackson, V. Asher, G. van Schalkwyk, A. Warren, A. Keightley, D. Hay, A. Bali, H. Sowter and R. Khan (2013). "Expression and effects of modulation of the K₂P potassium channels TREK-1 (KCNK2) and TREK-2 (KCNK10) in the normal human ovary and epithelial ovarian cancer." *Clin Transl Oncol* **15**(11): 910-918.

Ishihara, K., N. Sarai, K. Asakura, A. Noma and S. Matsuoka (2009). "Role of Mg²⁺ block of the inward rectifier K(+) current in cardiac repolarization reserve: A quantitative simulation." *J Mol Cell Cardiol* **47**(1): 76-84.

January, C. T., Q. Gong and Z. Zhou (2000). "Long QT syndrome: cellular basis and arrhythmia mechanism in LQT2." *J Cardiovasc Electrophysiol* **11**(12): 1413-1418.

Jopling, C., E. Sleep, M. Raya, M. Marti, A. Raya and J. C. Izpisua Belmonte (2010). "Zebrafish heart regeneration occurs by cardiomyocyte dedifferentiation and proliferation." *Nature* **464**(7288): 606-609.

Jopling, C., G. Sune, A. Faucherre, C. Fabregat and J. C. Izpisua Belmonte (2012). "Hypoxia induces myocardial regeneration in zebrafish." *Circulation* **126**(25): 3017-3027.

Jopling, C., G. Sune, C. Morera and J. C. Izpisua Belmonte (2012). "p38alpha MAPK regulates myocardial regeneration in zebrafish." *Cell Cycle* **11**(6): 1195-1201.

Kang, D., C. Choe, E. Cavanaugh and D. Kim (2007). "Properties of single two-pore domain TREK-2 channels expressed in mammalian cells." *J Physiol* **583**(Pt 1): 57-69.

Kang, D., C. Choe and D. Kim (2005). "Thermosensitivity of the two-pore domain K⁺ channels TREK-2 and TRAAK." *J Physiol* **564**(Pt 1): 103-116.

Kang, J., J. R. Huguenard and D. A. Prince (2000). "Voltage-gated potassium channels activated during action potentials in layer V neocortical pyramidal neurons." *J Neurophysiol* **83**(1): 70-80.

Kennard, L. E., J. R. Chumbley, K. M. Ranatunga, S. J. Armstrong, E. L. Veale and A. Mathie (2005). "Inhibition of the human two-pore domain potassium channel, TREK-1, by fluoxetine and its metabolite norfluoxetine." *Br J Pharmacol* **144**(6): 821-829.

Kido, M., L. Du, C. C. Sullivan, X. Li, R. Deutsch, S. W. Jamieson and P. A. Thistlethwaite (2005). "Hypoxia-inducible factor 1-alpha reduces infarction and attenuates progression of cardiac dysfunction after myocardial infarction in the mouse." *J Am Coll Cardiol* **46**(11): 2116-2124.

Kikuchi, K. and K. D. Poss (2012). "Cardiac regenerative capacity and mechanisms." *Annu Rev Cell Dev Biol* **28**: 719-741.

Kim, D. (1992). "A mechanosensitive K⁺ channel in heart cells. Activation by arachidonic acid." *J Gen Physiol* **100**(6): 1021-1040.

Kim, N., A. L. Stiegler, T. O. Cameron, P. T. Hallock, A. M. Gomez, J. H. Huang, S. R. Hubbard, M. L. Dustin and S. J. Burden (2008). "Lrp4 is a receptor for Agrin and forms a complex with MuSK." *Cell* **135**(2): 334-342.

Klein-Nulend, J., R. G. Bacabac and M. G. Mullender (2005). "Mechanobiology of bone tissue." *Pathol Biol (Paris)* **53**(10): 576-580.

Koh, S. D., K. Monaghan, G. P. Sergeant, S. Ro, R. L. Walker, K. M. Sanders and B. Horowitz (2001). "TREK-1 regulation by nitric oxide and cGMP-dependent protein kinase. An essential role in smooth muscle inhibitory neurotransmission." *J Biol Chem* **276**(47): 44338-44346.

Kohl, P., C. Bollensdorff and A. Garny (2006). "Effects of mechanosensitive ion channels on ventricular electrophysiology: experimental and theoretical models." *Exp Physiol* **91**(2): 307-321.

Kumar, S., I. Z. Maxwell, A. Heisterkamp, T. R. Polte, T. P. Lele, M. Salanga, E. Mazur and D. E. Ingber (2006). "Viscoelastic retraction of single living stress fibers and its impact on cell shape, cytoskeletal organization, and extracellular matrix mechanics." *Biophys J* **90**(10): 3762-3773.

Kuwahara, K., Y. Wang, J. McAnally, J. A. Richardson, R. Bassel-Duby, J. A. Hill and E. N. Olson (2006). "TRPC6 fulfills a calcineurin signaling circuit during pathologic cardiac remodeling." *J Clin Invest* **116**(12): 3114-3126.

Laflamme, M. A., K. Y. Chen, A. V. Naumova, V. Muskheli, J. A. Fugate, S. K. Dupras, H. Reinecke, C. Xu, M. Hassanipour, S. Police, C. O'Sullivan, L. Collins, Y. Chen, E. Minami, E. A. Gill, S. Ueno, C. Yuan, J. Gold and C. E. Murry (2007). "Cardiomyocytes derived from human embryonic stem cells in pro-survival factors enhance function of infarcted rat hearts." *Nat Biotechnol* **25**(9): 1015-1024.

Laigle, C., S. Confort-Gouny, Y. Le Fur, P. J. Cozzone and A. Viola (2012). "Deletion of TRAAK potassium channel affects brain metabolism and protects against ischemia." *PLoS One* **7**(12): e53266.

Lehoux, S. and A. Tedgui (2003). "Cellular mechanics and gene expression in blood vessels." *J Biomech* **36**(5): 631-643.

Lei, M., S. A. Jones, J. Liu, M. K. Lancaster, S. S. Fung, H. Dobrzynski, P. Camelliti, S. K. Maier, D. Noble and M. R. Boyett (2004). "Requirement of neuronal- and cardiac-type sodium channels for murine sinoatrial node pacemaking." *J Physiol* **559**(Pt 3): 835-848.

Lengyel, M., G. Czirjak and P. Enyedi (2016). "Formation of Functional Heterodimers by TREK-1 and TREK-2 Two-pore Domain Potassium Channel Subunits." *J Biol Chem* **291**(26): 13649-13661.

Leri, A., J. Kajstura, P. Anversa and W. H. Frishman (2008). "Myocardial regeneration and stem cell repair." *Curr Probl Cardiol* **33**(3): 91-153.

Lesage, F. and M. Lazdunski (2000). "Molecular and functional properties of two-pore-domain potassium channels." *Am J Physiol Renal Physiol* **279**(5): F793-801.

Lev, S., I. Kehat and L. Gepstein (2005). "Differentiation pathways in human embryonic stem cell-derived cardiomyocytes." *Ann N Y Acad Sci* **1047**: 50-65.

Levental, K. R., H. Yu, L. Kass, J. N. Lakins, M. Egeblad, J. T. Emler, S. F. Fong, K. Csiszar, A. Giaccia, W. Weninger, M. Yamauchi, D. L. Gasser and V. M. Weaver (2009). "Matrix crosslinking forces tumor progression by enhancing integrin signaling." *Cell* **139**(5): 891-906.

Levitz, J., P. Royal, Y. Comoglio, B. Wdziekonski, S. Schaub, D. M. Clemens, E. Y. Isacoff and G. Sandoz (2016). "Heterodimerization within the TREK channel subfamily produces a diverse family of highly regulated potassium channels." *Proc Natl Acad Sci U S A* **113**(15): 4194-4199.

Li, F., X. Wang, J. M. Capasso and A. M. Gerdes (1996). "Rapid transition of cardiac myocytes from hyperplasia to hypertrophy during postnatal development." *J Mol Cell Cardiol* **28**(8): 1737-1746.

Li, J., B. Hou, S. Tumova, K. Muraki, A. Bruns, M. J. Ludlow, A. Sedo, A. J. Hyman, L. McKeown, R. S. Young, N. Y. Yuldasheva, Y. Majeed, L. A. Wilson, B. Rode, M. A. Bailey, H. R. Kim, Z. Fu, D. A. Carter, J. Bilton, H. Imrie, P. Ajuh, T. N. Dear, R. M. Cubbon, M. T. Kearney, R. K. Prasad, P. C. Evans, J. F. Ainscough and D. J. Beech (2014). "Piezo1 integration of vascular architecture with physiological force." *Nature* **515**(7526): 279-282.

Li, M., J. Liu and C. Zhang (2011). "Evolutionary history of the vertebrate mitogen activated protein kinases family." *PLoS One* **6**(10): e26999.

Liang, J., B. Huang, G. Yuan, Y. Chen, F. Liang, H. Zeng, S. Zheng, L. Cao, D. Geng and S. Zhou (2017). "Stretch-activated channel Piezo1 is up-regulated in failure heart and cardiomyocyte stimulated by AngII." *Am J Transl Res* **9**(6): 2945-2955.

Liang, Q. and J. D. Molkentin (2003). "Redefining the roles of p38 and JNK signaling in cardiac hypertrophy: dichotomy between cultured myocytes and animal models." *J Mol Cell Cardiol* **35**(12): 1385-1394.

Lin, E., C. Craig, M. Lamothe, M. V. Sarunic, M. F. Beg and G. F. Tibbits (2015). "Construction and use of a zebrafish heart voltage and calcium optical mapping system, with integrated electrocardiogram and programmable electrical stimulation." *Am J Physiol Regul Integr Comp Physiol* **308**(9): R755-768.

Lin, L., S. McCroskery, J. M. Ross, Y. Chak, B. Neuhuber and M. P. Daniels (2010). "Induction of filopodia-like protrusions by transmembrane agrin: role of agrin glycosaminoglycan chains and Rho-family GTPases." *Exp Cell Res* **316**(14): 2260-2277.

Liu, S., D. A. Calderwood and M. H. Ginsberg (2000). "Integrin cytoplasmic domain-binding proteins." *J Cell Sci* **113** (Pt 20): 3563-3571.

Liu, W. and D. A. Saint (2004). "Heterogeneous expression of tandem-pore K⁺ channel genes in adult and embryonic rat heart quantified by real-time polymerase chain reaction." *Clin Exp Pharmacol Physiol* **31**(3): 174-178.

Lopatin, A. N. and C. G. Nichols (2001). "Inward rectifiers in the heart: an update on I(K1)." *J Mol Cell Cardiol* **33**(4): 625-638.

Lugenbiel, P., F. Wenz, P. Syren, P. Geschwill, K. Govorov, C. Seyler, D. Frank, P. A. Schweizer, J. Franke, T. Weis, C. Bruehl, B. Schmack, A. Ruhparwar, M. Karck, N. Frey, H. A. Katus and D. Thomas (2017). "TREK-1 (K2P2.1) K(+) channels are suppressed in patients with atrial fibrillation and heart failure and provide therapeutic targets for rhythm control." *Basic Res Cardiol* **112**(1): 8.

Luo, T., K. Mohan, V. Srivastava, Y. Ren, P. A. Iglesias and D. N. Robinson (2012). "Understanding the cooperative interaction between myosin II and actin cross-linkers mediated by actin filaments during mechanosensation." *Biophys J* **102**(2): 238-247.

Maingret, F., M. Fosset, F. Lesage, M. Lazdunski and E. Honore (1999). "TRAAK is a mammalian neuronal mechano-gated K⁺ channel." *J Biol Chem* **274**(3): 1381-1387.

Maingret, F., E. Honore, M. Lazdunski and A. J. Patel (2002). "Molecular basis of the voltage-dependent gating of TREK-1, a mechano-sensitive K(+) channel." *Biochem Biophys Res Commun* **292**(2): 339-346.

Maingret, F., I. Lauritzen, A. J. Patel, C. Heurteaux, R. Reyes, F. Lesage, M. Lazdunski and E. Honore (2000). "TREK-1 is a heat-activated background K(+) channel." *Embo j* **19**(11): 2483-2491.

Maingret, F., A. J. Patel, F. Lesage, M. Lazdunski and E. Honore (1999). "Mechano- or acid stimulation, two interactive modes of activation of the TREK-1 potassium channel." *J Biol Chem* **274**(38): 26691-26696.

Maingret, F., A. J. Patel, F. Lesage, M. Lazdunski and E. Honore (2000). "Lysophospholipids open the two-pore domain mechano-gated K(+) channels TREK-1 and TRAAK." *J Biol Chem* **275**(14): 10128-10133.

Marion, E., O. R. Song, T. Christophe, J. Babonneau, D. Fenistein, J. Eyer, F. Letournel, D. Henrion, N. Clere, V. Paille, N. C. Guerineau, J. P. Saint Andre, P. Gersbach, K. H. Altmann, T. P. Stinear, Y. Comoglio, G. Sandoz, L. Preisser, Y. Delneste, E. Yeramian, L. Marsollier and P. Brodin (2014). "Mycobacterial toxin induces analgesia in buruli ulcer by targeting the angiotensin pathways." *Cell* **157**(7): 1565-1576.

Matrone, G., C. S. Tucker and M. A. Denvir (2017). "Cardiomyocyte proliferation in zebrafish and mammals: lessons for human disease." *Cell Mol Life Sci* **74**(8): 1367-1378.

Mazella, J., O. Petrault, G. Lucas, E. Deval, S. Beraud-Dufour, C. Gandin, M. El-Yacoubi, C. Widmann, A. Guyon, E. Chevet, S. Taouji, G. Conductier, A. Corinus, T. Coppola, G. Gobbi, J. L. Nahon, C. Heurteaux and M. Borsotto (2010). "Spadin, a sortilin-derived peptide, targeting rodent TREK-1 channels: a new concept in the antidepressant drug design." *PLoS Biol* **8**(4): e1000355.

Mercola, M., P. Ruiz-Lozano and M. D. Schneider (2011). "Cardiac muscle regeneration: lessons from development." *Genes Dev* **25**(4): 299-309.

Mikut, R., T. Dickmeis, W. Driever, P. Geurts, F. A. Hamprecht, B. X. Kausler, M. J. Ledesma-Carbayo, R. Maree, K. Mikula, P. Pantazis, O. Ronneberger, A. Santos, R. Stotzka, U. Strahle and N. Peyrieras (2013). "Automated processing of zebrafish imaging data: a survey." *Zebrafish* **10**(3): 401-421.

Milan, D. J., T. A. Peterson, J. N. Ruskin, R. T. Peterson and C. A. MacRae (2003). "Drugs that induce repolarization abnormalities cause bradycardia in zebrafish." *Circulation* **107**(10): 1355-1358.

Moha ou Maati, H., R. Peyronnet, C. Devader, J. Veyssiere, F. Labbal, C. Gandin, J. Mazella, C. Heurteaux and M. Borsotto (2011). "A human TREK-1/HEK cell line: a highly efficient screening tool for drug development in neurological diseases." *PLoS One* **6**(10): e25602.

Moha Ou Maati, H., J. Veyssiere, F. Labbal, T. Coppola, C. Gandin, C. Widmann, J. Mazella, C. Heurteaux and M. Borsotto (2012). "Spadin as a new antidepressant: absence of TREK-1-related side effects." *Neuropharmacology* **62**(1): 278-288.

Momin, A. and J. N. Wood (2008). "Sensory neuron voltage-gated sodium channels as analgesic drug targets." *Curr Opin Neurobiol* **18**(4): 383-388.

Murata, M., S. Tohyama and K. Fukuda (2010). "Impacts of recent advances in cardiovascular regenerative medicine on clinical therapies and drug discovery." *Pharmacol Ther* **126**(2): 109-118.

Murbartian, J., Q. Lei, J. J. Sando and D. A. Bayliss (2005). "Sequential phosphorylation mediates receptor- and kinase-induced inhibition of TREK-1 background potassium channels." *J Biol Chem* **280**(34): 30175-30184.

Murry, C. E., M. H. Soonpaa, H. Reinecke, H. Nakajima, H. O. Nakajima, M. Rubart, K. B. Pasumarthi, J. I. Virag, S. H. Bartelmez, V. Poppa, G. Bradford, J. D. Dowell, D. A. Williams and L. J. Field (2004). "Haematopoietic stem cells do not transdifferentiate into cardiac myocytes in myocardial infarcts." *Nature* **428**(6983): 664-668.

Murthy, S. E., A. E. Dubin and A. Patapoutian (2017). "Piezos thrive under pressure: mechanically activated ion channels in health and disease." *Nat Rev Mol Cell Biol* **18**(12): 771-783.

Nadal-Ginard, B., J. Kajstura, A. Leri and P. Anversa (2003). "Myocyte death, growth, and regeneration in cardiac hypertrophy and failure." *Circ Res* **92**(2): 139-150.

Nakada, Y., D. C. Canseco, S. Thet, S. Abdisalaam, A. Asaithamby, C. X. Santos, A. M. Shah, H. Zhang, J. E. Faber, M. T. Kinter, L. I. Szweda, C. Xing, Z. Hu, R. J. Deberardinis, G. Schiattarella, J. A. Hill, O. Oz, Z. Lu, C. C. Zhang, W. Kimura and H. A. Sadek (2017). "Hypoxia induces heart regeneration in adult mice." *Nature* **541**(7636): 222-227.

Nemtsas, P., E. Wettwer, T. Christ, G. Weidinger and U. Ravens (2010). "Adult zebrafish heart as a model for human heart? An electrophysiological study." *J Mol Cell Cardiol* **48**(1): 161-171.

Nilius, B. and V. Flockerzi (2014). "Mammalian transient receptor potential (TRP) cation channels. Preface." *Handb Exp Pharmacol* **223**: v - vi.

Nishida, M., K. Watanabe, Y. Sato, M. Nakaya, N. Kitajima, T. Ide, R. Inoue and H. Kurose (2010). "Phosphorylation of TRPC6 channels at Thr69 is required for anti-hypertrophic effects of phosphodiesterase 5 inhibition." *J Biol Chem* **285**(17): 13244-13253.

Nyman, J. S., H. Leng, X. N. Dong and X. Wang (2009). "Differences in the mechanical behavior of cortical bone between compression and tension when subjected to progressive loading." *J Mech Behav Biomed Mater* **2**(6): 613-619.

O'Connell, A. D., M. J. Morton and M. Hunter (2002). "Two-pore domain K⁺ channels-molecular sensors." *Biochim Biophys Acta* **1566**(1-2): 152-161.

Oberpriller, J. and J. C. Oberpriller (1971). "Mitosis in adult newt ventricle." *J Cell Biol* **49**(2): 560-563.

Oeztuerk-Winder, F. and J. J. Ventura (2012). "The many faces of p38 mitogen-activated protein kinase in progenitor/stem cell differentiation." *Biochem J* **445**(1): 1-10.

Ohba, T., H. Watanabe, M. Murakami, Y. Takahashi, K. Iino, S. Kuromitsu, Y. Mori, K. Ono, T. Iijima and H. Ito (2007). "Upregulation of TRPC1 in the development of cardiac hypertrophy." *J Mol Cell Cardiol* **42**(3): 498-507.

Olson, T. M., A. E. Alekseev, X. K. Liu, S. Park, L. V. Zingman, M. Bienengraeber, S. Sattiraju, J. D. Ballew, A. Jahangir and A. Terzic (2006). "Kv1.5 channelopathy due to KCNA5 loss-of-function mutation causes human atrial fibrillation." *Hum Mol Genet* **15**(14): 2185-2191.

Ono, K. and J. Han (2000). "The p38 signal transduction pathway: activation and function." *Cell Signal* **12**(1): 1-13.

Orr, A. W., B. P. Helmke, B. R. Blackman and M. A. Schwartz (2006). "Mechanisms of mechanotransduction." *Dev Cell* **10**(1): 11-20.

Ozaita, A. and E. Vega-Saenz de Miera (2002). "Cloning of two transcripts, HKT4.1a and HKT4.1b, from the human two-pore K⁺ channel gene KCNK4. Chromosomal localization, tissue distribution and functional expression." *Brain Res Mol Brain Res* **102**(1-2): 18-27.

Patel, A. J., E. Honore, F. Lesage, M. Fink, G. Romey and M. Lazdunski (1999). "Inhalational anesthetics activate two-pore-domain background K⁺ channels." *Nat Neurosci* **2**(5): 422-426.

Patel, A. J., E. Honore, F. Maingret, F. Lesage, M. Fink, F. Duprat and M. Lazdunski (1998). "A mammalian two pore domain mechano-gated S-like K⁺ channel." *Embo j* **17**(15): 4283-4290.

Patel, S. K., L. Jackson, A. Y. Warren, P. Arya, R. W. Shaw and R. N. Khan (2013). "A role for two-pore potassium (K2P) channels in endometrial epithelial function." *J Cell Mol Med* **17**(1): 134-146.

Pedrozo, Z., A. Criollo, P. K. Battiprolu, C. R. Morales, A. Contreras-Ferrat, C. Fernandez, N. Jiang, X. Luo, M. J. Caplan, S. Somlo, B. A. Rothermel, T. G. Gillette, S. Lavandero and J. A. Hill (2015). "Polycystin-1 Is a Cardiomyocyte Mechanosensor That Governs L-Type Ca²⁺ Channel Protein Stability." *Circulation* **131**(24): 2131-2142.

Pelster, B. and W. W. Burggren (1996). "Disruption of hemoglobin oxygen transport does not impact oxygen-dependent physiological processes in developing embryos of zebra fish (*Danio rerio*)." *Circ Res* **79**(2): 358-362.

Peyronnet, R., J. M. Nerbonne and P. Kohl (2016). "Cardiac Mechano-Gated Ion Channels and Arrhythmias." *Circ Res* **118**(2): 311-329.

Porrello, E. R., A. I. Mahmoud, E. Simpson, J. A. Hill, J. A. Richardson, E. N. Olson and H. A. Sadek (2011). "Transient regenerative potential of the neonatal mouse heart." *Science* **331**(6020): 1078-1080.

Priest, B. T. and J. S. McDermott (2015). "Cardiac ion channels." *Channels (Austin)* **9**(6): 352-359.

Provenzano, P. P. and P. J. Keely (2011). "Mechanical signaling through the cytoskeleton regulates cell proliferation by coordinated focal adhesion and Rho GTPase signaling." *J Cell Sci* **124**(Pt 8): 1195-1205.

Puente, B. N., W. Kimura, S. A. Muralidhar, J. Moon, J. F. Amatruda, K. L. Phelps, D. Grinsfelder, B. A. Rothermel, R. Chen, J. A. Garcia, C. X. Santos, S. Thet, E. Mori, M. T. Kinter, P. M. Rindler, S. Zacchigna, S. Mukherjee, D. J. Chen, A. I. Mahmoud, M. Giacca, P. S. Rabinovitch, A. Aroumougame, A. M. Shah, L. I. Szweda and H. A. Sadek (2014). "The oxygen-rich postnatal environment induces cardiomyocyte cell-cycle arrest through DNA damage response." *Cell* **157**(3): 565-579.

Rahimov, F. and L. M. Kunkel (2013). "The cell biology of disease: cellular and molecular mechanisms underlying muscular dystrophy." *J Cell Biol* **201**(4): 499-510.

Ranade, S. S., Z. Qiu, S. H. Woo, S. S. Hur, S. E. Murthy, S. M. Cahalan, J. Xu, J. Mathur, M. Bandell, B. Coste, Y. S. Li, S. Chien and A. Patapoutian (2014). "Piezo1, a mechanically activated ion channel, is required for vascular development in mice." *Proc Natl Acad Sci U S A* **111**(28): 10347-10352.

Raouf, R., F. Rugiero, H. Kieseewetter, R. Hatch, E. Hummler, M. A. Nassar, F. Wang and J. N. Wood (2012). "Sodium channels and mammalian sensory mechanotransduction." *Mol Pain* **8**: 21.

Raya, A., C. M. Koth, D. Buscher, Y. Kawakami, T. Itoh, R. M. Raya, G. Sternik, H. J. Tsai, C. Rodriguez-Esteban and J. C. Izpisua-Belmonte (2003). "Activation of Notch signaling pathway precedes heart regeneration in zebrafish." *Proc Natl Acad Sci U S A* **100** Suppl 1: 11889-11895.

Retailleau, K., F. Duprat, M. Arhatte, S. S. Ranade, R. Peyronnet, J. R. Martins, M. Jodar, C. Moro, S. Offermanns, Y. Feng, S. Demolombe, A. Patel and E. Honore (2015). "Piezo1 in Smooth Muscle Cells Is Involved in Hypertension-Dependent Arterial Remodeling." *Cell Rep* **13**(6): 1161-1171.

Richardson, S. M., J. A. Hoyland, R. Mobasheri, C. Csaki, M. Shakibaei and A. Mobasheri (2010). "Mesenchymal stem cells in regenerative medicine: opportunities and challenges for articular cartilage and intervertebral disc tissue engineering." *J Cell Physiol* **222**(1): 23-32.

Rinne, S., V. Renigunta, G. Schlichthorl, M. Zuzarte, S. Bittner, S. G. Meuth, N. Decher, J. Daut and R. Preisig-Muller (2014). "A splice variant of the two-pore domain potassium channel TREK-1 with only one pore domain reduces the surface expression of full-length TREK-1 channels." *Pflugers Arch* **466**(8): 1559-1570.

Rossi, M. A. and S. V. Carillo (1991). "Cardiac hypertrophy due to pressure and volume overload: distinctly different biological phenomena?" *Int J Cardiol* **31**(2): 133-141.

Rumyantsev, P. P. (1977). "Interrelations of the proliferation and differentiation processes during cardiac myogenesis and regeneration." *Int Rev Cytol* **51**: 186-273.

Ruwhof, C. and A. van der Laarse (2000). "Mechanical stress-induced cardiac hypertrophy: mechanisms and signal transduction pathways." *Cardiovasc Res* **47**(1): 23-37.

Sabeh, M. K., H. Kekhia and C. A. Macrae (2012). "Optical mapping in the developing zebrafish heart." *Pediatr Cardiol* **33**(6): 916-922.

Sadoshima, J. and S. Izumo (1997). "The cellular and molecular response of cardiac myocytes to mechanical stress." *Annu Rev Physiol* **59**: 551-571.

Sander, V., G. Sune, C. Jopling, C. Morera and J. C. Izpisua Belmonte (2013). "Isolation and in vitro culture of primary cardiomyocytes from adult zebrafish hearts." *Nat Protoc* **8**(4): 800-809.

Sandoz, G., D. Douguet, F. Chatelain, M. Lazdunski and F. Lesage (2009). "Extracellular acidification exerts opposite actions on TREK1 and TREK2 potassium channels via a single conserved histidine residue." *Proc Natl Acad Sci U S A* **106**(34): 14628-14633.

Sandoz, G., M. P. Tardy, S. Thummler, S. Feliciangeli, M. Lazdunski and F. Lesage (2008). "Mtap2 is a constituent of the protein network that regulates twik-related K⁺ channel expression and trafficking." *J Neurosci* **28**(34): 8545-8552.

Sandoz, G., S. Thummler, F. Duprat, S. Feliciangeli, J. Vinh, P. Escoubas, N. Guy, M. Lazdunski and F. Lesage (2006). "AKAP150, a switch to convert mechano-, pH- and arachidonic acid-sensitive TREK K⁽⁺⁾ channels into open leak channels." *Embo j* **25**(24): 5864-5872.

Sauter, D. R., C. E. Sorensen, M. Rapedius, A. Bruggemann and I. Novak (2016). "pH-sensitive K⁽⁺⁾ channel TREK-1 is a novel target in pancreatic cancer." *Biochim Biophys Acta* **1862**(10): 1994-2003.

Schindler, R. F., C. Scotton, J. Zhang, C. Passarelli, B. Ortiz-Bonnin, S. Simrick, T. Schwerte, K. L. Poon, M. Fang, S. Rinne, A. Froese, V. O. Nikolaev, C. Grunert, T. Muller, G. Tasca, P. Sarathchandra, F. Drago, B. Dallapiccola, C. Rapezzi, E. Arbustini, F. R. Di Raimo, M. Neri, R. Selvatici, F. Gualandi, F. Fattori, A. Pietrangelo, W. Li, H. Jiang, X. Xu, E. Bertini, N. Decher, J. Wang, T. Brand and A. Ferlini (2016). "POPDC1(S201F) causes muscular dystrophy and arrhythmia by affecting protein trafficking." *J Clin Invest* **126**(1): 239-253.

Schroeder, M. C. and G. Halder (2012). "Regulation of the Hippo pathway by cell architecture and mechanical signals." *Semin Cell Dev Biol* **23**(7): 803-811.

Schwerte, T., C. Prem, A. Mairosi and B. Pelster (2006). "Development of the sympatho-vagal balance in the cardiovascular system in zebrafish (*Danio rerio*) characterized by power spectrum and classical signal analysis." *J Exp Biol* **209**(Pt 6): 1093-1100.

Schwingshackl, A., B. Teng, M. Ghosh, A. N. West, P. Makena, V. Gorantla, S. E. Sinclair and C. M. Waters (2012). "Regulation and function of the two-pore-domain (K2P) potassium channel Trek-1 in alveolar epithelial cells." *Am J Physiol Lung Cell Mol Physiol* **302**(1): L93-L102.

Sehnert, A. J. and D. Y. Stainier (2002). "A window to the heart: can zebrafish mutants help us understand heart disease in humans?" *Trends Genet* **18**(10): 491-494.

Seth, M., Z. S. Zhang, L. Mao, V. Graham, J. Burch, J. Stiber, L. Tsiokas, M. Winn, J. Abramowitz, H. A. Rockman, L. Birnbaumer and P. Rosenberg (2009). "TRPC1 channels are critical for hypertrophic signaling in the heart." *Circ Res* **105**(10): 1023-1030.

Shiba, Y., S. Fernandes, W. Z. Zhu, D. Filice, V. Muskheli, J. Kim, N. J. Palpant, J. Gantz, K. W. Moyes, H. Reinecke, B. Van Biber, T. Dardas, J. L. Mignone, A. Izawa, R. Hanna, M. Viswanathan, J. D. Gold, M. I. Kotlikoff, N. Sarvazyan, M. W. Kay, C. E. Murry and M. A. Laflamme (2012). "Human ES-cell-derived cardiomyocytes electrically couple and suppress arrhythmias in injured hearts." *Nature* **489**(7415): 322-325.

Shotan, A., S. Dacca, M. Shochat, M. Kazatsker, D. S. Blondheim and S. Meisel (2005). "Fluid overload contributing to heart failure." *Nephrol Dial Transplant* **20 Suppl 7**: vii24-27.

Skerjanc, I. S., H. Petropoulos, A. G. Ridgeway and S. Wilton (1998). "Myocyte enhancer factor 2C and Nkx2-5 up-regulate each other's expression and initiate cardiomyogenesis in P19 cells." *J Biol Chem* **273**(52): 34904-34910.

Spector, A. A. (2009). "Arachidonic acid cytochrome P450 epoxygenase pathway." *J Lipid Res* **50 Suppl**: S52-56.

Streicher, J. M., S. Ren, H. Herschman and Y. Wang (2010). "MAPK-activated protein kinase-2 in cardiac hypertrophy and cyclooxygenase-2 regulation in heart." *Circ Res* **106**(8): 1434-1443.

Tajima, M., J. Bartunek, E. O. Weinberg, N. Ito and B. H. Lorell (1998). "Atrial natriuretic peptide has different effects on contractility and intracellular pH in normal and hypertrophied myocytes from pressure-overloaded hearts." *Circulation* **98**(24): 2760-2764.

Takahashi, K., Y. Kakimoto, K. Toda and K. Naruse (2013). "Mechanobiology in cardiac physiology and diseases." *J Cell Mol Med* **17**(2): 225-232.

Takahashi, K., K. Tanabe, M. Ohnuki, M. Narita, T. Ichisaka, K. Tomoda and S. Yamanaka (2007). "Induction of pluripotent stem cells from adult human fibroblasts by defined factors." *Cell* **131**(5): 861-872.

Tan, J. H., W. Liu and D. A. Saint (2002). "Trek-like potassium channels in rat cardiac ventricular myocytes are activated by intracellular ATP." *J Membr Biol* **185**(3): 201-207.

Thomson, J. A., J. Itskovitz-Eldor, S. S. Shapiro, M. A. Waknitz, J. J. Swiergiel, V. S. Marshall and J. M. Jones (1998). "Embryonic stem cell lines derived from human blastocysts." *Science* **282**(5391): 1145-1147.

Thubrikar, M. J. and F. Robicsek (1995). "Pressure-induced arterial wall stress and atherosclerosis." *Ann Thorac Surg* **59**(6): 1594-1603.

Tong, L., M. Cai, Y. Huang, H. Zhang, B. Su, Z. Li and H. Dong (2014). "Activation of K(2)P channel-TREK1 mediates the neuroprotection induced by sevoflurane preconditioning." *Br J Anaesth* **113**(1): 157-167.

Turczynska, K. M., P. Hellstrand, K. Sward and S. Albinsson (2013). "Regulation of vascular smooth muscle mechanotransduction by microRNAs and L-type calcium channels." *Commun Integr Biol* **6**(1): e22278.

Uhm, C. S., B. Neuhuber, B. Lowe, V. Crocker and M. P. Daniels (2001). "Synapse-forming axons and recombinant agrin induce microprocess formation on myotubes." *J Neurosci* **21**(24): 9678-9689.

Unudurthi, S. D., X. Wu, L. Qian, F. Amari, B. Onal, N. Li, M. A. Makara, S. A. Smith, J. Snyder, V. V. Fedorov, V. Coppola, M. E. Anderson, P. J. Mohler and T. J. Hund (2016). "Two-Pore K+ Channel TREK-1 Regulates Sinoatrial Node Membrane Excitability." *J Am Heart Assoc* **5**(4): e002865.

Urbanek, K., F. Quaini, G. Tasca, D. Torella, C. Castaldo, B. Nadal-Ginard, A. Leri, J. Kajstura, E. Quaini and P. Anversa (2003). "Intense myocyte formation from cardiac stem cells in human cardiac hypertrophy." *Proc Natl Acad Sci U S A* **100**(18): 10440-10445.

Veale, E. L., K. A. Rees, A. Mathie and S. Trapp (2010). "Dominant negative effects of a non-conducting TREK1 splice variant expressed in brain." *J Biol Chem* **285**(38): 29295-29304.

Verkerk, A. O. and C. A. Remme (2012). "Zebrafish: a novel research tool for cardiac (patho)electrophysiology and ion channel disorders." *Front Physiol* **3**: 255.

Veyssiere, J., H. Moha Ou Maati, J. Mazella, G. Gaudriault, S. Moreno, C. Heurteaux and M. Borsotto (2015). "Retroinverso analogs of spadin display increased antidepressant effects." *Psychopharmacology (Berl)* **232**(3): 561-574.

Vogel, V. and M. Sheetz (2006). "Local force and geometry sensing regulate cell functions." *Nat Rev Mol Cell Biol* **7**(4): 265-275.

Vollrath, M. A., K. Y. Kwan and D. P. Corey (2007). "The micromachinery of mechanotransduction in hair cells." *Annu Rev Neurosci* **30**: 339-365.

Voloshyna, I., A. Besana, M. Castillo, T. Matos, I. B. Weinstein, M. Mansukhani, R. B. Robinson, C. Cordon-Cardo and S. J. Feinmark (2008). "TREK-1 is a novel molecular target in prostate cancer." *Cancer Res* **68**(4): 1197-1203.

Wang, C., B. Xiong and J. Huang (2016). "The Role of Omega-3 Polyunsaturated Fatty Acids in Heart Failure: A Meta-Analysis of Randomised Controlled Trials." *Nutrients* **9**(1).

Wang, J., D. Panakova, K. Kikuchi, J. E. Holdway, M. Gemberling, J. S. Burris, S. P. Singh, A. L. Dickson, Y. F. Lin, M. K. Sabeh, A. A. Werdich, D. Yelon, C. A. Macrae and K. D. Poss (2011). "The regenerative capacity of zebrafish reverses cardiac failure caused by genetic cardiomyocyte depletion." *Development* **138**(16): 3421-3430.

Wang, L. and D. H. Wang (2005). "TRPV1 gene knockout impairs postischemic recovery in isolated perfused heart in mice." *Circulation* **112**(23): 3617-3623.

Wang, W., M. Zhang, P. Li, H. Yuan, N. Feng, Y. Peng, L. Wang and X. Wang (2013). "An increased TREK-1-like potassium current in ventricular myocytes during rat cardiac hypertrophy." *J Cardiovasc Pharmacol* **61**(4): 302-310.

Woo, S. H., S. Ranade, A. D. Weyer, A. E. Dubin, Y. Baba, Z. Qiu, M. Petrus, T. Miyamoto, K. Reddy, E. A. Lumpkin, C. L. Stucky and A. Patapoutian (2014). "Piezo2 is required for Merkel-cell mechanotransduction." *Nature* **509**(7502): 622-626.

Wozniak, M. A. and C. S. Chen (2009). "Mechanotransduction in development: a growing role for contractility." *Nat Rev Mol Cell Biol* **10**(1): 34-43.

Wu, X., P. Eder, B. Chang and J. D. Molkentin (2010). "TRPC channels are necessary mediators of pathologic cardiac hypertrophy." *Proc Natl Acad Sci U S A* **107**(15): 7000-7005.

Xian Tao, L., V. Dyachenko, M. Zuzarte, C. Putzke, R. Preisig-Muller, G. Isenberg and J. Daut (2006). "The stretch-activated potassium channel TREK-1 in rat cardiac ventricular muscle." *Cardiovasc Res* **69**(1): 86-97.

Yamakage, M. and A. Namiki (2002). "Calcium channels--basic aspects of their structure, function and gene encoding; anesthetic action on the channels--a review." *Can J Anaesth* **49**(2): 151-164.

Yoshida, Y. and S. Yamanaka (2011). "iPS cells: a source of cardiac regeneration." *J Mol Cell Cardiol* **50**(2): 327-332.

Yue, Z., Y. Zhang, J. Xie, J. Jiang and L. Yue (2013). "Transient receptor potential (TRP) channels and cardiac fibrosis." *Curr Top Med Chem* **13**(3): 270-282.

Zafeiridis, A., V. Jeevanandam, S. R. Houser and K. B. Margulies (1998). "Regression of cellular hypertrophy after left ventricular assist device support." *Circulation* **98**(7): 656-662.

Zaman, S. and P. Kovoor (2014). "Sudden cardiac death early after myocardial infarction: pathogenesis, risk stratification, and primary prevention." *Circulation* **129**(23): 2426-2435.

Zeng, T., G. C. Bett and F. Sachs (2000). "Stretch-activated whole cell currents in adult rat cardiac myocytes." *Am J Physiol Heart Circ Physiol* **278**(2): H548-557.

Zhang, G. M., F. N. Wan, X. J. Qin, D. L. Cao, H. L. Zhang, Y. Zhu, B. Dai, G. H. Shi and D. W. Ye (2015). "Prognostic significance of the TREK-1 K2P potassium channels in prostate cancer." *Oncotarget* **6**(21): 18460-18468.

Zhang, J., G. F. Wilson, A. G. Soerens, C. H. Koonce, J. Yu, S. P. Palecek, J. A. Thomson and T. J. Kamp (2009). "Functional cardiomyocytes derived from human induced pluripotent stem cells." *Circ Res* **104**(4): e30-41.

Zhang, M., H. J. Yin, W. P. Wang, J. Li and X. L. Wang (2016). "Over-expressed human TREK-1 inhibits CHO cell proliferation via inhibiting PKA and p38 MAPK pathways and subsequently inducing G1 arrest." *Acta Pharmacol Sin* **37**(9): 1190-1198.

Ziello, J. E., I. S. Jovin and Y. Huang (2007). "Hypoxia-Inducible Factor (HIF)-1 regulatory pathway and its potential for therapeutic intervention in malignancy and ischemia." *Yale J Biol Med* **80**(2): 51-60.

Zordoky, B. N., M. E. Aboutabl and A. O. El-Kadi (2008). "Modulation of cytochrome P450 gene expression and arachidonic acid metabolism during isoproterenol-induced cardiac hypertrophy in rats." *Drug Metab Dispos* **36**(11): 2277-2286.

Acknowledgements:

I owe my deepest gratitude to my PhD supervisors Chris Jopling and Hamid Moha Ou Maati for their support during my PhD, for their patience and their guidance that helped me during for writing thesis.

I would also like to thank all the members of my team: Dr Adele Faucherre, Dr Girisaran Gangataran, Dr Laurent Gamba, and Pierre Rambeau for their support and for the moments that we have spent together.

I would like to thank Dr Catherine Heurteaux, Dr Marc Borsotto, Dr Jean Mazella for providing me with spadin, Dr Frank Chatelain for providing me with mouse TREK-1 antibody.

Another person I would like to thank is Dr Angelo Torrente for his help with optical mapping experiments.

I would like to thank the members of my thesis committee: Dr Benedicte Delaval and Dr Jean-Yves Le Guennec for their follow-up and their ideas that they have provided me during my PhD.

I would like to thank people who I met during my 3 years of PhD and they become great friends. I would like to thank Antony.Chung-You-Chong, Leila Talssi, Monia Souidi, Joelle Obeid, Chadi Nasrallah, Luc Forichon, Pierre Cesses for their advices and for all the great moments that we have spent together.

I would like to thank a special person: Mazen El Ghoussainy who supported me especially during the tough period of my PhD.

Finally, I would like to thank my family for their support, without their help I couldn't have achieved my goals and done this PhD. Thank you for believing in me.